



INSTITUTO POLITÉCNICO NACIONAL  
ESCUELA NACIONAL DE MEDICINA Y HOMEOPATÍA  
SECCIÓN DE ESTUDIOS DE POSGRADO E INVESTIGACIÓN

DOCTORADO EN CIENCIAS EN BIOTECNOLOGÍA EN RED

**“Diseño y evaluación biológica de péptidos inmunológicamente activos  
contra la Influenza A Humana H1N1”**

**(Design and biological evaluation of immunological active peptides  
against Human Influenza A H1N1)**

TESIS

QUE PARA OBTENER EL GRADO DE DOCTORADO EN  
CIENCIAS EN BIOTECNOLOGÍA EN RED

**PRESENTA:**

Carrillo Vázquez Jonathan Pablo

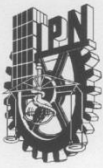
**DIRECTOR DE TESIS:**

Dr. Absalom Zamorano Carrillo

Dr. Marlon Rojas López



MÉXICO D.F. A 13 DE FEBRERO DEL 2015.



# INSTITUTO POLITÉCNICO NACIONAL SECRETARÍA DE INVESTIGACIÓN Y POSGRADO

## ACTA DE REVISIÓN DE TESIS

En la Ciudad de México siendo las 12:00 horas del día 13 del mes de Febrero del 2015 se reunieron los miembros de la Comisión Revisora de la Tesis, designada por el Colegio de Profesores de Estudios de Posgrado e Investigación de E.N.M.y H. para examinar la tesis titulada:  
Diseño y evaluación biológica de péptidos inmunológicamente activos contra la Influenza A Humana H1N1

Presentada por el alumno:

Carrillo	Vázquez	Jonathan Pablo							
Apellido paterno	Apellido materno	Nombre(s)							
		Con registro:							
		<table border="1"> <tr> <td>A</td> <td>1</td> <td>0</td> <td>0</td> <td>6</td> <td>6</td> <td>3</td> </tr> </table>	A	1	0	0	6	6	3
A	1	0	0	6	6	3			

aspirante de:

Doctorado en Ciencias en Biotecnología en Red

Después de intercambiar opiniones los miembros de la Comisión manifestaron **APROBAR LA TESIS**, en virtud de que satisface los requisitos señalados por las disposiciones reglamentarias vigentes.

### LA COMISIÓN REVISORA

Directores de tesis

\_\_\_\_\_  
Dr. Absalom Zamorano Carrillo

\_\_\_\_\_  
Dr. Marlon Rojas López

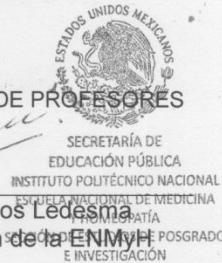
\_\_\_\_\_  
Dr. José Correa Basurto

\_\_\_\_\_  
Dr. Cesar A.S. Reyes López

\_\_\_\_\_  
Dra. Claudia G. Benítez Cardoza

PRESIDENTE DEL COLEGIO DE PROFESORES

\_\_\_\_\_  
M. en C. Manuel Landeros Ledesma  
Encargado de la Dirección de la ENMyH



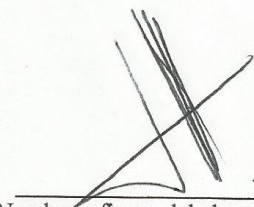


**INSTITUTO POLITÉCNICO NACIONAL**  
**SECRETARÍA DE INVESTIGACIÓN Y POSGRADO**

*CARTA CESIÓN DE DERECHOS*

En la Ciudad de México, D.F. el día 13 del mes de febrero del año 2015, el (la) que suscribe Jonathan Pablo Carrillo Vázquez alumno(a) del Programa de Doctorado en Biotecnología en Red, con número de registro A100663, adscrito(a) al Programa de Doctorado en Biotecnología en Red, manifiesto(a) que es el (la) autor(a) intelectual del presente trabajo de Tesis bajo la dirección del (de la, de los) Doctor Absalom Zamorano Carrillo y del Doctor Marlon Rojas López y cede los derechos del trabajo titulado “Diseño y evaluación biológica de péptidos inmunológicamente activos contra la Influenza A Humana H1N1”, al Instituto Politécnico Nacional para su difusión, con fines académicos y de investigación.

Los usuarios de la información no deben reproducir el contenido textual, gráficas o datos del trabajo sin el permiso expreso del (de la) autor(a) y/o director(es) del trabajo. Este puede ser obtenido escribiendo a las siguientes direcciones [cdln\\_jp@hotmail.com](mailto:cdln_jp@hotmail.com); [absalomz2002@gmail.com](mailto:absalomz2002@gmail.com); [marlonlrojas@gmail.com](mailto:marlonlrojas@gmail.com). Si el permiso se otorga, el usuario deberá dar el agradecimiento correspondiente y citar la fuente del mismo.

  
\_\_\_\_\_  
Nombre y firma del alumno(a)

Este trabajo fue realizado en la Escuela Nacional de Medicina y Homeopatía en el laboratorio de Investigación Bioquímica y Biofísica, en el laboratorio de Investigación de Inmunología Molecular de la Escuela Superior de Medicina y en el Centro de Investigación en Biotecnología Aplicada de Tlaxcala en el Laboratorio de Instrumentación Analítica y Biosensores, todos ellos pertenecientes al Instituto Politécnico Nacional. Jonathan Carrillo Vázquez fue becario del CONACYT (No. 211129), becario también del Programa Institucional de Formación de Investigadores (PIFI) de la COFFA- IPN. Este trabajo fue patrocinado por el la Secretaria de Posgrado e Investigación del IPN (Proyectos SIP: 20130466, 20121480, 20121516, 20130432, 20130447, 20140252); también fue patrocinado por el ICyTDF (Instituto de Ciencia y Tecnología del Distrito Federal (Proyecto: PIRIVE09-9), CYTED (Proyecto: 214RT0482) PIFI-EDI-COFAA/IPN and the CONACYT (Proyecto: 132352). Agradecemos especialmente a Teresita Rocío Cruz-Hernández, Jazmín García Machorro y mi amigo el M. en C. Arturo Contis Montes de Oca por su apoyo técnico en los experimentos inmunológicos. En los experimentos teóricos agradezco la colaboración especial de mis amigos la MD Paola Reyes Loyola y al Dr. Jorge Luis Rosas Trigueros. Finalmente agradezco a mi amigo Dr. José Luis Ordoñez Librado y a la técnico Patricia Aley Medina con las imágenes de MET y a la responsable del Laboratorio de Neuromorfología de la FES Iztacala la Dra. Rosa María Avila Costa.

## AGRADECIMIENTOS

A Dios, sin él no existe nada.

Al Doctor Absalom, por continuar con la aventura de dirigir esta nueva tesis

Al Doctor Marlon por apoyarme incondicionalmente y mostrarme una forma diferente de interpretar la naturaleza

Al Doctor José Correa, sin su apoyo nada hubiera sido posible. Gracias por adoptarme.

A la Doctora Violaine Moreau por apoyarme con las predicciones desde Francia.

Al Dr. Rafael Campos, por su apoyo en los ensayos inmunológicos en su laboratorio y el diseño del péptido.

A la Doctora Claudia por darme siempre sus comentarios que alientan a mejorar siempre (la presentación y la primer derivada son suyas)

Al Doctor Cesar por sus consejos y su apoyo en los aspectos inmunológicos y estructurales (las imágenes llevan sus enseñanzas)

A la Doctora Jazmín García Machorro por su apoyo en los ensayos de Neutralización.

Al Dr. José Luis Ordoñez por su apoyo con el MET y otras tantas cosas.

A mis amigos y compañeros, con quienes compartí el día a día y que algunos ya se fueron, en ENMH: Lili, Normandé, Brenda, César, Roberto Isaac, Roberto Carlos, Ian, Oscar. A Marisol y Hugo por su apoyo en el Lab. A los de la ESM: Arturo Contis y Paola. En la ESCOM a George RT.

## DEDICATORIA

A las personitas que amo y que dan razón a mi vida: Sofía y Valentina.

A ti mi amor, por darme vida de nuevo, te amo Gabriela.

## **ABSTRACT**

Influenza is a widespread disease produced by the influenza virus that generates more than 15% of the flu in the entire world. Since 2009 the health system in Mexico after the breakout of the H1N1 virus the INDRE document (April 2010) 72,462 cases and 1,185 deaths. This situation alerts the world population because the idea of a mortal pandemia would be a real threat. Two principal types of therapies lead the fight against this virus, antiviral drugs and vaccines. In the search of antifu vaccines many techniques were developed. Peptide design has become a powerful tool to create intelligent and rational vaccines. First using bioinformatical tools to predict immunological epitopes and second testing these peptides with programs that predict the accuracy of the binding of these peptides with the Major Histocompatibility Complex (MHC). It's necessary to test this peptide in animal assays to analyze the capability to produce and efficient immunological response. Finally we analyze serum of pandemic and prepandemic subjects' serums to quantify the indirect levels of recognition to our designed peptides. Its molecular analysis and identification contributes in our searching of new vaccine targets. Bioinformatical tools could make easier the searching and analysis vaccines. In this work we propose the rational design of antigenic peptides based on epitope prediction of the surface protein hemagglutinin of the influenza A H1N1 virus and the affinity of this peptide to the MHC II molecule. Also one of this peptide bioconjugation with gold nanoparticles is confirmed by UV spectroscopy and Transmission Electron Microscopy was performed. This approach might contribute to the design of a new therapeutically target.

## RESUMEN

La influenza es una enfermedad ampliamente distribuida a nivel mundial y es producida por el virus de la influenza, la cual genera más del 15% de las gripes a nivel mundial. En México desde el 2009 se reportaron después del brote más de 72,462 casos y 1,185 muertes, según un documento del INDRE (Abril 2010). Esta situación alertó a la población mundial por la posibilidad de una pandemia mortal. Dos tipos de terapias se usan principalmente contra este virus, los fármacos antivirales y las vacunas. En la búsqueda de una vacuna anti-influenza se han desarrollado diferentes técnicas entre las que se encuentran el diseño de péptidos inmunogénicos, convirtiéndose en una herramienta poderosa inteligente y racional para vacunas. Primero utilizando herramientas bioinformáticas para predecir epítomos inmunogénicos y segundo probando estos péptidos con programas que predigan la exactitud de la “unión” entre los péptidos y las moléculas del complejo mayor de histocompatibilidad (CMH). Es necesario probar estos péptidos en pruebas con animales para analizar la capacidad de estos péptidos de producir una respuesta inmunológica eficiente. Finalmente se analizaron sueros de voluntarios pandémicos y pre-pandémicos y cuantificamos el reconocimiento indirecto a nuestros péptidos. El análisis molecular y de identificación contribuirá en nuestra búsqueda de un nuevo blanco vacunal. Las herramientas bioinformáticas podrían mejorar la búsqueda y análisis de estas vacunas. En este trabajo nosotros proponemos un diseño racional de péptidos inmunogénicos basados en la predicción de epítomos de la proteína de superficie hemaglutinina del virus de la influenza A H1N1 y la afinidad del péptido al CMH tipo II. Además se realizó una bioconjugación de este péptido con nanopartículas de oro que se confirma por técnicas espectroscopia de luz visible y Microscopia Electrónica de Transmisión. Este avance podría contribuir al diseño de un nuevo blanco terapéutico.



## CONTENTS

ABSTRACT .....	vi
RESUMEN .....	vii
CONTENTS .....	viii
ABBREVIATIONS .....	xi
TABLE LIST .....	xii
FIGURE & GRAPHICS LIST.....	xii
<b>Chapter I. Introduction .....</b>	<b>1</b>
1.1. Influenza Virus.....	1
1.2. Epidemiology.....	1
1.2.1. Influenza Pandemics and Outbreaks .....	1
1.2.2. Recent epidemiology: Outbreak H1N1 2009.....	2
1.2.3. Morbidity and Mortality .....	3
1.3. Pathology .....	3
1.3.1. Transmission and incubation period.....	4
1.3.2. Cellular Infection.....	4
1.3.3. Immune response.....	5
1.4. Structure, evolution and genetics .....	6
1.4.1. Genome.....	6
1.4.2. Antigenic drift and antigenic shift: H1N1 .....	7
1.5. Influenza virus proteins .....	8
1.5.1. Hemagglutinin.....	9
1.5.2. Antigenic sites of HA .....	10
1.6. Immunoinformatics and vaccine design .....	11
1.6.1. Immunoinformatics .....	11
1.6.2. Vaccine design .....	11
1.6.3. HLA recognition and epitope prediction .....	12
1.6.4. Docking and antigens .....	13
1.6.5. Molecular Dynamics: Equilibrium and convergence .....	13
1.7. Bioconjugation.....	14

1.8. Justification .....	15
1.9. Objectives .....	16
1.9. Objectives .....	16
<b>Chapter II. Materials and methods .....</b>	<b>17</b>
2.1. Epitope prediction .....	17
2.2. Docking the epitope with the Major Histocompatibility Complex Class II .....	17
2.3. Molecular Dynamics Simulation.....	18
2.4. Contact Map.....	18
2.5. Peptide synthesis .....	18
2.6. Elisa Assays .....	18
2.7. Immunization of the rabbits .....	19
2.8. Cells and Influenza Viruses .....	19
2.9. ConA envELISA .....	19
2.10. Neutralization assay.....	19
2.11. Isotype response in serum from patients infected with pandemic influenza A H1N1 2009 .....	20
2.12. Statistical analysis .....	20
2.13. Synthesis of gold nanoparticles.....	20
2.14. Conjugation of peptide with gold nanoparticles .....	20
2.15. UV/VIS spectroscopy .....	21
2.16. Raman spectroscopy.....	21
2.17. Transmission electron microscopy .....	21
<b>Chapter III. Results .....</b>	<b>22</b>
3.1. Results <i>in silico</i> analysis.....	22
3.1.1. 3D model selection of the HA of the Human Influenza H1N1 .....	22
3.1.2. Prediction of the epitope .....	22
3.1.3. Docking and MD simulations of the peptide with the MHC Class II .....	24
3.2 Results of experimental strategy .....	26
3.2.1. Design of the peptides .....	26
3.2.2. Human IgG antibodies to the peptides .....	27
3.2.3. Isotype response in serum from patients infected with influenza A p/H1N1/2009 .....	28

3.2.4. Peptide 1 is immunogenic and induced antibodies to native form of HA .....	28
3.2.5. Neutralizing antibodies induced by Hemagglutinin peptides in rabbits.....	29
3.3. Conjugation of peptide .....	30
3.4. UV/VIS spectra of single and peptide-conjugated gold nanoparticles.....	31
3.5. SERS spectra of peptide conjugated to gold nanoparticles .....	31
<b>Chapter IV. Discussion .....</b>	<b>36</b>
<b>Chapter V. Conclusions .....</b>	<b>40</b>
<b>References.....</b>	<b>41</b>

## ABBREVIATIONS

HA	Hemagglutinin or Haemagglutinin
NA	Neuraminidase
Ig	Immunoglobulin
AB	Antibody or Antibodies
MHC	Major Histocompatibility Complex
HLA	Human Leukocyte Antigen
MS	Molecular Simulation
MD	Molecular Dynamics
kDa	Kilodalton
PDB	Protein Data Bank
nm	Nanometer
RMSD	Root mean square deviation
RMSF	Root mean square fluctuation
ELISA	Enzyme Linked Immunosorbent Assay
AuNp	Gold Nanoparticles
TEM	Transmission Electron Microscopy

## TABLE LIST

1. Influenza subtypes and characteristics .....	3
2. The influenza A virus proteins, length, number of conserved sequences and the total length of the conserved sequences of each protein .....	9
1. Influenza subtypes and characteristics .....	3

## FIGURE & GRAPHICS LIST

1. Influenza representation .....	6
2. Hemagglutinin antigenic sites: Sa, Sb, Ca and Cb.....	10
3. Antigenic sites of HA and scores obtained from computational epitope predictors.....	23
4. Pockets of the MHC and their interaction with the epitope .....	25
5. RMSD and RMSF parameters .....	26
6. Detection of the p1 and p2 peptides by the human IgG Ab .....	25
7. Levels of IgG against viral particle in serum of infected individuals or from rabbit immunized with peptide 1 .....	25
8. Plaque reduction neutralization test .....	30
9. UV/VIS spectra of gold nanoparticles (control) synthesized and used in this work .....	31
10. UV/VIS spectra of gold nanoparticles conjugated to the peptide at several concentrations .....	32
11. First derivative of UV/VIS spectra of gold nanoparticles conjugated to the peptide at several concentrations .....	33
12. SERS spectra of gold nanoparticles conjugated to the peptide at several concentrations..	34
13. TEM.....	35

## **Chapter I. Introduction.**

### 1.1. Influenza Virus.

Poison is the translation for the latin word “Virus”, but they are really parasites in the cells, using their own chemical energy and genetic material to reproduce (Smith 1962; Kupperberg 2008). Influenza was originated by a latin etymology in Italy during the fifteenth-century, where the cause of the disease was blamed to unfavorable astrological “influences”. In the last 300 years exists some reports about Influenza epidemics and pandemics, but it’s not until 1580 A.D. when reports from medical historians confirms outbreaks in Asia, Africa and Europe to finally in 1743 during the European Outbreak all the world know it as Influenza. In our days the medical definition for Influenza is: Acute contagious respiratory infection produce by Influenza Virus (Potter 2001; Kupperberg 2008).

### 1.2. Epidemiology.

Before the isolation of the virus, Influenza can only be identified by signs and symptoms and the explosive nature of outbreaks. Most of the doctors of the age thought that was caused by bacteria. The difference with other respiratory infections presents a problem, nevertheless the influenza presents without warning a sudden onset three-day fevers, muscle pain and prostration out of proportion with the severity of the symptoms. The surprising appearance of these symptom in a special time and region becomes outbreaks that can be identified in the historical record without difficulty; like a reference to influenza found in scientific publications since 1650. Historically the first report of an influenza epidemic occurred in 1173±4, but the first convincing report was by Molineux in 1694. Normally epidemics occur in winter months when cold, crowding of people and higher humidities are common but in recent times epidemics are arising in Eastern and Southern Hemisphere countries to spread later to Europe and North America (Potter 2001; Kupperberg 2008).

#### *1.2.1. Influenza Pandemics and Outbreaks.*

Influenza pandemics differs from epidemics cause this occur when a new influenza virus subtype arise and is not related to preexisting influenza viruses (arisen from those viruses by mutations) circulating immediately before the outbreak and there is little or no existing immunity. Second, emerges in a specific area and efficiently infects worldwide (Potter 2001; Garten et al. 2009). To prevent Influenza pandemics the WHO create in 1952 the Global Influenza Surveillance Network composed of four WHO Collaborating Centers and 112 institutions in 83 countries. The importance of preventing these outbreaks becomes with the history. The most important background was the infamous Spanish Flu (1918-1920) at the end of the World War I this is interesting because some reviewers localize the origin in China; others in

North America where the virus were ship to Europe, nevertheless all authors agree that the infection spread with the British Expeditionary Force and reach Italy and Spain in April 1918. This pandemic caused approximately 50 million deaths worldwide. Some medical historians called as 'the greatest medical holocaust in history'. This pandemic ranks only with the "Plague of Justinian" and the "Black Death". When the pandemic achieves the peak, deaths in the hospital exceeded 25% per night. It is estimated that the pandemic infect 50% of the world's population, 25% suffered a clinical infection. In Mexico was reported that ten percent of the entire population of the Mexican state of Chiapas died during the outbreak of the Spanish flu (Potter 2001; Kupperberg 2008; Taubenberger et al. 2006). An interesting note is that people over 60 years old in 1918 had minor risk to be infected with 1918 influenza, simply because of immunity acquired from a previous epidemic originating in 1840 (Brownlee et al. 2001).

In recent times using molecular tools three RNA fragments (HA, NA and NS1) have been recovered from formalin-preserved lung tissues from victims who died of influenza in 1918. The antibody study of sera indicates that the 1918 pandemic was caused by influenza A (H1). Sequence and phylogenetic analysis of the completed 1918 influenza virus genes and a 1918 HA protein crystal structure resolved shows to be the most avian-like among the mammalian adapted viruses, nevertheless, other researchers put the 1918 influenza close related to the virus found in pigs (Potter 2001; Kupperberg 2008; Taubenberger 2006(2); Brownlee et al. 2001).

### *1.2.2. Recent epidemiology: Outbreak H1N1 2009.*

In April 21 2009, the Centers for Disease Control and Prevention (CDC) confirmed 2 cases identified by the Department of Defense of a febrile respiratory illness in children from southern California caused by infection with a novel influenza A (H1N1) virus. Several days later, the CDC reported that H1N1 viruses of the same strain had been confirmed among samples from patients in Mexico, where there was a cluster of 47 cases of rapidly progressive severe pneumonia that resulted in 12 known deaths. For May 18 of 2009, there have been 8829 laboratory confirmed cases in 40 countries, resulting in 74 deaths. Finally on June 11th of 2009, WHO declared a global pandemic of 2009 H1N1 infection. WHO classified this alert as level 5 of 6. A striking data was when the sequence identification was completed and it was reported like an H1N1 subtype, this became an emergency because is world known that H1N1 influenza virus caused the deadly "Spanish Flu". Sequence analysis of the U.S. and Mexico shows clearly a H1N1 subtype (Taubenberger 1997; Smith et al. 2009; Garten et al. 2009; Sullivan et al. 2009; Igarashi et al. 2010).

The 2009 H1N1 resulted from genetic reassortment between the recently circulating swine H1 viruses in North America and the avian-like swine viruses in Europe. Phylogenetic analysis showed that the HA gene of 2009 H1N1 was derived from the so-called "classical swine H1N1" virus, which likely shares a common ancestor with the recent human H1N1 virus (Igarashi et al. 2010; Smith et al. 2009).

### 1.2.3. Morbidity and Mortality.

Every year 500 million people get sick of influenza A worldwide, of them 3 or 5 million become grave cases that produce 250 to 500 thousand deaths. For the pandemic (H1N1) 2009 influenza A virus (pH1N1) is reported more than 19,000 deaths worldwide since it appeared in April 2009. The health secretary in Mexico reported until July 2009. The number of confirmed cases was 72,538 with 1,326 deaths. On August 10th of 2010, WHO has announced that the world is no longer in phase 6 of influenza pandemic alert and we are now moving into the post pandemic period. Because of resource limitations, both the CDC and WHO stopped reporting confirmed and probable cases of 2009 H1N1 on July 24, 2009 (Arias et al. 2009; Sanjay et al. 2009; Sullivan et al. 2010).

### 1.3. Pathology.

The World Health Organization (WHO) published the guidelines for the nomenclature of influenza viruses as follows: the type of virus is designated (A, B, or C), the host (if non-human), place of isolation or geographical origin, strain or isolation number and year of isolation (separated by slashes). Specifically for influenza A, exists 16 hemagglutinins (HA), so there are H1 to H16 and nine neuraminidases (NA) so N1 to N9 subtypes. Nevertheless the WHO classification Influenza virus family contains five genera, classified by variations in nucleoprotein (NP and M) antigens: Influenza A, Influenza B, Influenza C, Thogotovirus, and Isavirus, in table 1 other features were shown (Taubenberger (2) 2008; Sullivan et al. 2009; Goh et al. 2009).

	INFLUENZA A	INFLUENZA B	INFLUENZA C
HOST	MAMMALS & BIRDS	HUMAN & SEALS	HUMAN & PIGS & DOGS
SEQUENCE VARIABILITY	+++	+	+
VIRULENCE AND PATHOGENICITY	+++	++	+
SURFACE PROTEINS	HA, NA, M1 & M2	HA, NA, M1 & M2	HEF
RNA	8 SEGMENTS	8 SEGMENTS	7 SEGMENTS

Table 1. Influenza subtypes and characteristics

Influenza A viruses infect a wide variety of warm-blooded animals, including birds, swine, horses, humans, and other mammals, this explain the origin of virulence of influenza A type is



the most dangerous strain. For example an avian influenza virus serves as the natural reservoir for all known subtypes of influenza A virus and are the most important source of human pandemic influenza strains. Type B and C influenza viruses are isolated almost exclusively from humans, although influenza B viruses have been isolated from seals and influenza C viruses have been isolated from pigs and dogs, Influenza C have seven gene segments and only one surface glycoprotein, the HEF protein, that made HA and NA functions. In general, influenza C virus causes less severe respiratory illness, which rarely progresses to the lower respiratory tract (Steinhauer et al. 2002; Taubenberger 2008).

Influenza afflicts school-age children and elderly population, in this etary group afflicts especially those with chronic pulmonary or cardiac disease and diabetes mellitus. These two groups develop severe complications which include hemorrhagic bronchitis, pneumonia (primary viral or secondary bacterial), weakness and fatigue may linger for weeks till the death of the patient. Influenza is characterized by acute symptoms and fever often persist for 7 to 10 days, chills, headaches, myalgia, prostration and sometimes coryza, cough and sore throat (Taubenberger 2008; Kupperberg 2008). The pathogenesis and transmission of the pandemic H1N1 in humans is not completely known and many studies are underway some of these reports mentioned it is due in part by replication efficiency in human cells, which is the net effect of complex virus-host interactions (Steinhauer et al. 2002; Sanjay et al. 2002).

### *1.3.1. Transmission and incubation period.*

Usually the transmission is via fine particles the virus enters the body through nose or mouth, requiring close contact (<1.83 m) to infect the respiratory tract cells through sialic acid surface receptors on the cells. Evidence suggests that 2009 H1N1 is transmitted via large particle droplets that remain suspended in the air for a short time. Indirect transmission became a threat through fomites (body fluids) and contaminated surfaces. The incubation period for the 2009 H1N1 virus has been estimated to be between 1 and 7 days, similar to that of seasonal influenza. Recent data have suggested that up to 80% of patients are still shedding virus at 5 days, 40% at 7 days, and 10% at 10 days. Children and younger adults may shed as long as 10 or more days and immunosuppressed persons may shed virus for weeks (Arias et al. 2009; Sullivan et al. 2009).

### *1.3.2. Cellular Infection.*

The influenza virus life cycle can be divided into the following stages: entry into the host cell; entry of virus RNP (vRNP) into the nucleus; transcription and replication of the viral genome; export of the vRNPs from the nucleus; and assembly and budding at the host cell plasma membrane. To enter the cell, Influenza virus binds to the sialic acid receptor on target cell, via the receptor binding domain on the HA. After binding to the host cell, the virus is incorporated into the cell by receptor-mediated endocytosis. Within the endosome, the HA undergo acid-induced conformational change so that the HA promotes fusion of the viral membrane with the endosomal membrane. Finally, the envelope fusion is a critical process for

infection provoking the penetration of the virus genome into the cytoplasm, followed by transportation to the nucleus to initiate genome transcription and replication (Taubenberger 2006; Saito et al. 2000; Samji et al. 2009).

### *1.3.3. Immune response.*

Palese et al. propose that the future efforts should be undertaken to better understand viral pathogenicity and human immunology in response to infection. Nevertheless it is believed that one of the major reasons for the inability of the global population to have effective neutralizing antibodies against influenza virus A is the predisposition of the viral genomes for the genetic reassortment. Humans normally generate polyvalent antibody responses to a given antigen, based on the analysis of post-infection human sera indicates that antibody responses are composed of a limited antibody repertoire. Due to the limited number of changes in the viral glycoproteins the virus is capable to evade the immune response generated by any particular individual to a previously circulating virus (Steinhauer et al. 2002; Palese et al. 2004; Goh et al. 2009).

Goh and coworkers propose that the high mobility of the exposed region of the HA trimer accounts for the evasion of the initial immune response. This highly dynamic nature of the potentially immunogenic region weakens the binding of antibodies and other immune response-related molecules to the HA molecule. Nevertheless exists other mechanisms to evade, like the antigenic shift and drift to evade existing human immunity, this produced a continually evolving variants of influenza viruses that results in enhanced virus propagation or survival by adaptation to the host cell immune response. All these features add information to identify and characterized the binding site of neutralizing antibodies (Steinhauer et al. 2002; Heiny et al. 2007; Goh et al. 2009).

Heiny and coworkers explains that the initial response of naive CD8+ T-cells to antigen requires only a brief stimulation with antigen early in the immune response, this initial activation can occur in the absence of T-cell help, but without the CD4+ response. The data of several studies indicate that generation of long term CD8+ T-cell immune memory requires the concurrent function of professional antigen presenting cells for class II antigen processing and presentation to CD4 + helper T-cells during the initial antigen priming period. Also Heiny and coworkers mentioned that it is likely that the major sources of T-cell epitopes, both class I and II, early after influenza infection are those proteins delivered to the immune system by the virus, including the highly variable structural proteins, HA and NA. Thus, this initial response, and the memory T-cells elicited by this response, may lack the highly conserved epitope sequences of the non-structural proteins that would be synthesized at a later stage of infection and, as cytoplasmic proteins. In this context, it is noteworthy that 29 of the reported influenza T-cell epitopes are found in conserved sequences and there was only a single class II epitope, suggesting that following natural infection, the conserved sequences elicit primarily cytotoxic T-cell responses (Heiny et al. 2007).

#### 1.4. Structure, evolution and genetics.

Influenza A belongs to *Orthomyxoviridae* virus family that is characterized by an envelope with a genome made up of negative sense, single-stranded, segmented RNA. Influenza A viruses have eight segments that encode for the 11 viral genes: hemagglutinin (HA), neuraminidase (NA), matrix 1 (M1), matrix 2 (M2), nucleoprotein (NP), non-structural protein 1 (NSP1), non-structural protein 2 (NS2; also known as nuclear export protein, NEP), polymerase acidic protein (PA), polymerase basic protein 1 (PB1), polymerase basic protein 2 (PB2) and polymerase basic protein 1 – F2 (PB1-F2) (Steinhauer et al. 2002; Goh et al. 2009; Samji et al. 2009).

According virus strain and history, the influenza A virions (i.e. a complete virus particle with its RNA core and protein coat) can exhibit different shapes and sizes, the most abundant are spherical particles of approximately 100 nm in diameter to the most strange forms like the elongated filamentous forms. The viral envelope is a lipid bilayer derived from the human host cell membrane that contains three of the viral transmembrane proteins: HA, NA, and M2. HA is the most abundant envelope protein with 80 percent, followed by NA, with 17 percent of the viral envelope proteins. They are distributed evenly over the virion surface, forming characteristic spike-shaped structures (Figure 1) (Steinhauer et al. 2002; Samji et al. 2002; Goh et al. 2009).

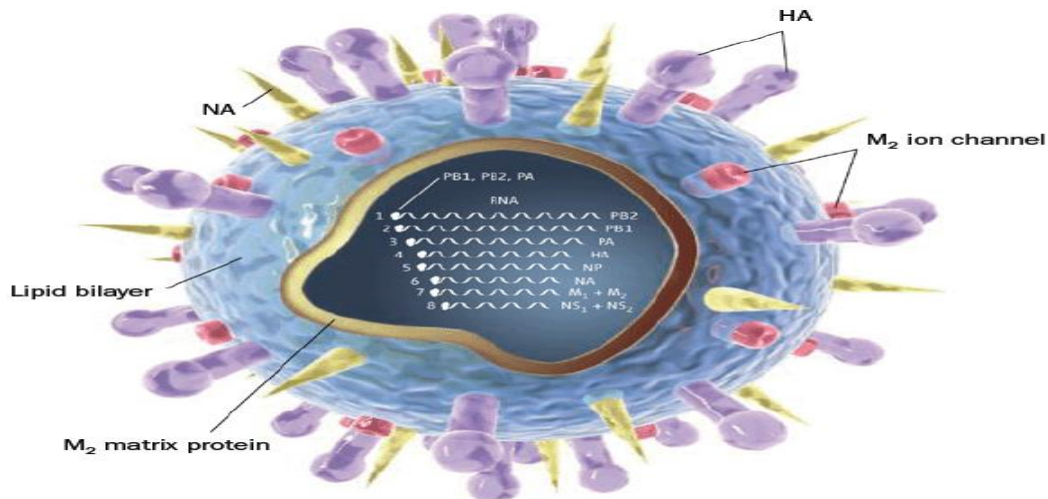


Figure 1. Influenza representation (Kaiser 2006, Science)

##### 1.4.1. Genome

Almost all cases of influenza A worldwide (excepting human infections from avian virus such as H5N1 and H7N7) have been caused by descendants of the 1918 virus including “drifted” H1N1 viruses and reassorted H2N2 and H3N2 viruses. Nevertheless, the genomes of the last three pandemic influenza viruses (1918 H1N1, 1957 H2N2, and 1968 H3N2) all originated in

whole or in part from nonhuman reservoirs, and the HA genes of all of the pandemic viruses ultimately originated from avian influenza viruses. Supporting these asseverations, the sequence and phylogenetic analyses suggest that the genes encoding the HA and NA surface proteins of the 1918 virus were derived from an avian-like influenza virus shortly before the start of the pandemic and that the precursor virus had not circulates widely in humans of swine in the few decades before (Brownlee et al. 2001; Taubenberger 2006; Garten et al. 2009).

Analysis of influenza virus genomes during the emergence of pandemic 2009 H1N1 virus provides a unique opportunity to track the transmission dynamics of a new influenza virus in an immunologically naïve population. To understand the influenza genome evolution we have to describe the influenza A viral genome. The viral genome consists of the eight segments of ribonucleic acid single chain of different sizes, ranging from 890 nucleotides to 2,350 nucleotides. In total, the genome is 13,000,588 nucleotides. All segments have their 5 and 3 untranslated regions that are conserved among the viral segment and containing binding signals for RNA polymerase of the virus and the signals required for encapsidation (packaging) viral genome (Palese et al. 2004; Arias et al. 2009; Goh et al. 2009; Baillie et al. 2011).

#### *1.4.2. Antigenic drift and antigenic shift: H1N1.*

The numerous observations of high-frequency recombination by influenza viruses and the studies on influenza virus defective interfering particles, permit to propose that the influenza genome was composed of RNA fragments. These studies postulate that influenza virus have two kinds of recombination, the first claims is that the influenza genome was composed of RNA fragments of high-frequency recombination by influenza viruses compared with other RNA viruses (Poliovirus and Newcastle disease virus). The second postulate is that influenza virus have a special recombination, in which individual gene segments or combinations of segments are exchanged during mixed infections, is referred to as reassortment, and the viruses that result from such genetic exchanges are termed reassortant viruses (Steinhauer et al. 2002).

In order to understand this postulates we have to explain briefly what is a Drift and a Shift. Drift refers to frequent, minor changes on the HA and/or NA antigens. Antigenic drifts in the HA subtype are associated with seasonal epidemics and often reduce the effectiveness of the previous seasonal vaccines. Annual epidemics are due to antigenic drift (Potter 2001; Steinhauer et al. 2002; Sullivan et al. 2010).

Different phenomenon is antigenic shift. *Shift* refers to the introduction of influenza A virus subtype to which the population has no preexisting immunity. Shifts are widely assumed to be facilitated by the virus's segmented genome and the genetic diversity it achieves by infecting a varied reservoir of animals. Antigenic shifts in HA subtypes are associated with pandemics, 3 of which occurred in the past century and occurring at 10 to 50 years intervals are due to new virus subtypes resulting from virus reassortment (Potter et al. 2001; Steinhauer et al. 2002; Sullivan et al. 2010).

According to Sullivan and coworkers the 2009 H1N1 virus does not fit the classic definition of a new subtype for which most of the population has no previous infection experience. Since

1977, H1N1 viruses have been in continuous circulation, and most persons born before 1956 have previous infection experience with H1N1. The 2009 H1N1 virus also does not fit the classic definition of drift because it has no direct evolutionary relationship with recently circulating H1N1 viruses of human origin (Sullivan et al. 2010).

Influenza viruses accumulate point mutations during replication because their RNA polymerase complex has no proofreading activity. Their genes have high mutation rates (ranging from approximately  $1 \times 10^{-3}$  to  $8 \times 10^{-3}$  substitutions per site per year). Mutations that change amino acids in the antigenic portions of surface glycoproteins may produce selective advantages for viral strains by allowing them to evade preexisting immunity (Potter et al. 2001; Taubenberger 2008).

### 1.5. Influenza virus proteins.

The eight strands of negative-sense RNA encodes eleven viral proteins mentioned before PB1, PB2, PA, HA, NP, NA, M1, M2 and NEP. Four of these viral proteins are localized in the surface of the viral particle: HA, NA, M1 and M2. These proteins are indispensable for the virus particle formation that occurs at the membrane of infected cells, where budding occurs from regions of the membrane at which the viral glycoproteins HA and NA have accumulated. Heiny and coworkers demonstrate that HA and NA have extreme sequence diversity, illustrative of the reassortment of the genome segments among the many subtypes of the avian group A viruses. Also, these sequences present a rapid rate of point at virtually every position except at a single region in HA that has remained remarkably conserved despite the extreme sequence modification of every other nonamer of the protein. The viral matrix protein (M1) is the most abundant component of the virion and is thought to play a pivotal role in the process of assembly and budding, nevertheless the details on the mechanism of assembly are still in analysis. It is assumed that M1 interacts with the RNPs and the cytoplasmic domains of HA, NA, and possibly the third integral membrane protein M2. The two other viral proteins, NS1 and NS2, were initially designated as nonstructural proteins, but there is now evidence for the presence of NS2 in virions (Steinhauer et al. 2002; Heiny et al. 2002; Shaw et al. 2008; Goh et al. 20009).

Heiny and coworkers reported a total of 55 peptide sequences, ranging from 9 to 58 amino acids in length, and containing a total of 965 amino acids, 21% of the total proteome, were completely conserved in 80% to 100% of the human and avian type A viruses recorded in the past decade. Twenty-six sequences were present in 90% to 100% of the viruses. The majority of the conserved sequences were in the nonstructural (NS) proteins. PB2 was the most conserved with 23 sequences, comprising 50% of the protein, conserved in 80% to 100% of the documented viruses (Table 2) PB1 was also highly conserved (11 sequences, 36%) and the PA, NP, and M1 proteins contained significant fractions (16% to 27%) of conserved sequences. HA contained one sequence, FGAIAGFIE (AA388-396), that was conserved in all type A viruses despite the extreme variability of all other HA amino acids. There were no sequences in the PB1-F2, NA, M2, NS1 or NS2 proteins that were completely conserved in at least 80% of the viruses. The H1N1, H3N2, and H1N2 viruses circulating in humans had the highest representation of

conserved sequences, with almost all of the 55 sequences present in 95% to 100% of the isolates of each virus (Heiny et al. 2007).

Protein	Length (aa) <sup>a</sup>	Number of highly conserved sequences <sup>b</sup>	Total length of conserved sequences (aa) <sup>c</sup>
PB2	759	23	379 (50%)
PB1	757	11	271 (36%)
PB1-F2	90	0	0
PA	716	7	111 (16%)
HA	568	1	9 (2%)
NP	498	9	126 (25%)
NA	469	0	0
M1	252	4	69 (27%)
M2	97	0	0
NS1	230	0	0
NS2	121	0	0
Total	4,557	55	965 (21%) <sup>d</sup>

Table 2. The influenza A virus proteins, length, number of conserved sequences and the total length of the conserved sequences of each protein. (Heiny 2007 - PlosOne)

### 1.5.1. Hemagglutinin.

Principally immunity to influenza comes from the HA antigenic sites, but when a new virus strain appears, acquired immunity confers no protections against the new subtype due to evolution or mutation in these antigenic sites in the hemagglutinin. The antigenic properties were studied by antibody characterization, these specific antibodies against the HA protein prevent receptor binding and are effective at preventing re-infection with the same strain. The HA can evade previously acquired immunity by either antigenic drift or antigenic shift, appearing or reappearing in a frequency of 15 to 30 years (Brownlee et al. 2001; Potter et al. 2002; Taubenberger 2008).

HA is synthesized as a precursor named HA0 polypeptide that must be cleaved into the disulfide linked subunits HA1 that contains receptor binding domain and HA2 which contains the fusion peptide in order to activate membrane fusion function by binding the sialic acid receptors (Samji et al. 2001; Steinhauer et al. 2002; Goh et al. 2009).

HA is a homotrimeric type I transmembrane surface glycoprotein and is the most abundant antigen on the viral surface and harbors the primary neutralizing epitopes for antibodies. This trimer has a tightly intertwined "stem" domain at its membrane-proximal base, which is composed of HA1 residues 11 to 51 and 276 to 329, and HA2 residues 1 to 176. The dominant feature of this stalk region in the HA trimer is the three long, parallel  $\alpha$ -helices (~50 amino acids in length each), one from each monomer, that associate to form a triple-stranded coiled coil. The membrane distal domain consists of a globular "head", which is formed by HA1 and which can be further subdivided into the R region (residues 108–261), containing the receptor binding site

and major epitopes for neutralizing antibodies, and the E region (residues 56–108 and 262–274). The HA2 chain contains two membrane-interacting hydrophobic peptide sequences: an N-terminal "fusion peptide" (residues 1–23), which interacts with the target membrane bilayer, and a C-terminal transmembrane segment that passes through the viral membrane (Goh et al. 2009).

### 1.5.2. Antigenic sites of HA.

Four main antigenic sites were identified near the top of the globular head of the haemagglutinin. Despite this common feature there were differences in the exact positions of two of the four antigenic sites because of the presence of N-linked carbohydrate, which masked potential antigenic sites. The four sites are the common and the specific; these are Sa, Sb, Ca and Cb (Fig 2). As a result, these sites consist of the most variable amino acids in the HA molecule of the seasonal human H1N1 viruses that have been subjected to antibody-mediated immune pressure since its emergence in 1918 (Brownlee et al. 2001; Xu et al. 2010; Igarashi et al. 2010; Huang et al. 2013).

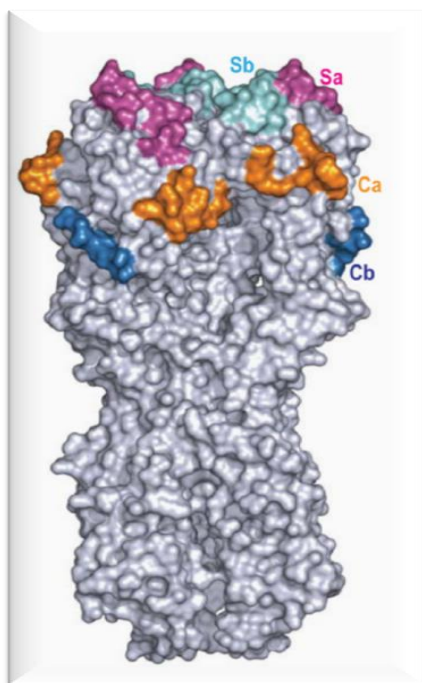


Fig. 2. Hemagglutinin antigenic sites: Sa, Sb, Ca and Cb.

The locations of the antigenic regions identified in studies on neutralizing anti-HA monoclonal antibodies are representative of the distribution on the structure of the sites that evolve during antigenic drift. The observation that these sites are proximal to the relatively conserved receptor binding pocket of HA, in conjunction with the structural data on HA antibody complexes indicates that interference with virus attachment to host cells may constitute the principal mechanism for antibody-mediated virus neutralization (Steinhauer et al. 2002).

Antigenically, the 2009 A(H1N1) viruses are homogeneous, and among historical viruses, are antigenically most similar to classical swine A(H1N1) viruses, as well as to North American lineage triple reassortant A(H1N1) viruses that have circulated in swine over the past 10 years in the United States and that have occasionally infected humans during the same period. There have been only a few amino acid substitutions in the HA among the 2009 H1N1 viruses analyzed. Since antigenic changes occur more slowly in swine than in the human population (Garten et al. 2009; Igarashi et al 2010).

Igarashi and coworkers constructed 3D structures of the representative strains of seasonal H1 viruses that had been isolated since 1934, and tracked the amino acid substitutions on their HA molecules. They confirmed that amino acid substitutions associated with the antigenic changes gradually accumulated on the globular head region of HA and were distributed over four distinct antigenic sites. It is well-documented that antigenic changes of HA occasionally result in the acquisition of carbohydrate side chains on the HA molecule. Since the carbohydrate side chains in the vicinity of antigenic sites mask the neutralizing epitopes on the HA surface, amino acid substitutions associated with acquisition of carbohydrate chains are believed to efficiently generate antigenic variants (Igarashi et al. 2010).

The fact that a pandemic resulted illustrates the concept that neutralizing antibody responses targeting the HA provide the key component for protection against influenza, although residual immunity to the NA may have reduced the severity of disease resulting from the 1968 viruses for example (Steinhauer et al. 2002). Igarashi and coworkers suggests too that antibodies elicited by natural infection with the 1918 pandemic or its early descendant viruses play a role in specific immunity against 2009 H1N1, and provides an insight into future likely antigenic changes in the evolutionary process of 2009 H1N1 in the human population (Igarashi et al. 2010).

## 1.6. Immunoinformatics and vaccine design.

### *1.6.1. Immunoinformatics.*

Immunoinformatics uses bioinformatic tools to perform analysis and obtain predictions of immunology research. Some of these approaches are epitope prediction, epitope analysis sequence and HLA recognition. Many reports described a strategic advantage in the use of computational analysis and conserved sequences for vaccine design (Diaz et al 2009; Prabdial et al. 2012; Lohia et al. 2014).

### *1.6.2. Vaccine design.*

The ideal way to reduce the impact of an emerging pandemic is vaccination (Palese et al. 2004; Sullivan et al 2009). A critical aspect of vaccine development is a demonstration that immunization is capable of inducing a protective immune response in an epidemic season or in the case of a global influenza pandemic due to emergence of a novel subtype of influenza (Wood et al. 2001; Saito et al. 2001; West et al. 2013).



The rapid mutation of the viral HA facilitates the selective replication of new virus strains and is a serious obstacle to the effectiveness of these vaccines (Heiny et al 2007). The fact that production of the current vaccine depends solely on chicken eggs will be a limiting factor for the vaccine supply. Based on data from vaccine production will be necessary increase production capacity at least 30-fold in case of a pandemic according to Saito and coworkers (Saito et al 2000).

The study of highly conserved sequences of both human and avian influenza proteomes becomes the first step in the selection of sequences for the synthesis of a super-type, epitope-based genetic vaccine. An important suggestion is the intelligent selection of the length of peptides that are bound by HLA molecules for presentation to T-cell receptors, typically from 8–20 amino acids, with nine amino acids being the predominant length of class I peptides and the core of class II peptides (Heiny et al. 2007). Some results demonstrate that structure/ function relationships between MHC class II binding and T cell activation may be a useful tool for design of subunit vaccines (Gogolak et al. 2000).

The design of the immunogen has to be compatible with the requirements for appropriate immune processing and presentation of the protein, and the epitopes have sufficient HLA-representation to cover the global distribution of HLA genotypes. It appears that these requirements can be satisfied given the large number of predicted super-type MHC binding sequences in the conserved regions of the influenza proteins (Heiny et al. 2007).

### *1.6.3. HLA recognition and epitope prediction.*

Cell-mediated immunity is based upon the binding of short sequences of antigen proteins, termed T-cell epitopes, to specialized cellular proteins, known as human leukocyte antigens (HLAs), class I (HLA I) and class II (HLA II) they are also known as Major Histocompatibility Complex I and II (MHC I –MHC –II). Of particular relevance for vaccine design are super-type groupings of similar HLA alleles that display overlapping peptide-binding capacities. The super-types cover a large fraction of the HLA diversity in the human population and antigen epitopes that bind to the super-types are considered prime candidates for vaccine formulations (Heiny et al. 2007). It is important to identify potentially active peptides of minimal size that would fit into a given MHC class II allele (Gogolak et al. 2000). An example of in silico prediction were performed by Heiny and coworkers, they use four computational software: NetCTL MULTIPRED, ARB, and TEPITOPE. They found over 500 HLA class I and over 100 class II HLA binding sequences of super-type alleles and many of the nonamer sequences binds multiple (2 to 9) individual class I alleles. Similarly, all of the DR binding predictions were selected as super-types on the basis of predicted binding to multiple DR-alleles (Heiny et al. 2007).

Two kind of epitope predictor arise in the last few years, the sequence predictors, which use the information of different databases with experimental information and structural predictors that analyses protein structure providing structural basis to discover antigenic sites of 2009

pandemic Influenza H1N1 (Veljkovic et al. 2009; Igarashi et al. 2010). Advantages and disadvantages are widely reported for both kinds of predictors. Initially the sequence predictors were the best because has enough evidence brought to the experimental data and combined with some HLA alleles determinants (Gowthaman et al. 2008; Mallios et al. 2003; Diaz et al. 2009).

Evidence show that peptide vaccines can offer a strong therapeutic weapon against Influenza because of the advantages (Rosendahl et al. 2014; Sette et al. 2003; Obeid et al. 1995; Schubert et al. 2013; Dormitzer et al. 2008). One of these advantages were supported in structural benefits founded in the antigenic sites exposed on the surface of the viral particles like the HA (Apostolopoulos et al. 2002; Correia et al. 2010). Other advantages come from the specificity that can come with the structural analysis and confirmation by in experimental analysis (Amicosante et al. 2002). Using these advantage with conserved sequences (De Groot et al. 2014; Huang et al. 2013) can we design a peptide that function like a good immunogen (Ben-Yedidia et al. 1997) and finally we can achieve a universal T-Cell vaccine (Liao et al. 2013) that could be a obtained by rational design (Walker et al. 2010).

#### *1.6.4. Docking and antigens.*

New validation technology is needed to obtain results in vaccine design, the bioinformatic arise like a good option to analyze the immunological interaction between the molecules and accelerate the identification of new targets (Moise et al. 2009; Camacho et al. 2005). The highest goal with docking programs is achieved the best interaction between HLA molecules and proposed peptides to understand how does the HLA recognition groove interacts with the peptides or antigens (Ballester et al. 2014; Ghersi et al. 2009). This will be performed with blind docking programs and restricted docking program (Comeau et al. 2005; Hetényi et al. 2002; Rocklin et al. 2013).

#### *1.6.5. Molecular Dynamics: Equilibrium and convergence.*

Finding the binding sites are not enough to understand the theoretical models, refinement is needed (Vorobjev et al. 2010), a refinement of the epitope-HLA II complex model can be necessary (Alonso et al. 2006; Platania et al. 2012). Is suggested by some authors that the refinement is reached with the equilibration and convergence of the model with short and long time simulation depending on the molecules (Brünger et al. 1987; Vorobjev et al. 2010; Raval et al. 2012; Kim et al. 2011). Molecular dynamics permits to establish the behavior of the complex using RMSD calculus to demonstrate the stability after the equilibration period (Sohn et al. 2005; Maganti et al. 2014; Takemura et al. 2012).

### 1.7. Bioconjugation.

Among the biological applications of the colloidal gold nanoparticles it has been reported their ability to work as affinity labels in the diagnostic field and as probes in light and electron microscopy (Horisberger 1992; Sonvico et al. 2005; Jennings et al. 2007). Noble metal nanoparticles exhibit unique optical properties due to their surface plasmon resonance (SPR). The SPR absorption band of silver and gold nanoparticles is strongly dependent on their size, shape and aggregation (Slocik et al. 2005). Nanoparticles are similar in size to common biomolecules like proteins and genes, have strong absorbing and scattering properties and are easy to prepare (Adegboyega et al., 2007; Kogan et al. 2007). Their surface can be enhanced for aqueous solubility, biocompatibility, and biorecognition, which permits the interaction between metals and biomolecules (De la Fuente et al. 2005). Specifically, gold nanoparticles are synthesized in water and subsequently linked to biomolecules that have been used in drug-delivery, gene transfer, bioprobes (immunocytochemical probes) in tissue analysis, and studies of biological processes at the nanoscale (McLean et al. 2004; Chen et al. 2008; Oh et al. 2011).

Peptides are involved in molecular recognition of antibodies, which is relevant in the field of clinical diagnosis of infectious diseases and in the design of new drugs and vaccines (Raman et al. 2006). Peptides can be attached (conjugated) to a single nanoparticle making individual targeting signals more accessible to cell receptors or allowing them to participate in ligand-receptor interactions (Brewer et al. 2005). Specifically conjugation of gold nanoparticles with peptides and proteins not only affords stabilization of the system, also introduces biocompatible functionalities into these nanoparticles for further biological interactions. Although gold is an inert metal, its effect on normal cell proliferation cannot be underestimated because metallic nanoparticles used in therapy and diagnosis must be nontoxic, biocompatible and stable in biological media (Tkachenko et al. 2003; Wangoo et al. 2008). Immunoinformatics allow the selection of possible epitopes (peptides) than can be used for conjugation; many successful examples of immunological molecules exist and can be used to improve the immunological response or used as biosensors.

Conjugated gold nanoparticles, are obtained from the negative charge on the gold colloids, (synthesized by citrate reduction) having an affinity for peptides and proteins that are positively charged at neutral or physiological pH and some evidence support that capping nanoparticles with peptides increases stability and biocompatibility (Norde 1986; Hayat 1989; Hermanson 2008). Proteins, in particular antibodies, can adsorb strongly to colloidal gold to form stable conjugates, in this case the peptide can adsorb strongly to colloidal gold to form a stable conjugate retaining its biological property (El-Sayed et al. 2005).

## 1.8. JUSTIFICATION

- Influenza is a worldwide health problem. Influenza virus can cause a mortal pandemic due to its genetics and animal reservoirs.
- It is necessary to propose and design novel vaccine methodologies against Influenza virus.
- Peptides might be an alternative capable of generating an immunologic response. In this task bioinformatics offers the best economic and biological cost.

## 1.9. OBJECTIVES

### *GENERAL.*

To design and evaluate immunogenic peptides of the Human Influenza A H1N1 Hemagglutinin.

### *SPECIFIC.*

1. To predict and to analyze the possible epitopes of the Influenza A H1N1 by bioinformatic tools.
2. To design antigenic peptide computationally.
3. To test the immunogenicity of the peptide experimentally.
4. To analyze the conjugation of the peptide with gold nanoparticles.

## **Chapter II. Materials and methods.**

### 2.1. Epitope prediction.

The crystal structure used for this study was the HA reported by XU and coworkers (PDB code: 3LZG) (Xu et al. 2010). All predictions were performed with the sequence and structure of 3LZG. Six programs of epitope prediction were used, four sequential predictors and two structural predictors. To obtain MHC II epitope predictions, PROPED2 was utilized (<http://www.imtech.res.in/raghava/propred/>); its predictions are based on locating the promiscuous regions that can bind HLA-DR alleles (Singh et al. 2001), including the 47 HLA-DRB1s, which are the most representative. The MHC2PRED program (<http://www.imtech.res.in/raghava/mhc2pred/info.html>) was also used to obtain MHC II epitope predictions. Each peptide is represented by a 20-dimensional vector (SMV) using 12 alleles of its matrix (10 HLA-DRB1, 1 HLA-DRB5, and 1 HLADRB4) (Lata et al. 2007). NetCTL 1.2 server predicts CTL epitopes in protein sequences that expand the MHC class I binding prediction to 12 MHC supertypes (Larsen et al. 2007). Finally, the last sequential predictor used was Vaxign (He et al. 2010) that is a vaccine target prediction and analysis system based on the principle of reverse vaccinology. Using 3D coordinates of the two chains of the model we submit to both structural predictors, PEPOP (<http://pepop.sysdiag.cnrs.fr/PEPOP/>) (Moreau et al. 2008) and SEPPA (<http://lifecenter.sgst.cn/seppa/>) (Sun et al. 2009).

### 2.2. Docking the epitope with the Major Histocompatibility Complex Class II.

Once the best epitope was obtained, a docking study was employed to describe the epitope and MHC type II (MHC II) interactions. The crystal structure of MHC II for this analysis was HLA-DRB1\*0401 (PDB ID: 1D5M). HLA-DRB1 was previously reported predicting response profiles in donors when HLA haplotypes in the H1N1 virus were chosen at random (Schanen et al. 2011). Importantly, this HLA-DR allele is present in the majority of the human population (Southwood et al. 2011). We performed a non-restricted docking with CLUSPRO automated docking program (Comeau et al. 2004). Docking calculations were also performed with Autodock 4.0.1 (Morris et al. 2008). The search space was restricted to a rectangular box that included  $\beta$ -folded chains and  $\alpha$ -helix chains targeting the binding site of the epitope and the MHC II. A rectangular grid (70 x 100 x 90 Å) with points separated by 0.375 Å was generated. The docking parameters of 100 runs with 100 million energy evaluations for each test and a population size of 100 individuals were used. The docking results were analyzed with AutoDock Tools and PyMol software (Seeliger et al. 2010).

### 2.3. Molecular Dynamics Simulation.

The software GROMACS performed the MD simulations. First, the system was embedded in a solvated water box, and then the system was neutralized. The system had undergone an equilibration process before MD simulations were performed. The equilibration started with an initial minimization and was followed by whole minimization. MD simulation of water molecules was performed with all backbone atoms fixed. During 100 ns, MD simulation was achieved under ensemble NTV. Tools of GROMACS were used to calculate the RMSD and RMSF (Hess et al. 2008).

### 2.4. Contact Map.

To analyze the contacts and distances of the complex, a program of the Weizmann Institute of Science in Israel (<http://ligin.weizmann.ac.il/cma>) was performed to generate the contact map.

### 2.5. Peptide synthesis.

Three peptides were purchased for immunological assays as crude material from Mimotopes (Minneapolis, MN and Clayton, Victoria, Australia). Peptide 1 (p1: KKFKPEIAIRPKVRD), Peptide 2 (p2: KLH-CKKFKPEIAIRPKVRD) conjugated with hemocyanin (KLH) linked by a cysteine with the sequence of the p1, and peptide 3 (p3: KKFKPEIAIRPKVRGD) with the addition of a glycine between the arginine and the aspartate.

### 2.6. Elisa Assays.

Blood were obtained according to previously reported procedures (Loyola et al. 2013) from healthy individuals who were living in Mexico City before the outbreak of the influenza H1N1 virus in 2009 and volunteers after the peak of the pandemic. Anti-hemagglutinin peptide levels were evaluated in serum samples from infected and asymptomatic individuals. The Ab levels in the serum samples were determined using an indirect enzyme-linked immunosorbent assay (ELISA). 96-well plates were coated with either p1 or p2. 1 µg of peptide/mL in carbonate bicarbonate buffer (15 mM Na<sub>2</sub>CO<sub>3</sub>, 35 mM NaHCO<sub>3</sub>, at pH 9.6). The plates were incubated for 2 h at 37 C and washed three times with 0.05 % Tween-20 in PBS (PBST). Blocking was performed by treating with PBST plus 6 % fat-free milk and by further washing with PBST. Each sample was tested in duplicate. Serum samples from individuals were diluted 1:50 or 1:100. After the plates were incubated overnight at 4 C and washed with PBST. 1:1000, 1:2000, and 1:4000 dilutions of goat anti-mouse IgG (Santa Cruz Biotechnology) or rabbit anti-human IgG (1:1,000, Santa Cruz Biotechnology) were added to each well, and the plates were incubated for 2 h at room temperature. The plates were washed with PBST, and the enzymatic reactions were started by adding substrate solution (0.5 mg of o-phenylenediamine/mL plus 0.01 % H<sub>2</sub>O<sub>2</sub> in 0.05 M citrate buffer 291 at pH 5.2). After 15 min, the reactions were stopped with 25 µL of 2.5 M H<sub>2</sub>SO<sub>4</sub>, and the absorbance at 492 nm (A<sub>492</sub>) was measured using a Multiscan Ascent (Thermo Labsystems) microplate reader (Ciacci et al. 2009).

### 2.7. Immunization of the rabbits.

Three rabbits were immunized with the three designed peptides (p1, p2, and p3). The immunization schedule was as follows. On day 1 (first immunization), 300 µg of peptide plus complete Freund's adjuvant (Sigma Chemical Co.) was administered through the subcutaneous route. On day 8 (second immunization), 300 µg of peptide plus incomplete Freund's adjuvant was administered through the subcutaneous route. On day 15 (third immunization), 300 µg of peptide in 5 mL of saline solution was administered through the intramuscular route. Seven days after the last immunization, the rabbits were anesthetized with pentobarbital, and serum samples were obtained from blood extracted by cardiac puncture and stored at -70 °C (Loyola et al. 2013).

### 2.8. Cells and Influenza Viruses.

Madin Darby Canine Kidney (MDCK) cells were cultured in Dulbecco's Modified Eagle Medium Nutrient Mixture F-12 (DMEM/F-12) (Gibco), supplemented with 10% fetal bovine serum (Invitrogen) at 37 °C and 5% CO<sub>2</sub>. The strain influenza A Puerto Rico/916/34 (PMID: 24146939) was gently donated by Dra. Blanca Lilia Barrón, the stock was prepared and stored as previously described (Rimmelzwaan et al. 1998).

### 2.9. ConA envELISA.

Viral particles isolated and purified (FBS free) from infected MDCK cells was immobilized in wells coated with Concanavalin A (Con A), which binds the glycoproteins of enveloped viruses. Briefly, 96-well plates (Costar) were coated with 100 µL per well of Con A (Sigma-Aldrich) at 50 µg/mL in PBS, pH 7.4 for 1 h. The wells were washed and incubated with solubilized influenza A Puerto Rico/916/34 (serum-free virus stock) in PBS containing 0.1% Triton-X (PBS-Tx) for 1 h. After the wells had been washing with PBS-Tx, the unbound ConA binding sites were blocked with RPMI medium 1640 containing 10% FBS for 1 h. Serial dilutions of the serum samples were incubated for 1 h at room temperature. Serum from influenza positive patients was used as a positive control. Rabbit pre-immune serum samples were used as negative controls. After the wells were washed again, they were incubated with 100 µL of peroxidase-conjugated secondary antibody anti-IgG (H+L) (Invitrogen) (Robinson et al. 1990).

### 2.10. Neutralization assay.

Neutralizing antibodies were titrated as described by Morens and coworkers (1985). Briefly serial dilutions of the heat-inactivated test sera in triplicate started from 1:20 were mixed with 20 PFU of influenza A Puerto Rico/916/34 virus for 1 h at 37 °C and added to MDCK at a density of  $1.2 \times 10^5$  cells per well in 24-well plates. At 1 h after infection serum-free DMEM/F-12 medium with 2 µg of TPCK (L-1-tosylamide-2-phenyl ethyl chloromethyl ketone)-treated trypsin was added to each well for 10 min at 37°C. Then 500 µL of overlay medium were added to each well and plates were incubated for three days under the same conditions. The supernatant was discarded, and the plaques were visualized with naphthol blue-black dye. The cytopathic effect was observed in order to determine the highest serum dilution that protected 50% of the



cells from cytopathology in these wells. Positive and negative control sera and virus back titration were included in each assay to confirm the viral inoculum (Chan et al. 2011; Morens et al. 1985).

#### 2.11. Isotype response in serum from patients infected with pandemic influenza A H1N1 2009.

IgG isotypes antibodies against p1 peptide were measured by ELISA in 96-well polyvinyl plates (Nunc) coated with each peptide (2 $\mu$ g/mL). We assayed 40 serums from patients infected with influenza A H1N1 2009 and 40 prepandemic serums at 1:100 dilution, 1h at 37°C. Then the anti-human immunoglobulin peroxidase-conjugated secondary antibodies were added (anti-human IgG1, 2, 3 or 4 all Invitrogen) for 1h at 37°C. After H<sub>2</sub>O<sub>2</sub> and 2, 2'-azino-bis (3-ethylbenzothiazoline-6-sulfonic acid) (ABTS) (Sigma-Aldrich) were added as substrates. The absorbance values were determined at 405 nm (Burlington et al. 1983).

#### 2.12. Statistical analysis.

Statistical analyses were performed using JMP Statistical Software (SAS Institute, Cary, NC) (<http://www.jmp.com/>). Normally distributed data were analyzed by ANOVA ONEWAY test to compare the groups. The differences among the groups were analyzed by a Tukey–Kramer HSD test, differences were considered significant at  $p < 0.05$ . Isotype differences were analyzed by ANOVA and Mann–Whitney U test, T-test nonparametric test and Mann-Whitney post-test using GraphPad prism 6 program to determine the significance of the differences between groups, denoted by asterisks as follows: \* $p < 0.05$ , \*\* $p < 0.01$ .

#### 2.13. Synthesis of gold nanoparticles.

Tetrachloroauric acid trihydrate 99.5% (HAuCl<sub>4</sub> • 3H<sub>2</sub>O) as precursor purchased from Sigma-Aldrich, sodium citrate dehydrate (Na<sub>3</sub>C<sub>6</sub>O<sub>7</sub> • 2H<sub>2</sub>O) as a reducing agent was from JT Baker. Citrate-reduction or chemical reduction was used in the synthesis of gold nanoparticles (20nm). It is based on the use of sodium citrate which reduces ions of a metal salt in this case tetrachloroauric acid (HAuCl<sub>4</sub>) in zero valence atoms in presence of heat. This method involved the preparation of 1 ml of tetrachloroauric acid (HAuCl<sub>4</sub>) at 4% in deionized water, then 0.5 ml was added to this solution to 200 ml of deionized water and brought to boiling, the solution was kept under constant stirring. Once the sample began to boil were added 3 ml of sodium citrate to 1%. The addition of sodium citrate, the solution began to darken and turn bluish-gray or purple. After 30 min, the reaction was completed and the final color of solution was a deep wine red indicating that the colloidal solution of gold nanoparticles was obtained. After the solution was cooled, the gold nanoparticles were centrifuged at 3500 rpm for 40 min, the supernatant was removed and the nanoparticles were re-suspended to 4 ml with deionized water (Kogan et al. 2007).

#### 2.14. Conjugation of peptide with gold nanoparticles.

Peptide was linked to the surface of gold nanoparticles by adding a constant volume of this molecule in solution at several concentrations on a fixed volume of the colloidal solution (Wang

et al. 2005). The volume ratio between the solutions of peptide and colloid was 1:9, to obtain conjugated solutions at several concentrations of peptide from 0.1 to 1 ug/ml. Each conjugated solution was incubated at room temperature during 5 minutes to be measured later by UV-vis spectroscopy, and later by Raman and TEM techniques.

#### 2.15. UV/VIS spectroscopy.

UV/VIS absorption spectra were recorded at room temperature with a Thermo Scientific Evolution 606 spectrophotometer. A volume of 500  $\mu$ l of each colloidal solution (control and conjugates) was placed on a quartz cuvette to obtain the absorption spectra for all the samples in the spectral interval of 300-900 nm. Origin software was used to calculate the first derivative of the UV/VIS absorption spectra.

#### 2.16. Raman spectroscopy.

A Raman spectrometer Thermo Scientific Smart DRX in the backscattering acquisition mode was used to obtain the surface enhanced Raman scattering (SERS) spectra of both gold nanoparticles and conjugates. The wavelength of the laser used as excitation source was 785 nm with a power supplied to the sample of 10 mW. To obtain an efficient SERS signal, the colloidal samples were centrifuged at 6000 rpm for 10 minutes, and after removing the supernatant, the concentrate sample was deposited on the surface of a monocrystalline silicon substrate to be analyzed then with the Raman spectrometer.

#### 2.17. Transmission electron microscopy.

This technique was used to observe the morphology of the gold nanoparticles and also of the conjugates peptide-nanoparticle. Images obtained of the particles were acquired using a JEOL GEM 100 CX II system operating at 80kV. A drop of the colloidal sample was placed on a carbon-coated copper mesh grid, to be slowly evaporated and analyzed by TEM.

## Chapter III. Results.

### 3.1 Results of in silico analysis.

#### *3.1.1. 3D model selection of the HA of the Human Influenza H1N1*

Early 2009, Di and coworkers reported a homology model of the HA H1N1 influenza strain and predicted some epitopes by SEPPA program (Lata et al. 2007). Later, in 2010 Xu and coworkers reported the crystallographic coordinates of influenza HA trimer with a PDB code 3LZG (Xu et al. 2010). Although both 3D models show a high similarity, in this work we used 3LZG and its corresponding protein sequence.

#### *3.1.2. Prediction of the epitope*

Two epitope prediction methods were used, sequence-based and the structure-based predictors. Structural predictors, according to their strategy, localize sequences of amino acids more exposed and discard epitopes in hidden domains. Likewise, epitopes located in  $\alpha$ -helix and  $\beta$ -folded regions were discarded because these regions have less mobility and could difficult the recognition by the MHC. In contrast, loops or tails are more recognizable and become accommodated in the corresponding pockets by the MHC molecule due to their flexibility. Furthermore, these structures were considered for the structural modeling of the immunogenic peptide (Yang et al. 2009; Jorgensen et al. 2010; Sinigaglia et al 1994; Ofek et al. 2010). The first system of prediction used was that implemented in the PEPOP server and its results were compared with the other predictors. PEPOP played the role of the initial reference due to its several features (length, type of amino acids, beta-turns, and hydrophobicity) that filter and refine the epitope search for the best structural prediction. In this initial approach, three more conditions were required: high score for MHC II recognition, presence of the epitope in a conserved region, and at the same time, to belong to a domain structurally exposed.

Therefore, we submitted into PEPOP server two main chains, those corresponding to the HA trimer retrieved from 3LZG (Moreau et al. 2008). A 20 residue length epitope was requested, to obtain a domain that can be recognized or processed by the immune system, in particular by the MHC I and II (Madden et al. 1993; Trombetta et al 2005; Villadangos 2001). Several amino acid sequences were predicted; however, due to its biological properties, absence of scientific reports, and to our knowledge about these sequences, the epitope sequence KFKPEIAIRPKVRDQEGRM (211 to 230 of Chain A) was selected. Located in the globular head of the HA, this surface portion is near Ca<sup>2+</sup> antigenic site, and includes the receptor binding region (Fig 3A, 3B) (Wiley et al. 1987). In terms of functionality, the residue 225 is already known to affect receptor-binding specificity of avian and human H1N1 viruses (Meroz et al. 2011). The epitope presents a core of ten amino acids (EIAIRPKVRD), according to the score of the PEPOP software these represent the highest content of immunogenicity. When we compared the result of PEPOP with the other predictors, this sub-sequence (core) was also preferred by epitope-MHC II and the epitope-B cell predictors (Fig 3C).

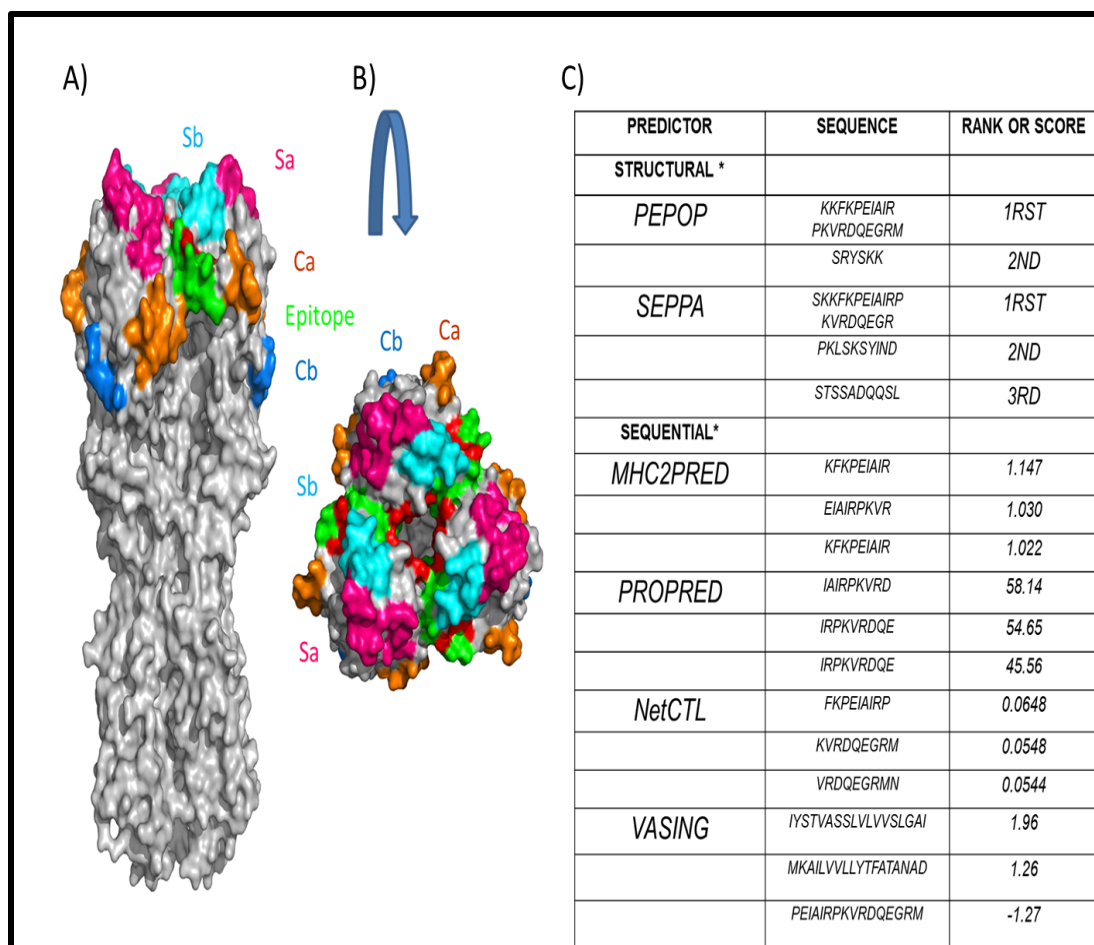


Figure 3. Antigenic sites of HA and scores obtained from computational epitope predictors. A) Three-dimensional representation of the HA trimer by Xu and coworkers. The antigenic sites of the HA highlighted in colors Sa, Sb, Ca, and Cb. The localization of the epitope predicted by PEPOP and its core are highlighted in green and red, respectively. B) Superior view of the globular head of the HA trimer. C) Rankings or scores of the sequence predicted according to the scale in the context of each software predictor.

A characterization of the predicted peptide was performed by the Peptide Property Calculator program ([www.genscript.com/ssl-bin/site2/peptide\\_calculation.cgi](http://www.genscript.com/ssl-bin/site2/peptide_calculation.cgi)) showing that its sequence has 40% of hydrophobicity, 50% of hydrophilicity, 15% of acidic composition, and 35% of basic. These proportions are essential for the peptide because they are related to immunogenicity (Menez et al. 2011; Kropshofer et al. 1992). The corresponding sequence of the epitope was submitted to a Protein-Protein Basic Local Alignment Search (BLASTP) and Position-Specific Iterated Basic Local Alignment Search (PSI-BLASTP) (<http://blast.ncbi.nlm.nih.gov/>), resulting that it has a complete identity (100 %) with a human protein related to a methyl-CpG-binding group (UNIPROT code: Q8WWY6) (Walavalkar et. 2013). This protein is localized in the nucleus and restricted to the round spermatids in the postmeiotic stages of the male germ cell development. The score for identity was 100% only in the residues KVRDQEGR, and in the rest of the BLAST alignments showed less than 90% of identity due to gaps. It is worthy to mention

that the predicted epitope might not induce an autoimmune response because the methyl-CpG-binding trait is localized in the nucleus.

### *3.1.3. Docking and MD simulations of the peptide with the MHC Class II*

Three-dimensional (3D) models of the peptides and MHC II were used to describe the interactions between them by docking studies with AUTODOCK 4.0.1 (focused) and blind docking with CLUSPRO program (Seeliger et al. 2010; Comeau et al. 2004). CLUSPRO program depicts free energy of the molecular interaction between the peptides and MHC II as the best free energy values. The results demonstrate that the epitope predicted by PEPOP can be bonded by the MHC II recognition groove, with blind or restricted docking. Characteristic of docking is that neglects the flexibility of the atomic configuration and the solvent effects (Amaro et al. 2008); therefore, from a complex obtained by AUTODOCK, MD simulations for 100 ns were performed to refine the epitope-MHC II complex with GROMACS (Platania et al. 2012; Karthick et al 2013; Strambi et al 2012; Terentiev et al. 2012; Carlsson et al. 2008 Iribarne et al. 2002; Shahlaei et al. 2011; Król et al. 2007).

To describe the epitope-MHC II interactions, we focused on the epitope recognition by the well-known MHC II pockets (P1, P4, P6, P7 and P9) located inside the recognition groove (Fig 2A). These regions are the necessary to produce an immune response because they participate in the formation of the epitope-MHC II complex necessary for the antigen presentation to T-cell and B-cell receptors (Sinigaglia et al. 1994; Villadangos 2001). MD simulations provided evidence that the epitope reaches the pocket 1, 4, 6, 7, and 9 which are reported as a determinant structure for the peptide recognition process (Bordner 2010).

The last structure reached by the MD simulations shows some changes in all the pockets, specially in P1 and P4. Also, during the simulations Lys1 approaches the P1 (Gly86 in chain B) rapidly, although it interacts with residues nearby the P4 (Cys79 and Arg80 in chain B). Lys2, with less mobility, also interacts with P4; in particular, sharing with the Lys1 an interaction with the Cys79. Phe3 plays an interesting role because during simulation interacts with residue of both chains: Ile8 (chain A) and His13 (chain B, P4); showing that hydrophobic amino acids play an important role for antigen processing. Also, the interaction formed by Tyr78 (chain B, P4) and Arg10 was evidenced as stabilizing. Regarding the P6 and P7, the Val65 (chain A) and Leu67 (chain B) were nearby Glu6 and Arg19, respectively (Fig. 4).

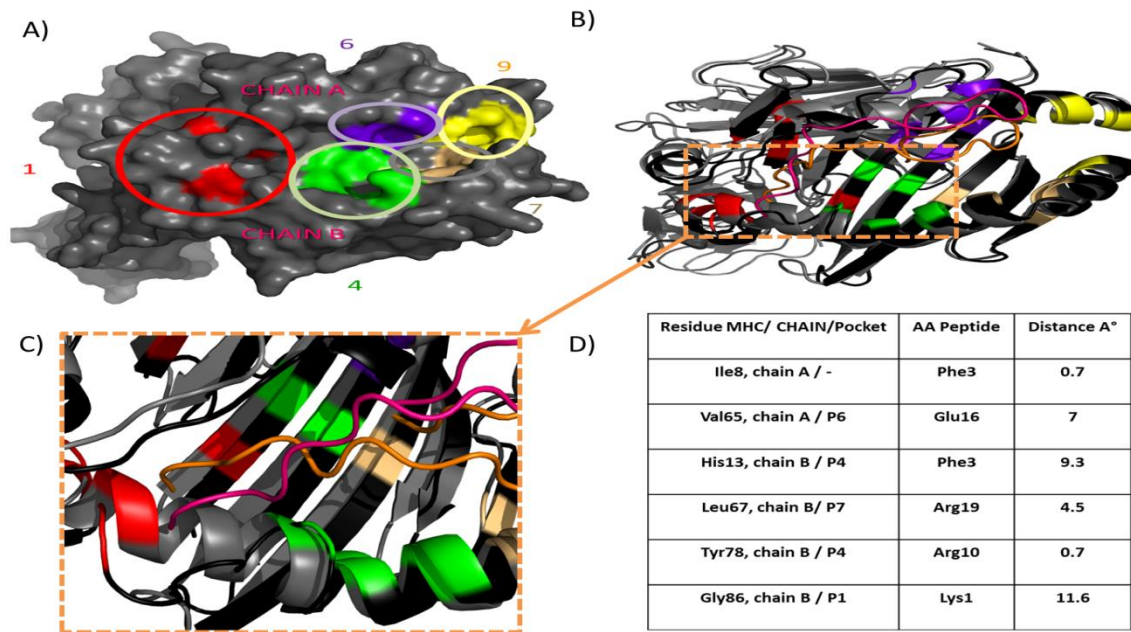


Figure 4. Pockets of the MHC and their interaction with the epitope. A) Three-dimensional surface representation of the MHC molecule, circled and highlighted in color the pockets that involve the interaction with the epitope predicted by PEPOP (P1=Red, P4=Green, P6=Blue, P7=Light Orange and P9=Yellow). B) Superposition of the final docking map (gray) and the 100 ns simulation (black). C) Zoom near the pockets 1 and 4 of the recognition groove. D) Distances obtained by a contact map analysis, some of these interactions are with specific amino acids of the pockets 1, 4 6 and 7.

To examine the epitope-MHC II complex interactions during the MD simulations we analyzed the RMSD and RMSF values (Fig.5) The RMSD analysis showed that the model reaches convergence approximately at 20 ns and remains stable during the rest of the MD simulation (100 ns)(Fig 5A) (Senda et al. 2012; Grossfield et al. 2007; Smith et al. 2002). Also, the RMSF values were retrieved from the three chains of the complex (Chain A spanning from 4 to 181, B from 2 to 190, both of the MHC molecule, and C corresponding to the 20 of the peptide) (Fig 5B and 5C). The MHC molecule was analyzed in each chain, the chain A shows many long movements in a region spanning from the residue 30 to 60 that involves the pocket 1 and the initial region of the pocket 6. The RMSF values studied from the chain B have an initial pick, this phenomena was due the flexibility of the amino acids in the amino-terminal region (residues 2, 3, and 4). Other regions present a local maximum, due to the lack of some amino acids in the chain, this gap span from residues 105 to 113 of chain B. The chain B residues that were involved in long movements were from the region near pocket 1, 7 and 9. (Fig 4B).The RMSF values show that the Phe3 of the peptide is the only amino acid that has limited movements compared with the rest of the peptide. The limited movements it is due the P1 and specially P4 with the His13, this is one of the special binding residues of the P4. All the rest of the residues have variable movements, but when the complex achieves the convergence the residues become more limited in their movements (Fig 5C).

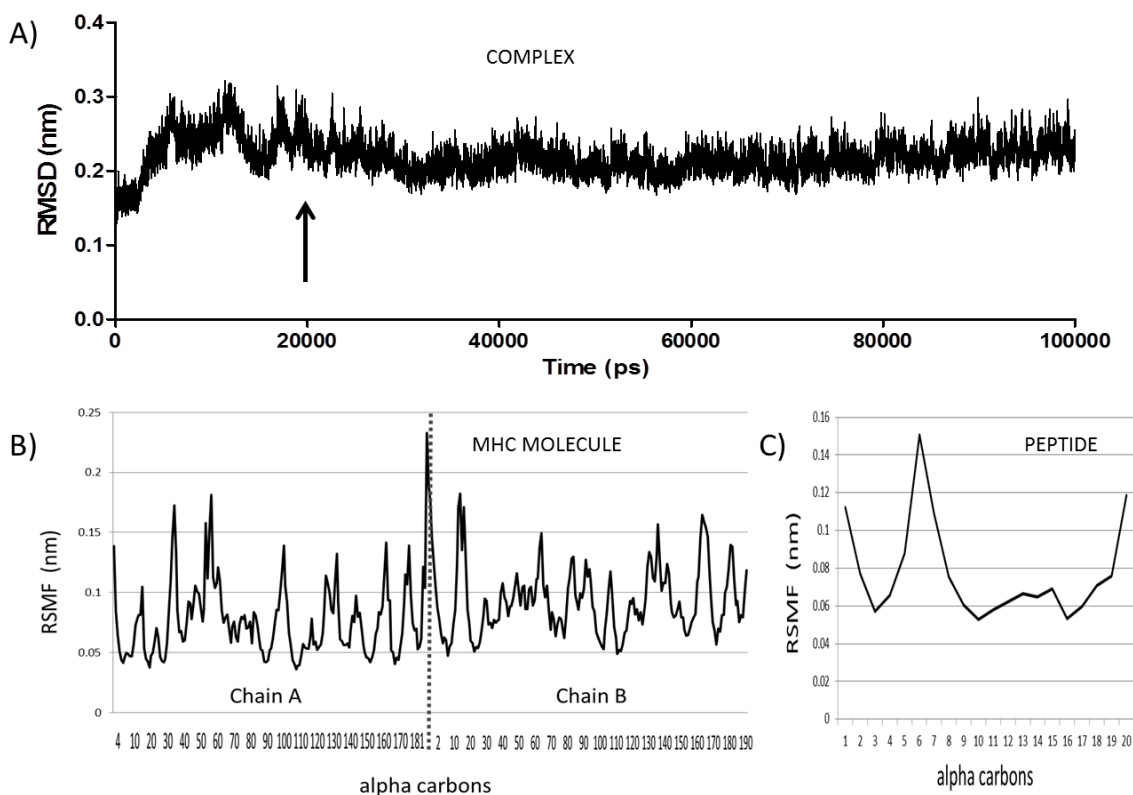


Figure 5. RMSD and RMSF parameters. A) RMSD of the complex. B) RMSF of the two chains of the MHC molecule. C) Epitope of 20 AA.

### 3.2 Results of experimental strategy.

#### *3.2.1. Design of the peptides*

The peptide was revised to explore the versatility of the epitope in order to improve it by editing its residue sequence according to the literature and the analysis *in silico* (Moreau et al. 2008; Burton et al, 2004; Sundaram et al. 2004; Kaumaya et al. 1992; Wang et al. 2002). The epitope predicted was modified to reduce its possible autoimmune response due to its complete homology with a human protein related to spermatogenesis. These modifications included the removal of the last five residues which belong to the homology region of the protein related to a methyl-CpG-binding group (KKFKPEIAIRPKVRDQEGRM). The second modification obeys to the MD simulations results where the amino terminal region showed a better interaction with the recognition groove. This coincides with the report of Yano and co-workers (2005), where it is mentioned that the KK linker sequence is preferred by cathepsin B to process antigens. Thus, it is also consistent with the presence of the Lys1 and Lys2 in the amino terminal region of the peptide; therefore, these residues remained unchanged. We named this peptide as p1 (KKFKPEIAIRPKVRD) (Yano et al. 2005). The second peptide, called Peptide 2 (p2), conserves the sequence of p1 with an additional Cysteine at the amino terminal that functions as a linker for Hemocyanin (KLH). This modification will provide evidence of the importance of

the amino terminal lysines (**KLH-C-KKFKPEIAIRPKVRD**) (Helling et al. 1994; Beekman et al. 1999). Another sequence of interest is RGD because it is preferred by the antigen process molecules and enhances the immune response (Yano et al. 2003). Fortunately, the sequence of the peptide presented an Arg and Asp residues in the carboxyl terminal sequence, and taking advantage of this situation, we inserted a Gly between these residues resulting in the peptide 3 (p3) (**KKFKPEIAIRPKVRGD**). In summary, we obtained four candidate peptides as potential immunogenic agents: the original predicted by PEPOP (**KKFKPEIAIRPKVRDQEGRM**) and its derivatives: p1 (**KKFKPEIAIRPKVRD**), p2 (**KLH-C-KKFKPEIAIRPKVRD**), and p3 (**KKFKPEIAIRPKVRGD**).

### 3.2.2. Human IgG antibodies to the peptides

To elucidate the immunogenic and antigenic potential of the p1 and p2, an ELISA assay was performed with sera of two volunteers groups. These groups were integrated by sera obtained of individuals who were considered prepandemic (*i. e.*, sera samples obtained before 2009); these were in storage before the 2009 outbreak. The second group of sera was considered pandemic because these samples were collected during the outbreak. This ELISA assay was based on the binding of human Ab (IgG) to the p1 and p2 (Figure 6) (Mavrouli et al. 2011; Loyola et al. 2013). The IgG antibodies identified the p1 in the sera of the two groups with no significant statistical difference (ANOVA). These results show that the general population had antibodies against the p1 prior to the immunization or infection with other viruses or exposure to influenza A virus (H1N1). In other words, this epitope presumably is conserved among the pandemic and seasonal strains. Thus, the peptide is antigenic in humans. Results are presented as box and whisker plots. The boxes define the 25th and 75th percentiles, with error bars defining the 10th and 90th percentiles. Human sera were recognized by both peptides.



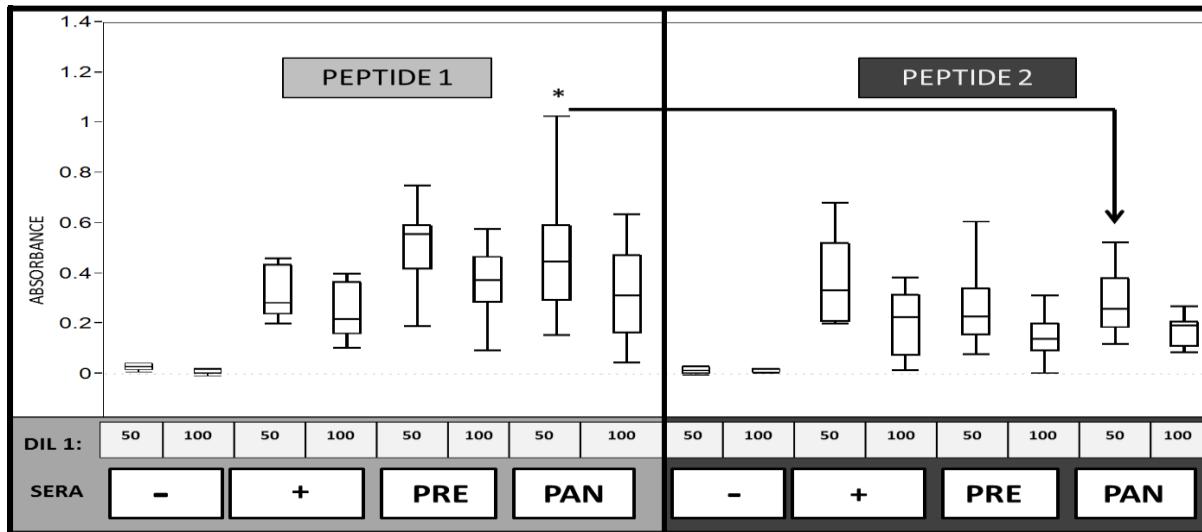


Figure 6. Detection of the p1 and p2 peptides by the human IgG Ab. Microplates were coated with p1 or p2, and two dilutions (1:50 and 1:100) of sera from pre-pandemic and pandemic individuals were used. The IgG Ab to the HA peptide was detected with a secondary Ab specific for human IgG. \*Statistical analysis of the ELISA  $p < 0.05$ , Pandemic – p1 vs Pandemic - p2, Dilution 1:50, Anova Oneway, Tuckey – Kramer HSD.

### 3.2.3. Isotype response in serum from patients infected with influenza A p/H1N1/2009

IgG2 is the main isotype of IgG antibodies against the p1. Although no differences were found in the levels of total IgG antibodies between pre-pandemic and pandemic sera, we analyzed the contribution of each subclass or isotype in response to p1 (Burlington et al. 1983). The antibody levels were significantly higher in the pandemic group compared to the pre-pandemic group (negative controls) for IgG2 ( $P = 0.025$ , Mann-Whitney U test) and IgG4 subclasses ( $P = 0.007$ ). In the rank order: IgG2 (0.6 vs 0.5, median) > IgG4 (0.08 vs 0.07, median).

### 3.2.4. Peptide 1 is immunogenic and induced antibodies to native form of HA

The rabbits immunized with p1 peptide and human infected with pH1N1 virus showed a clear antibody response against wild-type viral antigens immobilized with ConA (Figure 7). Rabbits immunized with p1 showed a stronger antibody response against the immobilized wild-type virus than human positive control. These results are important and demonstrate that the p1 is highly immunogenic in rabbits and probably in humans, and it induces antibodies capable of interacting with the native form of hemagglutinin (Robinson et al. 1990).

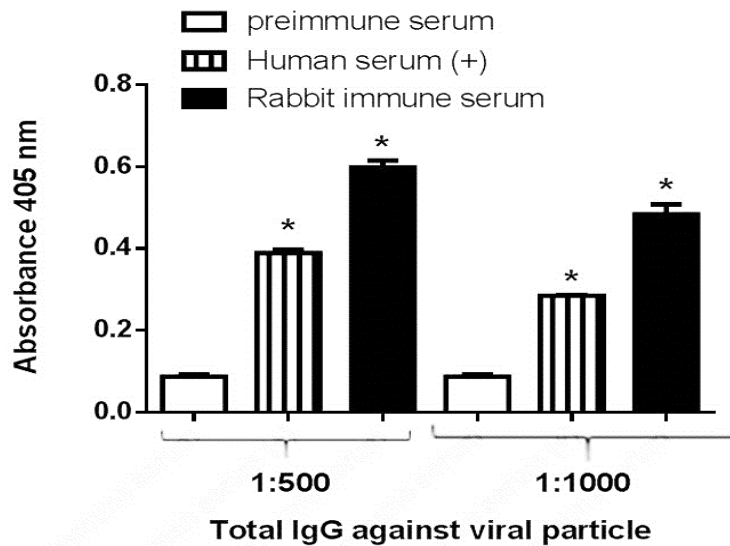


Figure 7. Levels of IgG against viral particle in serum of infected individuals or from rabbit immunized with peptide 1. IgG levels were determined by ELISA using viral antigens immobilized with ConA, and the IgG antibodies were detected with a secondary antibody specific for human or rabbit IgG. Data are expressed as the mean  $\pm$ SD. The levels were significantly higher in human serum and rabbit antiserum ( $P < 0.05$ , Kruskal Wallis).

### 3.2.5. Neutralizing antibodies induced by Hemagglutinin peptides in rabbits

Serum samples from rabbit immunized with p1 and from two vaccinated individuals and two patients infected with influenza A p/H1N1/2009 were titrated for neutralizing antibodies (PRNT50). p1 induces 1:533 neutralizing titers in rabbit, whereas in vaccinated individuals the titers were 1:246 and 1:600, and in infected patients were 1:400 and 1:250. On the other hand p2, which is the p1 conjugated to hemocyanin (KLH-CKKFKPEIAIRPKVRD), and the p3, in which a glycine was added between the arginine and the aspartate of the p1 sequence, induced neutralizing antibodies in minor quantity than the infected or vaccinated group (titer 1: 103, and 1: 160, respectively) (Fig. 8) (Chan et al. 2011, Morens et al. 1985).

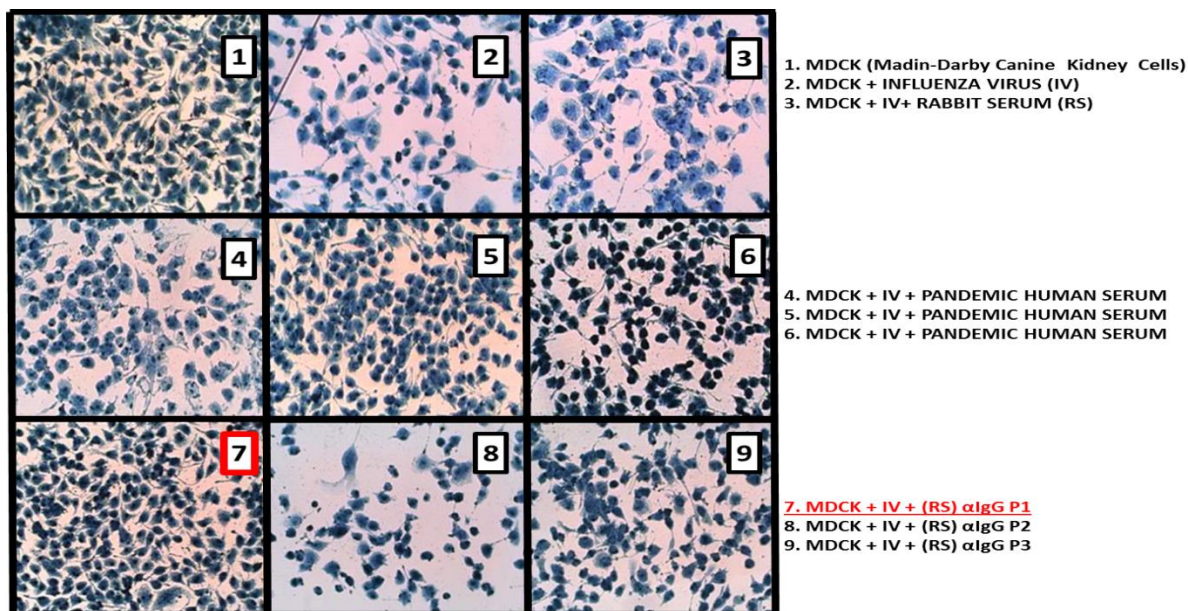


Figure 8. Plaque reduction neutralization test. Panel 1 -Madin Darby Canine Kidney (MDCK) cells, Panel 2. MDCK cell with 30 PFU influenza virus, Panel 3. MDCK cells with Influenza virus and rabbit serum (not immunized). Panel 4 to 6. MDCK cell with 30 PFU and Human sera, the three panels were controls. Panel 7 to 9. Infected MDCK cells with immunized rabbit sera with peptide 1, 2 and 3.

### 3.3. Conjugation of peptide.

The conjugates were prepared at several concentrations of peptide using the methods mentioned elsewhere (Wang et al., 2005). The color of the mixture is the first evidence of conjugation, when the concentration of peptide becomes very high, the mixture turns into a dark purple to blue gray color, and the original ruby red disappears. For this case, very small black particles appear in the mixture. However, as the concentration of peptide diminishes, the obtained colloidal solution begins to show the ruby red coloration characteristic of the gold nanoparticle solution used as control. Thus, we observe that for concentrations between 0.5 and 0.7  $\mu$ m/ml still retains its ruby red coloration, but with a lightly darker tone and never appear the small black color particles. It is well known that the permanence of the ruby red color of the colloidal solution is related to a stabilized state of the conjugated, whereas a change in the coloration to blue-gray is directly related to the aggregation of the gold nanoparticles caused by an excess of charge provided by the peptide, which uncharge the surface of the particles (De la Fuente 05). We suggest that the interaction is based on the charge attraction between the gold nanoparticle and the peptide. In our case, the gold nanoparticles were synthesized by the citrate reduction method, thus, a layer of citrate groups covers the surface of each nanoparticle, providing negative charge. In this way several amino acids of the peptide could be linked to a gold nanoparticle through a positively charged part (amino terminal or lysine groups), which

interacts with the citrate of the gold nanoparticle surface (Brewer et al., 2005; McLean et al., 2004).

### 3.4. UV/VIS spectra of single and peptide-conjugated gold nanoparticles.

The UV/VIS spectrum of gold nanoparticles (control) consists of a unique absorption band at 520 nm, as shown in Figure 9, which arises from the surface plasmon resonance (SPR) absorption. We have used a simple and fast method to evaluate the average size of gold nanoparticles (Haiss et al., 2007). This method use the information of the UV/VIS spectrum obtained experimentally as the intensity of the SPR absorption at 520 nm, and also the intensity of the absorption at 450 nm.

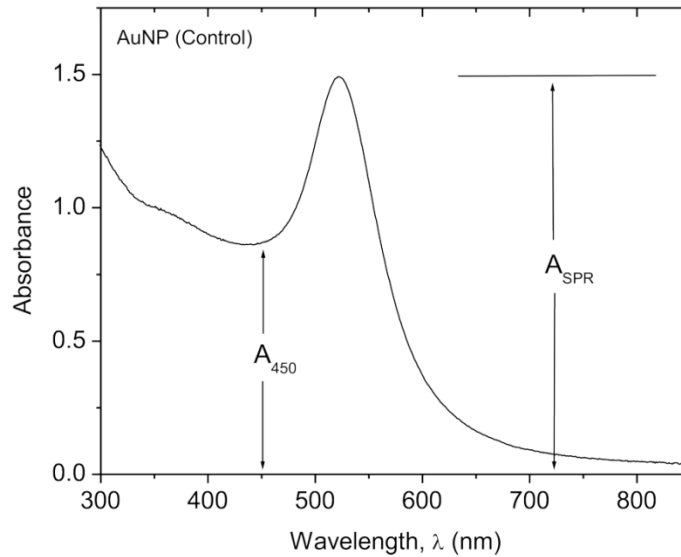


Figure 9. UV/VIS spectra of gold nanoparticles (control) synthesized and used in this work. Parameters  $A_{450}$  and  $A_{SPR}$  were used to estimate the particle size according to the model proposed by W. Haiss. The particle size was calculated by:

$$d = \exp(B1 A_{SPR} / A_{450} - B2) \quad (1)$$

where ( $A_{SPR}$ ) is the absorbance of the surface plasma resonance, and ( $A_{450}$ ) is the absorbance at 450 nm.  $B1$  is the inverse of the slope of the linear fit between ( $A_{SPR} / A_{450}$ ) and  $\ln(d)$ , whereas  $B2$  is the interception. Using experimental data reported in (Haiss et al., 2007),  $B1=3.0$  and  $B2=2.2$ . The calculation of particle diameter using equation (1) allows estimate the size of gold nanoparticles. From the UV/VIS spectrum of the gold nanoparticles used in this work  $A_{SPR}=1.491$  and  $A_{450}=0.869$ , thus using ec. (1) the estimated average size is  $d=19$  nm.

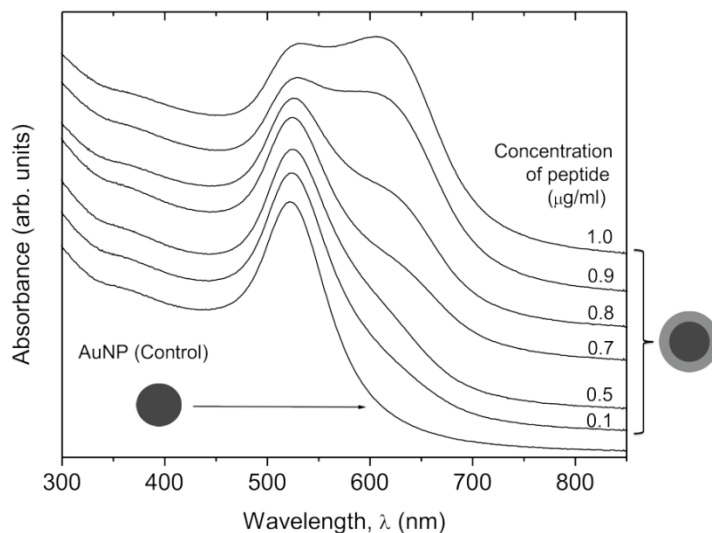


Figure 10. UV/VIS spectra of gold nanoparticles conjugated to the peptide at several concentrations (0.1 – 1.0)  $\mu\text{g/ml}$ .

Figure 10 shows the UV/VIS spectrum of the gold nanoparticles and also the spectra of the conjugated peptide-nanoparticle solutions at several concentrations of peptide. The concentration range of peptide is (0.1 – 1.0)  $\mu\text{g/ml}$ . It can be observed that the lineshape of the spectrum of the single nanoparticles (control) changes as the concentration of peptide increases, beginning with a little shift to long wavelengths (for 0.1  $\mu\text{g/ml}$ ) and also a widening of the absorption signal resulting from the conjugation of peptide with the surface of the gold nanoparticles. After 0.8  $\mu\text{g/ml}$  a second band near 607 nm is more evident, and is due to the aggregation of the conjugates. This effect is more accentuated for high concentrations of peptide (> 0.8  $\mu\text{g/ml}$ ). It is well known that the negative charged surface of the gold nanoparticles is neutralized by some part of the peptide positively charged, because high peptide concentrations can accentuate this effect and consequently cause aggregation (Raman et al., 2006). When this condition is reached the conjugated particles are aggregated and the colloidal single-particle condition disappears. This fact can be also observed from the first derivative of the UV/VIS spectra of the conjugates shown in figure 11.

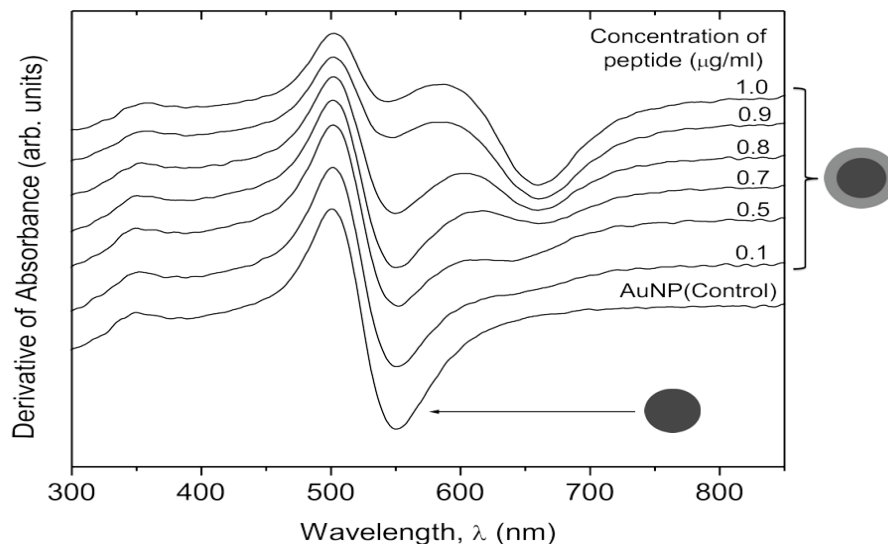


Figure 11. First derivative of UV/VIS spectra of gold nanoparticles conjugated to the peptide at several concentrations (0.1 – 1.0)  $\mu\text{g/ml}$ .

For concentrations of peptide ( $>0.8 \mu\text{g/ml}$ ) the line shape of the first derivative is distorted because of the presence of the second band at 607 nm which leads to the aggregation of the conjugates. The last can be observed as a discoloration of the colloidal solutions. Thus, an adequate conjugation can be achieved for concentrations of peptide ( $< 0.8 \mu\text{g/ml}$ ), where the lineshape of the spectrum of the conjugated is very similar to the spectra of gold nanoparticles (control).

### 3.5. SERS spectra of peptide conjugated to gold nanoparticles.

SERS spectra of peptide conjugated to gold nanoparticles. Once obtained the conjugates (peptide-gold nanoparticle) in colloidal state at several concentrations of peptide, they were centrifuged and deposited on monocrystalline silicon substrates as indicated in the experimental section, to obtain the SERS spectra by Raman spectroscopy. Figure 12 (bottom) shows the Raman spectra of peptide at 1  $\mu\text{g/ml}$  deposited on the monocrystalline silicon substrate. There is not observable any signal from the peptide due its low concentration. Only two bands at 520  $\text{cm}^{-1}$  (from optical single mode) and at 960  $\text{cm}^{-1}$  (from two phonon processes) of the crystal silicon are observed (Rojas-Lopez et al., 2006, Rojas-Lopez et al., 2010, Liu et al., 2002). The next Raman spectrum corresponds to the peptide at 1  $\text{mg/ml}$ , where the band at 1436  $\text{cm}^{-1}$  is assigned to deformations of  $\text{NH}_3$  species of the amino acid lysine (Aliaga, et al, 2009). For null concentration of peptide (AuNP gold nanoparticles), the SERS spectrum shows vibrational modes associated mainly to silicon oxides arising from the surface of the monocrystalline substrate, such as the bands at 630, 1054 and 2126  $\text{cm}^{-1}$  (Liu et al., 2002), which has been enhanced by the gold nanoparticles by the SERS process.

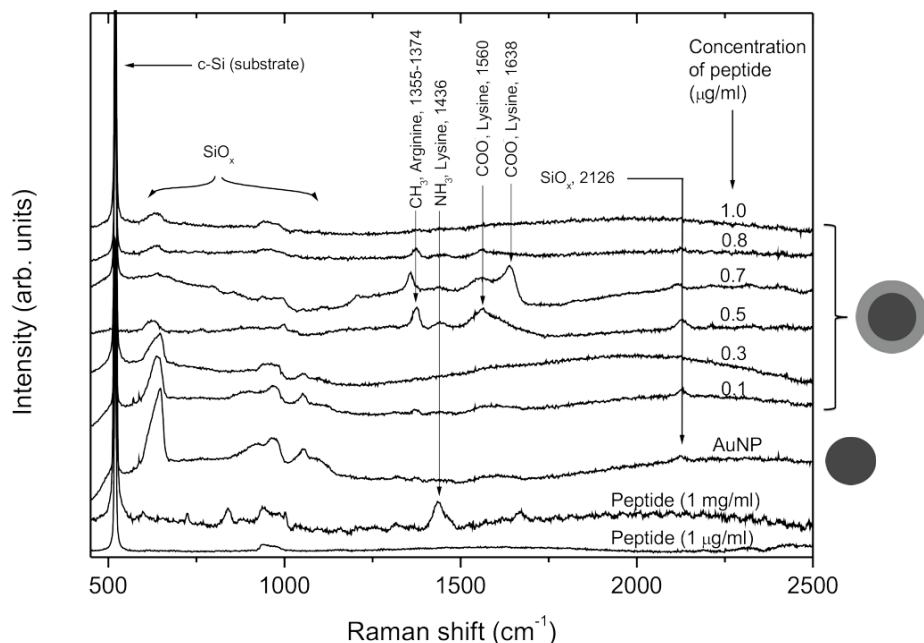


Figure 12. SERS spectra of gold nanoparticles conjugated to the peptide at several concentrations (0.1 – 1.0)  $\mu\text{g/ml}$ .

For low concentrations of peptide (0.1 and 0.3  $\mu\text{g/ml}$ ), the SERS spectra of the conjugate are very similar to the corresponding to the gold nanoparticles (control) with no signals from the peptide, may be because there is not enough amount of molecules covering the surface of the nanoparticle. However for the next concentrations: 0.5 and 0.7  $\mu\text{g/ml}$ , the SERS spectra of the conjugate shows intense bands arising from the conjugated peptide. The band at 1355-1374  $\text{cm}^{-1}$  is associated to vibrations of the aliphatic chain of  $\text{CH}_2$  from the amino acid arginine (Aliaga et al., 2010). The next band at 1436  $\text{cm}^{-1}$  is assigned to deformations of  $\text{NH}_3^+$  species from the amino acid lysine, whereas the bands at 1560 and 1638  $\text{cm}^{-1}$  could be ascribed to a asymmetric stretching of the  $\text{COO}^-$  group of lysine too (Aliaga, et al, 2009). According to that, SERS spectra indicate that lysine and arginine amino acids interact with the surface of gold nanoparticles adopting different conformations and orientations onto the surface, enhancing their intensity in this interval of concentration of peptide (0.5-0.7)  $\mu\text{g/ml}$ . This observation can be used as evidence of the immobilization of peptide on the surface of gold nanoparticles. For high concentrations of peptide: 0.8 and 1.0  $\mu\text{g/ml}$ , the intensity of the SERS signals diminish notably due to the aggregation effect of nanoparticles by the neutralizing of the negative charge of the gold nanoparticles. The last is consistent with the observation of a second band in the UV/VIS spectra attributed to the formation of aggregates, which is more evident for high concentrations of peptide (0.8-1.0)  $\mu\text{g/ml}$ . Therefore the interval of concentrations between 0.5 and 0.7  $\mu\text{g/ml}$  represent the optimal conditions to obtain a stable conjugate by using this hemagglutinin peptide. The so obtained conjugated could be especially useful for diagnostic or immunologic therapy in nanomedicine



### 3.6. Transmission electron microscopy of peptide conjugated to gold nanoparticles.

Figure 13 (A-B) shows the quasi spherical or icosahedral nature of gold nanoparticles (control) used to prepare the peptide conjugates. The average size of these particles is near 20 nm, which is consistent with the estimated size (19 nm) obtained using eq. (1) and the UV/VIS spectrum. Figure 4 (C-G) shows the morphological appearance of the AuNP-peptide conjugates at several scales. The peptide layer covering each gold nanoparticle can be observed. In this case the concentration of peptide used to be conjugated to the gold nanoparticle was 0.5  $\mu\text{g}/\text{ml}$ , because of UV/VIS, first derivative of UV/VIS and Raman results, it is suggested this concentration of peptide as the most viable to form the conjugates.

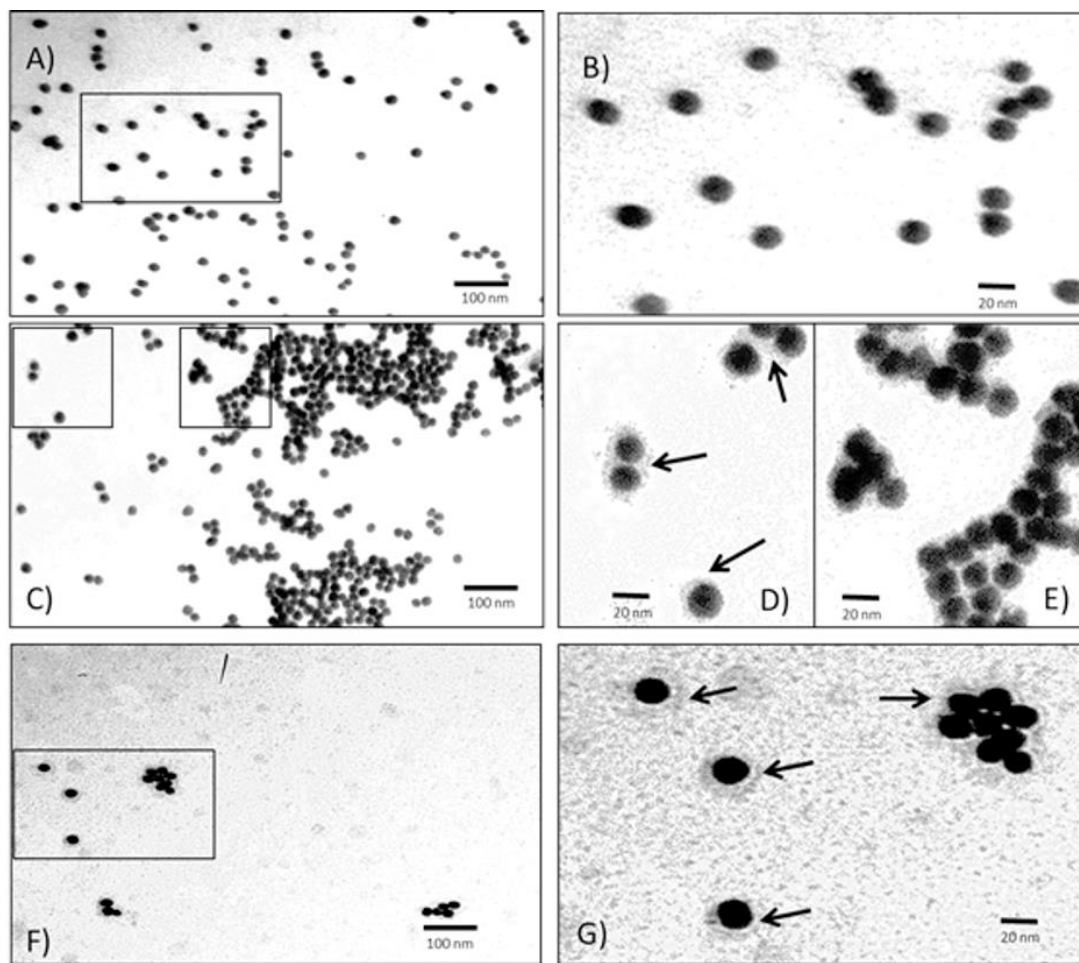


Fig. 13. TEM. A) AuNP Control B) Zoom AuNP Control C) Conjugation at 5  $\mu\text{g}/\text{ml}$  concentration D) and E) Zoom conjugation at 5  $\mu\text{g}/\text{ml}$  F) Conjugated AuNP peptide after 10 months 5  $\mu\text{g}/\text{ml}$  G) Zoom of the conjugated AuNP peptide after 10 months ( 5  $\mu\text{g}/\text{ml}$ ).



## Chapter IV. Discussion

Predicting of possible epitopes and testing its immunogenicity involve a wide effort and intervention of diverse scientific disciplines. There are different epitope prediction methods based on biochemical properties such as conserved sequences, special sequences, special amino acids, length, and hydrophobicity or secondary structure. Many studies focus in sequence and its relation with B-cell immunity response; other take into account the recognition by MHC molecules or the three-dimensional data of the proteins. Our workgroup has combined the epitope prediction and molecular modeling studies to obtain a peptide whose immunogenicity was assessed by experimental assays (Loyola et al. 2013). The area of opportunity of these studies is reflected by the fact that, until we know, websites such as Immune Epitope Data Base (<http://www.iedb.org/>) that gathers information about this topic are scarce (Tangri et al. 2001; Geysen et al 1985; Peters et al. 2005).

In this work, we used PEPOP epitope predictor because its features and previous results (Moreau et al. 2008). Later, we analyzed the localization of the epitope and its relationship with antigenic sites using the 3D model of HA (PDB ID 3LZG). Once localized the sequence in three-dimensional model of HA, we identified that the epitope was located among the amino acids that conform the Ca antigenic site, and near to Sa and Sb antigenic sites (Fig 1A and B). Interestingly, this finding initiates a discussion about the definition of continuous or discontinuous epitopes: if the sequence is not reported as a discontinuous epitope, at least it is part of a continuous epitope. Thus, the ELISA assay could suggest that this sequence is part of the same antigenic site, more experimental assays are necessary to prove this asseveration (Haste et al. 2006; Wieggers et al. 1990, Moreau et al. 2006). To confirm the immunological capabilities of the epitopes initially predicted, these were submitted to other epitope predictors to select those that were found at least in three of these predictors (Fig.3C) (Deavin et al. 1996; Flower 2003, Yu et al. 2002; Salimi et al. 2010). Also, the conservation of the sequence should be considered to design an epitope (Ekiert et al. 2009; Heiny et al. 2007; Xu et al. 2010; Gaschen et al. 2002; Igarashi et al. 2010; Du et al 2010). HA has different epitopes reported elsewhere; an example is the sequence IAI that is part of a peptide that produces efficient immune response for Paracoccidioidomycosis (PCM) granulomatous disease caused by *Paracoccidioides brasiliensis*, a thermal dimorphic fungus (Taborda et al 1998). In the peptide reported in this work, the sequence IAI is between residues 216 and 225 of the subunit 1 of the HA (3LZG).

Rothbard and coworkers (1988) reported an extensive analysis of the DR1 epitopes, proposing different sequences and combinations of residues that could be recognized (Rothbard et al. 1988). More recently Yano and coworkers proposed the use of RGD sequence in vaccine design (Yano et al 2005; Yano et al. 2013). Our results showed that p3, with the sequence RGD, produces neutralizing antibodies, but it has not the same reaction when are compared with p1 in the neutralization assays, possibly due to the introduction of the Gly. Some of the structural

changes have been studied by Dayan and coworkers explaining the reason of this of phenomena (Dayan et al. 2010). Other authors have analyzed how the loss of the recognition is due to the flexibility of the interaction of MHC with peptide (Insaiddoo et al. 2011). In the docking assay, we prepared the simulation to produce a high flexibility in the peptide and a rigid structure in the MHC molecule; however, the MD simulations allowed to increase the relaxing of the epitope-MHC II complex in order to refine the 3D model of interaction. The structural analysis showed that the carboxyl terminal sequence maintains a rigid behavior, preventing an unfolding of the extreme of the peptide or the stretching out of the recognition groove. This produced a strong turn that was maintained during the simulation between the P4 and P6 and it coincided with possible interaction with the Met20. The groove recognized three initial residues of the amino terminal sequence; however, the size of the residues spanning from Lys12 to Ile17 of the peptide hinders the anchoring with the groove completely. Also, the two Arg residues of the peptide, the Asp, and the Gln could be hindrance effects to an adequate docking given their hydrophobicity.

Several authors have reported that the binding with the pocket P1 stabilizes the epitope-MHC II complex (James et al. 2009; Cardenas et al 2005; Cardenas et al. 2007; Painter et al. 2008). Herein, the computational simulations show that the Lys1, Lys2, and Phe3 bind the hydrophobic pocket P1 and P4 (Fig 3). On the contrary, possibly the presence of KHL interferes (hindrance effects) with the recognition by the antibodies. Lys1 and Lys2 could facilitate the antigen processing and the pocket anchoring. Further analyses are needed to explain this phenomenon.

P4 was the most important anchoring element after the 100 ns of MD simulations. As it is shown by the interactions with at least four residues of the peptide (Lys1, Lys2, Phe3 and Arg10). Particularly, the P4 of the chain B play the most important role. Thus, the RMSF analysis shows fewer fluctuations in the P4, which containing the residues of anchorage. Furthermore, P4 has been reported that elicits a suitable spatial disposition of the residues nearby. In turn, certain residues in P6 modify the conformation of those in P9. For instance, the binding of positively charged amino acids at P6 can reduce the cavity of P9, limiting the ability to interact with residues with hydrophobic side chains. In contrast, the binding of negatively charged amino acids at P6 enlarges P9; render P9 capable of accepting residues with large side chains. According to MD simulations, the alpha helices of the recognition groove are unstable, particularly, in the alpha helices of both chains close to P1 and P4. Possibly, these changes are promoted by the interaction of the peptide (by Lys1, Lys2 and Phe3) with the lateral chains of MHC, searching an appropriate interaction (Knapp et al. 2010, James et al. 2009).

Peptide 1 manifested its immunogenicity by inducing antibodies in rabbits as it is shown in the neutralization assays. This property could be based on the molecular size, rigidity, chemical complexity, interaction with B-cell receptors or MHC and activation of helper T cells [Benjamin et al. 2009] The p1 proved to be an antigen that is recognized by the IgG Ab from immunized rabbits and infected individuals, using the methodology reported for other peptides (Madhumathi et al. 2010; Benkirane et al. 1993; Pandiaraja et al. 2010).

IgG antibodies in human serum, mainly the IgG2 isotype; demonstrate that clinical or subclinical infections with the influenza virus induced IgG to the peptide. Thus, the peptide is immunogenic and antigenic in humans. Although we did not directly demonstrate the interaction of p1 with MHC-II molecules in infected subjects, we believe that this interaction took place because class switching to produce IgG requires activated helper T cells that recognize the antigen (p1) in association with the MHC II protein on the surface of an antigen-presenting cell, such as B cells or dendritic cells. Moreover, the interaction of p1 with MHC-II molecules and T helper cells (CD4 T cells) was demonstrated by the class switch of the IgG isotype, which is mediated by cytokines produced by T helper cell activation after recognition of the peptide on MHC-II molecules and the engagement of the CD40 receptor on B cells by CD40 L (Rudolph et al. 2006; Stavnezer et al. 2008; Smith et al. 2009).

Peptides are protected against proteolytic degradation because B cells contain much lower levels of lysosomal proteases than macrophages. This favors the presentation of antigenic peptides on MHC class II molecules by limiting the complete destruction of the peptide determinants [Pandiaraja et al. 2010; Lennon et al. 2002; Delamarre et al. 2005]. In addition, the B-cell receptor may protect the peptide from proteolytic enzymes (selective processing) (Jemmerson et al. 1986). Through these two mechanisms, p1 could interact with MHC-II molecules as well as activate T helper cells and the production of IgG antibodies in humans and rabbits.

To serve as an antigen, a substance typically must have a relative molecular mass of at least 4,000 Daltons, and the peptide under study is approximately 1.9 kDa (1825.21 Daltons, 15 amino acid residues). Interestingly, this p1 is one of the few substances with low molecular weight (below 2,000) having antigenic properties (Loyola et al. 2013). Immunogenicity of a peptide is related to its amino acid composition and its diversity. As we mentioned above, Lys1, Lys2, and Phe3 contained in p1, interact with the pocket 1 and 4. In the native HA, the epitope corresponding to p1 is exposed, providing accessibility to Ab binding. Also, the polar residues are situated on the surface much more frequently than nonpolar residues; thus, the regions of highest average polarity within a polypeptide sequence have the highest likelihood of being targets for Ab binding. Evidence shows that mimic epitopes are continuous epitopes, specifically the sera from all the individual of our trial recognized the peptide p1. Therefore, we confirmed that is a B-cell epitope and it has been circulated previously in Mexican population, where clinical or subclinical infections with the influenza virus induced IgG Ab to the peptide p1.

The antibodies against p1 were mainly isotype IgG2, which is the most abundant in human sera. IgG2 isotype is less effective for complement activation and antibody-dependent cell-mediated cytotoxicity (ADCC) than other isotype, as IgG1 (Frazer et al. 1999; Srivastava et al. 2013). We propose that the effect of IgG2 isotype against peptide 1 could be the neutralization of the free virus, producing antiviral activity through the binding of antibodies to the receptor binding site of the HA, preventing the infection by the influenza virus (Xu et al. 2010). Moreover, the protection with IgG2 is noteworthy because patients with a severe infection with influenza H1N1

have lower levels of this isotype, and p1 peptide induces this specific isotype. Nevertheless, it is necessary to determine the neutralizing activity of the IgG2 isotype (Gordon et al. 2012). Finally, the results of the ConA and PRNT assays demonstrate that the antibodies produced peptides that are able to react with the protein of wild type virus and neutralize it. These results suggest that the p1 might be a candidate to be used as a peptide-based vaccine or in a diagnosis of the human influenza AH1N1.

An immunologic peptide obtained from the hemagglutinin protein structure of the influenza virus H1N1 has been conjugated to gold nanoparticles. UV/VIS absorption and first derivative of UV/VIS absorption suggest the formation of aggregates of gold nanoparticles for concentrations of peptide greater than 0.8  $\mu\text{g/ml}$ , whereas for concentrations lower than 0.8  $\mu\text{g/ml}$  the effect of the aggregation is less important. The net electric charge of peptide was estimated by using procedures of epitope predicting, obtaining a significant positive charge due to the contribution of lysine and arginine amino acids. This suggests that those groups can interact with the citrate groups of the surface of gold nanoparticles, which are negatively charged. SERS spectra of the conjugates with concentrations of peptide between 0.5 and 0.7  $\mu\text{g/ml}$  show enhance of the scattering of the most positively charged amino acids: lysine and arginine. Thus, this interval of concentrations 0.5-0.7  $\mu\text{g/ml}$  is adequate to immobilize the hemagglutinin peptide on the gold nanoparticles because of their enhanced Raman intensity compared with the rest of concentrations. Transmission electron microscopy images for concentration of 0.5  $\mu\text{g/ml}$  show the peptide layer covering each gold nanoparticle. This kind of nanostructure based on gold nanoparticles and immunologic peptide could be useful in biomedical applications.

## Chapter V. Conclusions

- Three peptides were designed using bioinformatic tools and tested as antigenic epitopes.
- A computational model of interaction between MHC II and a predicted epitope peptide was obtained by simulation of molecular recognition and molecular dynamics.
- The collected data of the MD showed how the peptide interacts with the pockets of the MHC II using two lysines as anchorage. These results also explain the conformational change in pockets 6 and 9.
- Improvement of the sequence enhanced the recognition by the immune system of the peptide. This knowledge offers a strategy to engineering immunogenic peptide.
- This thesis proposes an antigenic site unreported for H1N1 strain.
- Peptide 1 and 2 were recognized by sera considered as pre-pandemic and post-pandemic, showing that the epitope is recognized by circulating antibodies among Mexican population before the outbreak of 2009.
- Peptide 1 showed to be efficient in the production of neutralizing antibodies in a model of infected cells (MDCK) with human influenza virus A H1N1.
- This work establishes a concentration curve that allows a stable conjugated state between AuNPs and peptide 1.
- A SERS spectrum evidenced the amplification and modification of the spectrum by the conjugate.
- TEM images visualized the bioconjugation of the immunogenic peptide and gold nanoparticles.

## References

- Adegboyega KO, Chen PC, Xiaohua H, et al. (2007) Peptide-Conjugated Gold Nanorods for Nuclear Targeting. *Bioconjugate Chem* 18:1490-1497
- Aliaga AE, Osorio-Roman I, Garrido C, et al. (2009) Surface enhanced Raman scattering study of L-lysine. *Vibr Spect* 50:131-135
- Aliaga AE, Garrido C, Leyton P, et al. (2010) SERS and theoretical studies of arginine. *Spectrochem. Acta Part A* 76:458-463
- Alonso H, Bliznyuk AA, Gready JE (2006) Combining docking and molecular dynamic simulations in drug design. *Med Res Rev* 5:531-68
- Amaro RE, Baron R, McCammon JA (2008) An improved relaxed complex scheme for receptor flexibility in computer-aided drug design. *J Comput Aided Mol Des* 9:693-705
- Amicosante M, Gioia C, Montesano C, et al. (2002) Computer-based design of an HLA-haplotype and HIV-clade independent cytotoxic T-lymphocyte assay for monitoring HIV-specific immunity. *Mol Med* 12:798-807
- Apostolopoulos V, Yu M, Corper AL, et al. (2002) Crystal structure of a non-canonical low-affinity peptide complexed with MHC class I: a new approach for vaccine design. *J Mol Biol* 5:1293-305
- Arias CF and López S (2009) Anatomía del virus de la influenza A /H1N1-2009. *Ciencia* 14-24
- Baillie GJ, Galiano M, Agapow PM, et al. (2012) Evolutionary Dynamics of Local Pandemic H1N1/2009 Influenza Virus Lineages Revealed by Whole-Genome Analysis. *J Virol* 1:11
- Ballester PJ, Schreyer A, Blundell TL (2014) Does a more precise chemical description of protein-ligand complexes lead to more accurate prediction of binding affinity? *J Chem Inf Model* 3:944-55
- Beekman NJ, Schaaper WM, Turkstra JA, et al. (1999) Highly immunogenic and fully synthetic peptide-carrier constructs targeting GnRH. *Vaccine* 15-16:2043-50
- Benjamin DC, Berzofsky JA, East IJ, et al. (1984) The antigenic structure of proteins: a reappraisal. *Annu Rev Immunol* 2:67-101
- Benkirane N, Friede M, Guichard G, et al. (1993) Antigenicity and immunogenicity of modified synthetic peptides containing D-amino acid residues. *J Biol Chem* 268:26279-85
- Ben-Yedidia T and Arnon R (1997) Design of peptide and polypeptide vaccines. *Curr Opin Biotechnol* 4:442-8
- Bordner AJ (2013) Structure-based prediction of Major Histocompatibility Complex (MHC) epitopes. *Methods Mol Biol* 1061:323-43

- Brewer SH, Glomm WR, Johnson MC, et al. (2005) Probing BSA binding to citrate-coated gold nanoparticles and surfaces. *Langmuir* 20:9303-7
- Brownlee GG and Fodor E (2001) The predicted antigenicity of the haemagglutinin of the 1918 Spanish influenza pandemic suggests an avian origin. *Phil Trans R Soc Lond B* 356:1871-1876
- Brünger AT, Kuriyan J, Karplus M (1987) Crystallographic R factor refinement by molecular dynamics. *Science* 275:1478-1480
- Burlington DB, Clements ML, Meiklejohn G, et al (1983) Hemagglutinin-specific antibody responses in immunoglobulin G, A, and M isotypes as measured by enzyme-linked immunosorbent assay after primary or secondary infection of humans with influenza A virus. *Infect Immun* 2:540-5
- Burton DR, Desrosiers RC, Doms RW, et al. (2004) HIV vaccine design and the neutralizing antibody problem. *Nat Immunol* 3:233-6
- Camacho CJ and Zhang C (2005) FastContact: rapid estimate of contact and binding free energies *Bioinformatics* 10:2534-6
- Cárdenas C, Ortiz M, Balbín A, et al. (2005) Allele effects in MHC-peptide interactions: a theoretical analysis of HLA-DRbeta1\*0101-HA and HLA-DRbeta1\*0401-HA complexes. *Biochem Biophys Res Commun* 4:1162-7
- Cárdenas C, Obregón M, Balbín A, et al. (2007) Wave function analysis of MHC-peptide interactions. *J Mol Graph Model* 5:605-15
- Carlsson J, Boukharta L, Aqvist J (2008) Combining docking, molecular dynamics and the linear interaction energy method to predict binding modes and affinities for non-nucleoside inhibitors to HIV-1 reverse transcriptase. *J Med Chem* 9:2648-56
- Chan KH, To KK, Hung IF, et al. (2011) Differences in antibody responses of individuals with natural infection and those vaccinated against pandemic H1N1 2009 influenza. *Clin Vaccine Immunol* 5:867-73
- Chen YS, Hung YC, Lin WH et al. (2010) Assessment of gold nanoparticles as a size-dependent vaccine carrier for enhancing the antibody response against synthetic foot-and-mouth disease virus peptide. *Nanotechnology* 19:195101
- Ciacci-Zanella JR, Vincent AL, Prickett JR, et al. (2010) Detection of anti-influenza A nucleoprotein antibodies in pigs using a commercial influenza epitope-blocking enzyme-linked immunosorbent assay developed for avian species. *J Vet Diagn Invest* 1:3-9
- Comeau SR, Vajda S, Camacho CJ (2005) Performance of the first protein docking server ClusPro in CAPRI rounds 3-5. *Proteins* 2:239-44
- Comeau SR, Gatchell DW, Vajda S, Camacho CJ (2005) ClusPro: an automated docking and discrimination method for the prediction of protein complexes. *Bioinformatics* 1:45-50
- Correia BE, Ban YE, Holmes MA, et al. (2010) Computational design of epitope-scaffolds allows induction of antibodies specific for a poorly immunogenic HIV vaccine epitope. *Structure* 9:1116-26

- Dayan FE, Daga PR, Duke SO, et al. (2010) Biochemical and structural consequences of a glycine deletion in the alpha-8 helix of protoporphyrinogenoxidase. *Biochim Biophys Acta* 7:1548-56
- Dean R. Madden, David N. Garboczi and Don C. Wiley (1993) The antigenic identity of peptide-MHC complexes: A comparison of the conformations of five viral peptides presented by HLA-A2. *Cell* 4:693-708
- Deavin AJ, Auton TR, Greaney PJ (1996) Statistical comparison of established T-cell epitope predictors against a large database of human and murine antigens. *Mol Immunol* 2:145-55
- De Groot AS, Moise L, Liu R (2014) Cross-conservation of T-cell epitopes: now even more relevant to (H7N9) influenza vaccine design. *Hum Vaccin Immunother* 2:256-62
- De la Fuente JM and Berry C (2005) C Tat Peptide as an Efficient Molecule To Translocate Gold. Nanoparticles into the Cell Nucleus *Bioconjugate Chem* 5:1176–1180
- Delamarre, L., M. Pack, et al. (2005) Differential lysosomal proteolysis in antigen-presenting cells determines antigen fate. *Science* 5715:1630-4
- Díaz I, Pujols J, Ganges L, et al. (2009) In silico prediction and ex vivo evaluation of potential T-cell epitopes in glycoproteins 4 and 5 and nucleocapsid protein of genotype-I (European) of porcine reproductive and respiratory syndrome virus. *Vaccine* 41:5603-11
- Dormitzer PR, Ulmer JB, Rappuoli R (2008) Structure-based antigen design: a strategy for next generation vaccines. *Trends Biotechnol* 12:659-67
- Du L, Zhou Y, Jiang S (2010) Research and development of universal influenza vaccines. *Microbes Infect* 4:280-6
- El-Sayed IH, Huang X, El-Sayed MA (2005) Surface plasmon resonance scattering and absorption of anti-EGFR antibody conjugated gold nanoparticles in cancer diagnostics: applications in oral cancer. *Nano Lett* 5:829-34
- Flower DR (2003) Towards in silico prediction of immunogenic epitopes. *Trends Immunol* 12:667-74
- Frazer J and Capra J (1999) Immunoglobulins: structure and function. *Fundamental Immunology*. W. E. Paul Philadelphia-New York, Lippincott-Raven: 37-74
- Garten RJ, Davis CT, Russell CA, et al. (2009) Antigenic and Genetic Characteristics of Swine-Origin 2009 A(H1N1) Influenza Viruses Circulating in Humans *Science* 5937:197-201
- Gaschen B, Taylor J, Yusim K, et al. (2002) Diversity considerations in HIV-1 vaccine selection. *Science* 5577:2354-60
- Geysen HM, Barteling SJ, Meloan RH (1985) Small peptides induce antibodies with a sequence and structural requirement for binding antigen comparable to antibodies raised against the native protein. *Proc Natl Acad Sci* 1:178-82
- Ghersi D and Sanchez R (2009) Improving accuracy and efficiency of blind protein-ligand docking by focusing on predicted binding sites. *Proteins* 2:417-24



- Gogolak P, Simon A, Horvath A et al. (2000) Mapping of a Protective Helper T Cell Epitope of Human Influenza A Virus Hemagglutinin. *Biochem Biophys Res Comm* 270:190–198
- Goh GK, Dunker AK, Uversky VN (2009) Protein intrinsic disorder and influenza virulence: the 1918 H1N1 and H5N1 viruses. *Virology* 6:69
- Gordon CL, Holmes NE, Grayson ML, et al. (2012) Comparison of immunoglobulin G subclass concentrations in severe community-acquired pneumonia and severe pandemic 2009 influenza A (H1N1) infection. *Clin Vaccine Immunol* 3:446-8
- Gowthaman U, Agrewala JN (2008) In silico tools for predicting peptides binding to HLA-class II molecules: more confusion than conclusion. *J Proteome Res* 1:154-63
- Grossfield A, Feller SE, Pitman MC (2007) Convergence of molecular dynamics simulations of membrane proteins. *Proteins* 1:31-40
- Haiss W, Thanh N, Aveyard J, Fernig D (2007) Determination of size and concentration of gold nanoparticles from UV–Vis spectra. *Anal Chem* 79:4215–4221
- Haste-Andersen P, Nielsen M, Lund O (2006) Prediction of residues in discontinuous B-cell epitopes using protein 3D structures. *Protein Sci* 11:2558-67
- Hayat MA (1989) *Colloidal Gold: Principles, Method and Application*, Vol. 1. Academic Press Inc, New York
- He Y, Xiang Z, Mobley HL (2010) Vaxign: the first web-based vaccine design program for reverse vaccinology and applications for vaccine development. *J Biomed Biotechnol* 2010:297505
- Heiny AT, Miotto O, Srinivasan KN, et al (2007) Evolutionarily Conserved Protein Sequences of Influenza A Viruses, Avian and Human, as Vaccine Targets. *PLoS ONE* 11:e1190
- Helling F, Shang A, Calves M, et al. (1994) GD3 vaccines for melanoma: superior immunogenicity of keyhole limpet hemocyanin conjugate vaccines. *Cancer Res* 1:197-203
- Hermanson G (2008) *Bioconjugate Techniques* 2nd ed.: Academic Press Elsevier, San Diego
- Hess B, Carsten K, Van der Spoel D, et al. (2008) GROMACS 4: Algorithms for Highly Efficient, Load-Balanced, and Scalable Molecular Simulation. *J Chem Theory Comput* 3: 435–447
- Hetényi C and van der Spoel D (2002) Efficient docking of peptides to proteins without prior knowledge of the binding site. *Protein Sci.* 7:1729-37
- Horisberger M. (1992) Colloidal gold and its application in cell biology. *Int Rev Cytol Survey Cell Biology* 136: 227
- Huang P, Yu S, Wu C et al. (2013) Highly conserved antigenic epitope regions of hemagglutinin and neuraminidase genes between 2009 H1N1 and seasonal H1N1 influenza: vaccine considerations. *J Transl Med* 11:47

- Igarashi M, Ito K, Yoshida R, et al. (2010) Predicting the Antigenic Structure of the Pandemic (H1N1) 2009 Influenza Virus Hemagglutinin. *PLoS ONE* 1:e8553
- Insaïdoo FK, Borbulevych OY, Hossain M, et al. (2011) Loss of T cell antigen recognition arising from changes in peptide and major histocompatibility complex protein flexibility: implications for vaccine design. *J Biol Chem* 46:40163-73
- Iribarne F, Paulino M, Aguilera S, et al. (2002) Docking and molecular dynamics studies at trypanothione reductase and glutathione reductase active sites. *J Mol Model* 5:173-83
- James EA, Moustakas AK, Bui J, et al. (2009). The binding of antigenic peptides to HLA-DR is influenced by interactions between pocket 6 and pocket 9. *J Immunol* 5:3249-58
- Jemmerson, R. and Y. Paterson (1986) Mapping epitopes on a protein antigen by the proteolysis of antigen-antibody complexes. *Science* 4753:1001-4
- Jennings T and Strouse G (2007) Past, present, and future of gold nanoparticles. *Bio-Applications of Nanoparticles. Adv Exp Med Biol* 620:34-47
- Jørgensen KW, Buus S, Nielsen M (2010) Structural properties of MHC class II ligands, implications for the prediction of MHC class II epitopes. *PLoS One.* 12:e15877
- Karthick V, Ramanathan K (2013) Virtual screening for oseltamivir-resistant a (H5N1) influenza neuraminidase from traditional Chinese medicine database: a combined molecular docking with molecular dynamics approach. *Springerplus* 1:115
- Kaumaya PT, Van Buskirk AM, Goldberg E, Pierce SK (1992) Design and immunological properties of topographic immunogenic determinants of a protein antigen (LDH-C4) as vaccines. *J Biol Chem* 9:6338-46
- Kim S, Lee Y, Lazar P, et al. (2011) Binding conformation prediction between human acetylcholinesterase and cytochrome c using molecular modeling methods. *J Mol Graph Model* 8:996-1005
- Knapp B, Omasits U, Schreiner W, et al. (2010) A comparative approach linking molecular dynamics of altered peptide ligands and MHC with in vivo immune responses. *PLoS One* 7:e11653
- Kogan, MJ, Olmedo I, Hosta L et.al. (2007) Peptides and metallic nanoparticles for biomedical applications. *Nanomedicine* 2:287–306
- Król M, Chaleil RA, Tournier AL, et al. (2007) Implicit flexibility in protein docking: cross-docking and local refinement. *Proteins* 4:750-7
- Kupperberg P (2008) The influenza pandemic. 1918-1919. *Great Historic Disasters* Ed. Chelsea House USA.
- Larsen MV, Lundegaard C, Lamberth K, et al. (2007) Large-scale validation of methods for cytotoxic T-lymphocyte epitope prediction. *BMC Bioinformatics* 8:424
- Lata S, Bhasin M, Raghava GP (2007) Application of machine learning techniques in predicting MHC binders. *Methods Mol Biol* 409:201-15
- Lennon-Dumenil, Bakker A, et al. (2002) Analysis of protease activity in live antigen-presenting cells shows regulation of the phagosomal proteolytic contents during dendritic cell activation. *J Exp Med* 4:529-40

- Liao YC, Lin HH, Lin CH, et al. (2013) Identification of cytotoxic T lymphocyte epitopes on swine viruses: multi-epitope design for universal T cell vaccine. *PLoS One*. 12:e84443
- Liu FM, Ren B, Yan JW, et al. (2002) Initial oxidation processes on hydrogenated silicon surfaces studied by in situ Raman spectroscopy. *J. Electrochem. Soc* 149:G95-G99
- Lohia N and Baranwal M (2014) Conserved Peptides Containing Overlapping CD4+ and CD8+ T-Cell Epitopes in the H1N1 Influenza Virus: An Immunoinformatics Approach. *Viral Immunol* 27(5):225-34
- Loyola PK, Campos-Rodríguez R, Bello M, et al. (2013) Theoretical analysis of the neuraminidase epitope of the Mexican A H1N1 influenza strain, and experimental studies on its interaction with rabbit and human hosts. *J Immunol Res* 1:44-60
- Madhumathi J, Prince PR, Anugraha G, et al. (2010) Identification and characterization of nematode specific protective epitopes of *Brugia malayi* TRX towards development of synthetic vaccine construct for lymphatic filariasis. *Vaccine* 31:5038-48
- Maganti L and Ghoshal N (2014) Probing the structure of *Mycobacterium tuberculosis* MbtA: model validation using molecular dynamics simulations and docking studies. *J Biomol Struct Dyn* 2:273-88
- Mallios RR (2003) A consensus strategy for combining HLA-DR binding algorithms. *Hum Immunol* 9:852-6
- Mavrouli MD, Routsias JG, Maltezou HC, et al. (2011) Estimation of seroprevalence of the pandemic H1N1 2009 influenza virus using a novel virus-free ELISA assay for the detection of specific antibodies. *Viral Immunol* 3:221-6
- McLean JA, Stumpo KA, Russell DH (2005) Size-selected (2-10 nm) gold nanoparticles for matrix assisted laser desorption ionization of peptides. *J Am Chem Soc* 127:5304-5
- Meroz D, Yoon SW, Ducatez MF, et al. (2011) Putative amino acid determinants of the emergence of the 2009 influenza A (H1N1) virus in the human population. *Proc Natl Acad Sci* 33:13522-7
- Metropolis N, Rosenbluth, AW, Rosenbluth, MN et al. (1954) Equation of State Calculations by Fast Computing Machines. *J Chem Phys* 21:1087-1092
- Moise L, McMurry JA, Buus S, et al. (2009) .In silico-accelerated identification of conserved and immunogenic variola/vaccinia T-cell epitopes. *Vaccine* 46:6471-9
- Moreau V, Fleury C, Piquer D, Nguyen C, Novali N, et al. (2008) PEPOP: computational design of immunogenic peptides. *BMC Bioinformatics* 9: 71
- Moreau V, Granier C, Villard S, et al. (2006) Discontinuous epitope prediction based on mimotope analysis. *Bioinformatics* 9:1088-95
- Morens DM, Halstead SB, Repik PM, et al. (1985) Simplified plaque reduction neutralization assay for dengue viruses by semimicro methods in BHK-21 cells: comparison of the BHK suspension test with standard plaque reduction neutralization. *J Clin Microbiol* 2:250-4

- Morris GM, Huey R, Olson AJ (2008) Using AutoDock for ligand-receptor docking. *Curr Protoc Bioinformatics* 8:8.14
- Narambuena CF and Leiva EPM (2014) Monte Carlo Studies in Polyelectrolyte Solutions: Structure and Thermodynamics. *Polyelectrol Engin Mat* 349-379
- Norde W (1986) Adsorption of proteins from solution at the solid-liquid interface. *Adv. Colloid Interface Sci* 25: 267
- Obeid OE, Partidos CD, Howard CR, et al. (1995) Protection against morbillivirus-induced encephalitis by immunization with a rationally designed synthetic peptide vaccine containing B- and T-cell epitopes from the fusion protein of measles virus. *J Virol* 3:1420-8
- Ofek G, Guenaga FJ, Schief WR, et al. (2010) Elicitation of structure-specific antibodies by epitope scaffolds. *Proc Natl Acad Sci* 42:17880-7
- Oh E, Delehanty JB, Sapsford KE (2011) Cellular uptake and fate of PEGylated gold nanoparticles is dependent on both cell-penetration peptides and particle size. *ACS Nano* 8:6434-48
- Painter CA, Cruz A, López GE, et al. (2008) Model for the Peptide-Free Conformation of Class II MHC Proteins. *PLoS ONE* 6:e2403.
- Palese P (2004) Influenza: Old and new threats. *Nature Medicine Supplement* 12:s82-s87
- Pandiaraja P, Arunkumar C, Hoti SL, et al. (2010) Evaluation of synthetic peptides of WbSXP-1 for the diagnosis of human lymphatic filariasis. *Diagn Microbiol Infect Dis* 68:410-5
- Peters B, Sidney J, Bourne P, Bui HH, Buus S, et al. (2005) The immune epitope database and analysis resource: from vision to blueprint. *PLoS Biol* 3:e91
- Platania CB, Salomone S, Leggio GM, et al. (2012) Homology modeling of dopamine D2 and D3 receptors: molecular dynamics refinement and docking evaluation. *PLoS One* 9:e44316
- Prabdial-Sing N, Puren AJ, Bowyer SM (2012) Sequence-based in silico analysis of well-studied hepatitis C virus epitopes and their variants in other genotypes (particularly genotype 5a) against South African human leukocyte antigen backgrounds. *BMC Immunol* 13:67
- Potter CW (2001) A history of influenza. *J Appl Microbiology* 91: 572-579
- Raman S, Machaidze G, Lustig A (2006) Structure-based design of peptides that self-assemble into regular polyhedral nanoparticles. *Nanomedicine* 2:95-102
- Raval A, Piana S, Eastwood MP, et al. (2012) Refinement of protein structure homology models via long, all-atom molecular dynamics simulations. *Proteins* 8:2071-9
- Rimmelzwaan GF, Baars M, Claas EC, Osterhaus AD (1998) Comparison of RNA hybridization, hemagglutination assay, titration of infectious virus and immunofluorescence as methods for monitoring influenza virus replication in vitro. *J Virol Methods* 1:57-66

- Robinson JE, Holton D, Liu J, et al. (1990) A novel enzyme-linked immunosorbent assay (ELISA) for the detection of antibodies to HIV-1 envelope glycoproteins based on immobilization of viral glycoproteins in microtiter wells coated with concanavalin A. *J Immunol Methods* 1:63-71
- Rocklin GJ, Boyce SE, Fischer M, et al. (2013) Blind prediction of charged ligand binding affinities in a model binding site. *J Mol Biol* 22:4569-83
- Rojas-López M, Orduña-Díaz A, Delgado-Macuil R, et al. (2006) Morphological transformation and kinetic analysis in the aluminum-mediated a-Si:H crystallization. *J. Non-Cryst. Solids* 352:281-284
- Rojas-López M, Orduña-Díaz A, Delgado-Macuil R, et al. (2010) a-Si:H crystallization from isothermal annealing and its dependence on the substrate used. *Mat Sci Engineering B* 174:137–140
- Rosendahl HS, van Beek J, de Jonge J, et al. (2014) T cell responses to viral infections - opportunities for Peptide vaccination. *Front Immunol.* 5:171
- Rothbard JB and Taylor WR (1988) A sequence pattern common to T cell epitopes. *EMBO J* 1:93-100
- Rudolph MG, Stanfield RL, Wilson IA (2006) How TCRs bind MHCs, peptides, and coreceptors. *Annu Rev Immunol* 24:419-66
- Saito T and Masato T (2000) Vaccines and therapeutics against influenza virus infections. *Pediatrics International* 42: 219–225
- Salimi N, Fleri W, Peters B, Sette A (2010) Design and utilization of epitope-based databases and predictive tools. *Immunogenetics* 4:185-96
- Samji T (2009) Influenza A: Understanding the Viral Life Cycle. *Yale Journal of Biology and Medicine* 82:153-159
- Sanjay M, Veena CV, Akhilesh CM, Shailesh D. Pawar et al. (2011) Pandemic (H1N1) 2009 influenza virus induces weaker host immuneresponses in vitro: a possible mechanism of high transmissibility. *Virology* 8:140
- Schubert B, Lund O, Nielsen M (2013) Evaluation of peptide selection approaches for epitope-based vaccine design. *Tissue Antigens* 4:243-51
- Sette A and Fikes J (2003) Epitope-based vaccines: an update on epitope identification, vaccine design and delivery. *Curr Opin Immunol* 4:461-70
- Schanen BC, De Groot AS, Moise L, et al. (2011) Coupling sensitive in vitro and in silico techniques to assess cross-reactive CD4(+) T cells against the swine-origin H1N1 influenza virus. *Vaccine* 17:3299-309
- Shaw ML, Stone KL, Colangelo CM et al. (2008) Cellular Proteins in Influenza Virus Particles. *PLOS Pathogens* 6:e1000085
- Seeliger D and de Groot BL (2010) Ligand docking and binding site analysis with PyMOL and Autodock/Vina. *J Comput Aided Mol Des* 5:417-22
- Senda Y, Fujio M, Shimamura S, et al. (2012) Fast convergence to equilibrium for long-chain polymer melts using a MD/continuum hybrid method. *J Chem Phys* 15:154115

- Shahlaei M, Madadkar-Sobhani A, Mahnam K, Fassihi A, et al. (2011) Homology modeling of human CCR5 and analysis of its binding properties through molecular docking and molecular dynamics simulation. *Biochim Biophys Acta* 3:802-17
- Sinigaglia F and Hammer J (1994) Rules for peptide binding to MHC class II molecules. *APMIS* 102:241–8
- Singh H and Raghava GP (2001) ProPred: prediction of HLA-DR binding sites. *Bioinformatics* 12:1236-7
- Slocik JM, Stone MO, Naik RR (2005) Synthesis of gold nanoparticles using multifunctional peptides. *Small* 11:1048-52
- Smith JD, Vijaykrishna D, Bahl J, et al. (2009) Origins and evolutionary genomics of the 2009 swine-origin H1N1 influenza A epidemic. *Nature* 25:1122-1126
- Smith KM (1962) *Viruses*. Oxford Press London.
- Smith LJ, Daura X, Van Gunsteren WF (2002) Assessing equilibration and convergence in biomolecular simulations. *Proteins* 3:487-96
- Smith-Garvin JE, Koretzky GA, Jordan MS (2009) T cell activation. *Annu Rev Immunol* 27:591-619
- Sohn J, Parks JM, Buhrman G et al. (2005) Experimental validation of the docking orientation of Cdc25 with its Cdk2-CycA protein substrate. *Biochemistry* 50:16563-73
- Sonvico F, Dubernet C, Colombo P, et al. (2005) Metallic colloid nanotechnology, applications in diagnosis and therapeutics. *Curr Pharm Des* 11:2091
- Southwood S, Sidney J, Kondo A, et al. (1998) Several common HLA-DR types share largely overlapping peptide binding repertoires. *J Immunol* 7:3363-73
- Srivastava V, Yang Z, Hung IF, et al. (2013) Identification of dominant antibody-dependent cell-mediated cytotoxicity epitopes on the hemagglutinin antigen of pandemic H1N1 influenza virus. *J Virol* 10:5831-40
- Stavnezer J, Guikema JE, Schrader CE (2008) Mechanism and regulation of class switch recombination. *Annu Rev Immunol* 26:261-92.
- Steinhauer DA and Skehel JJ (2002) Genetics of influenza viruses. *Annu Rev Genet* 36:305–32
- Strambi A, Mori M, Rossi M, et al. (2013) Structure prediction and validation of the ERK8 kinase domain. *PLoS One* 1:e52011.
- Sullivan SJ, Jacobson RM, Dowdle WR et al. (2010) 2009 H1N1 Influenza *Mayo Clin Proc* 1:64-76
- Sun J, Di W, Tianlei X, Xiaojing W, et al. (2009) SEPPA: a computational server for spatial epitope prediction of protein antigens. *Nucleic Acids Res* 37:W612–W616
- Sundaram R, Lynch MP, Rawale SV, et al. (2004) De novo design of peptide immunogens that mimic the coiled coil region of human T-cell leukemia virus type-1 glycoprotein 21 transmembrane subunit for induction of native protein reactive neutralizing antibodies. *Biol Chem* 23:24141-51

- Taborda CP, Juliano MA, Puccia R, et al. (1998) Mapping of the T-cell epitope in the major 43-kilodalton glycoprotein of *Paracoccidioides brasiliensis* which induces a Th-1 response protective against fungal infection in BALB/c mice. *Infect Immun* 2:786-93
- Takemura K, Guo H, Sakuraba S, et al. (2012) Evaluation of protein-protein docking model structures using all-atom molecular dynamics simulations combined with the solution theory in the energy representation. *J Chem Phys* 21:215105
- Tangri S, Ishioka GY, Huang X, et al. (2001) Structural features of peptide analogs of human histocompatibility leukocyte antigen class I epitopes that are more potent and immunogenic than wild-type peptide. *J Exp Med* 6:833-46
- Taubenberger JK (1) and Morens D (2006) 1918 Influenza: the Mother of All Pandemics. *Emergency Infectious Diseases*. 1:15-22
- Taubenberger JK (2) (2006) The Origin and Virulence of the 1918 “Spanish” Influenza Virus. *Proc Am Philos Soc* 1:86–112
- Taubenberger JK (3), Reid AH, Krafft AE, et al. (1997) Initial genetic characterization of the 1918 "Spanish" influenza virus. *Science* 5307:1793-6
- Terentiev AA, Moldogazieva NT, Levtsova OV, et al. (2012) Modeling of three dimensional structure of human alpha-fetoprotein complexed with diethylstilbestrol: docking and molecular dynamics simulation study *J Bioinform Comput Biol* 2:1241012
- Teixeira AAR, Lund M, Barroso da Silva FL (2010) Fast Proton Titration Scheme for Multiscale Modeling of Protein Solutions *J Chem Theory Comput* 10:3259-3266
- Tkachenko AG, Xie H, Coleman D, Glomm, W (2003) Multifunctional gold nanoparticle-peptide complexes for nuclear targeting. *J Am Chem Soc* 125:4700–4701
- Trombetta ES and Mellman I (2005) Cell biology of antigen processing in vitro and in vivo. *Annu Rev Immunol* 23:975-1028
- Villadangos JA (2001) Presentation of antigens by MHC class II molecules: getting the most out of them. *Mol Immunol*. 5:329-46
- Vorobjev YN (2010) Blind docking method combining search of low-resolution binding sites with ligand pose refinement by molecular dynamics-based global optimization. *J Comput Chem*. 5:1080-92
- Walavalkar NM, Gordon N, Williams DC Jr. (2013) Unique features of the anti-parallel, heterodimeric coiled-coil interaction between methyl-cytosine binding domain 2 (MBD2) homologues and GATA zinc finger domain containing 2A (GATAD2A/p66 $\alpha$ ) *J Biol Chem* 5:3419-27
- Walker LM and Burton DR 2010 Rational antibody-based HIV-1 vaccine design: current approaches and future directions. *Curr Opin Immunol* 3:358-66
- Wang CY, Chang TY, Walfield AM, et al. (2002) Effective synthetic peptide vaccine for foot-and-mouth disease in swine. *Vaccine* 19-20:2603-10
- Wangoo N, Bhasin KK, Meht SK, et al. (2008) Synthesis and capping of water-dispersed gold nanoparticles by an amino acid: bioconjugation and binding studies. *J Colloid Interface Sci* 323:247

- Weidanz JA, Piazza P, Hickman-Miller H, et al. (2007) Development and implementation of a direct detection, quantitation and validation system for class I MHC self-peptide epitopes. *J Immunol Methods* (1-2):47-58
- West AP Jr, Scharf L, Horwitz J, et al (2013) Computational analysis of anti-HIV-1 antibody neutralization panel data to identify potential functional epitope residues. *Proc Natl Acad Sci* 26:10598-603
- Wieggers KJ, Wetz K, Dernick R (1990) Molecular basis for linkage of a continuous and discontinuous neutralization epitope on the structural polypeptide VP2 of poliovirus type 1. *J Virol* 3:1283-9
- Wiley DC, Skehel JJ (1987) The Structure and Function of the Hemagglutinin Membrane Glycoprotein of Influenza Virus. *Ann Rev Biochem* 56:365-394
- Wood JM (2001) Developing vaccines against pandemic influenza. *Phil Trans. R. Soc. Lond. B* 356:1953-1960
- Xu R, Damian CE, Krause JC, et al. (2010) Structural basis of pre-existing immunity to the 2009 H1N1 pandemic influenza virus. *Science* 5976:357–360
- Yang J, Aslimovska L, Glaubitz C (2011) Molecular dynamics of proteorhodopsin in lipid bilayers by solid-state NMR. *J Am Chem Soc.* 13:4874-81
- Yano A, Onozuka A, Asahi-Ozaki Y, et al. (2005) An ingenious design for peptide vaccines. *Vaccine* 17-18:2322-6
- Yano A, Miwa Y, Kanazawa Y, et al. (2013) A novel method for enhancement of peptide vaccination utilizing T-cell epitopes from conventional vaccines. *Vaccine* 11:1510-5
- Yu K, Petrovsky N, Schönbach C, et al. (2002) Methods for prediction of peptide binding to MHC molecules: a comparative study. *Mol Med* 3:137-48



## Journal of Molecular Recognition - Decision on Manuscript ID JMR-14-0114.R1

---

De: **onbehalfof+vanregen+esbs.u-strasbg.fr@manuscriptcentral.com** en nombre de **vanregen@esbs.u-strasbg.fr**

Enviado: jueves, 15 de enero de 2015 02:04:19 a.m.

Para: **cdln\_jp@hotmail.com; cdlnjpc@gmail.com**

15-Jan-2015

Dear Dr. Carrillo,

It is a pleasure to accept your manuscript entitled "A continuous peptide epitope reacting with pandemic influenza AH1N1 predicted by bioinformatic approaches" in its current form for publication in Journal of Molecular Recognition. The comments of the referee(s) who reviewed your manuscript are included at the bottom of this letter.

A signed copyright transfer agreement is needed for publication. If you have not already provided us with one you can access the copyright transfer agreement at:

<http://media.wiley.com/assets/1540/95/ctapsglobal.pdf>

To enable the publisher to disseminate the author's work to the fullest extent, the author must sign a Copyright Transfer Agreement, transferring the copyright of the article from the author to the publisher.

If you have not yet uploaded a CTA, please ensure that you have identified the form with the manuscript ID number; scan your signed CTA and e-mail to [ctaforms@wiley.com](mailto:ctaforms@wiley.com) stating the manuscript ID number in the subject line of the e-mail.

Please note that this does not take away your rights to reuse your own article after publication, and that if the copyright belongs to your employing institution, they should sign the form instead of you.

If you have already provided us with the signed form, you do not need to do anything at this stage. You will be contacted by our typesetters/copyeditors shortly.

Thank you for your fine contribution.

Sincerely,

Prof. Marc Van Regenmortel  
Editor, Journal of Molecular Recognition  
vanregen@esbs.u-strasbg.fr

Reviewer comments to Author (Please note that these comments may have been delivered to us as files. We attach a description at the bottom how to access them.)

Reviewer: 1

Comments to the Author

The authors has resubmitted the manuscript with a number of improvements and clarifications. No further revisions are deemed necessary prior to publication.

Reviewer: 2

Comments to the Author

I agree with the revision

# A continuous peptide epitope reacting with pandemic influenza AH1N1 predicted by bioinformatic approaches

Jonathan P. Carrillo-Vazquez<sup>a</sup>, José Correa-Basurto<sup>b</sup>, Jazmin García-Machorro<sup>c</sup>, Rafael Campos-Rodríguez<sup>d</sup>, Violaine Moreau<sup>e</sup>, Jorge L. Rosas-Trigueros<sup>f</sup>, Cesar A. Reyes-López<sup>a</sup>, Marlon Rojas-López<sup>g</sup> and Absalom Zamorano-Carrillo<sup>a\*</sup>



Q2

Computational identification of potential epitopes with an immunogenic capacity challenges immunological research. Several methods show considerable success, and together with experimental studies, the efficiency of the algorithms to identify potential peptides with biological activity has improved. Herein, an epitope was designed by combining bioinformatics, docking, and molecular dynamics simulations. The hemagglutinin protein of the H1N1 influenza pandemic strain served as a template, owing to the interest of obtaining a scheme of immunization. Afterward, we performed enzyme-linked immunosorbent assay (ELISA) using the epitope to analyze if any antibodies in human sera before and after the influenza outbreak in 2009 recognize this peptide. Also, a plaque reduction neutralization test induced by virus-neutralizing antibodies and the IgG determination showed the biological activity of this computationally designed peptide. The results of the ELISAs demonstrated that the serum of both pre-pandemic and pandemic recognized the epitope. Moreover, the plaque reduction neutralization test evidenced the capacity of the designed peptide to neutralize influenza virus in Madin-Darby canine cells. Copyright © 2015 John Wiley & Sons, Ltd. Additional supporting information may be found in the online version of this article at the publisher's web site.

**Keywords:** Peptide, Influenza, Bioinformatic

## INTRODUCTION

The study of viral infectious diseases is of interest in the public health of any community. Molecular basis and new technologies are investigated and developed to improve the diagnostic and treatment of these pathologies, requiring a considerable financial resource to reach results [1]. Influenza virus has been considered as the primary cause of severe flu, which is 15% of all cases worldwide [2]. High mortality rates produced by antigenic variation make the control of this illness difficult [3]. Influenza, transmitted by a negative single-stranded virus, presents antigenic drift and antigenic shift, resulting in epidemics and pandemics [4]. Currently, vaccine development for influenza is related to the search for a method or a group of methods to discover a universal epitope that allows a more comprehensive immunization [5,6]. Many epitopes and sequences of distinct influenza virus strains have been reported, and various arise from the viral surface proteins [7–9]. These proteins are the best source of epitope data because they are localized in the most external part of a viral particle, participating in the process of viral adhesion into the host cell [10]. The influenza virus has four surface proteins. Two of them, M1 and M2, are in the inner part of the particle and include the most conserved sequences of amino acids [11,12]. The others, hemagglutinin (HA) and neuraminidase (NA), exhibit the highest antigenic variation of all influenza proteins and confer antigenic exposure to the immune cells of the host during the

\* Correspondence to: A. Zamorano-Carrillo, Laboratorio de Bioquímica y Biofísica Computacional, Doctorado en Biotecnología, ENMH—IPN, Mexico, D.F., Mexico.  
E-mail: absalomz2002@gmail.com

a J. P. Carrillo-Vazquez, C. A. Reyes-López, A. Zamorano-Carrillo  
Laboratorio de Bioquímica y Biofísica Computacional, Doctorado en Biotecnología ENMH—IPN, Mexico, D.F., Mexico

b J. Correa-Basurto  
Laboratorio de Modelado Molecular y Diseño de Fármacos, Escuela Superior de Medicina—IPN, Mexico, D.F., Mexico

c J. García-Machorro  
Laboratorio de Medicina de Conservación, Escuela Superior de Medicina—IPN, Mexico, D.F., Mexico

d R. Campos-Rodríguez  
Laboratorio de Inmunología Molecular, Escuela Superior de Medicina—IPN, Mexico, D.F., Mexico

e V. Moreau  
CNRS FRE 3009, SysDiag, CAP DELTA, Montpellier, France

f J. L. Rosas-Trigueros  
Laboratorio Transdisciplinario de Investigación en Sistemas Evolutivos SEPI-ESCOM-IPN, Mexico, D.F., Mexico

g M. Rojas-López  
Centro de Investigación en Biotecnología Aplicada—IPN, Tlaxcala, Mexico

entrance of the virus [13–15]. Mainly, HA exhibits four antigenic sites known as Ca, Cb, Sa, and Sb (Figure 1A and B) [16–18].

Some theoretical and experimental methods identify epitopes that can be the initial candidates for peptide vaccine design or new targets for molecular diagnosis [19–21]. Computational tools used for the prediction of epitopes include theoretical understanding of molecular interactions [22,23]. Bioinformatics research has developed mainly two strategies to predict epitopes: structural-based [24,25] and sequence-based predictors [26–28]. In the former, the search is focused on three-dimensional (3D) structure information [29,30], whereas the second strategy uses sequences related to immunogenicity. Both strategies depend on the content of databases with theoretical and experimental information where individual epitopes or sequences have been described as antigenic or immunogenic. Some tools also use the information of epitopes capable of being recognized by the major histocompatibility complex (MHC) class II. However, this addition to these methods of prediction remains an open problem because of the difficulty to predict T-cell responses [31,32]. Also, a problem lies in the epitopes mimicked by synthetic peptides because a sequence size of 6–10 residues is needed for antigen reactivity; nevertheless, they have been studied extensively in animal models with various results [33,34].

Usually, promising results have the potential to not only decrease costs but also avoid unwanted responses that occur with vaccines derived from attenuated live or killed pathogens [35,36]. In this work, we identify an epitope of the H1N1 human influenza strain through combining bioinformatic tools such as structural and sequential epitope predictors. Furthermore, docking and molecular dynamics (MD) simulations were used to analyze the interaction between the epitope and the MHC II molecule [37,38]. These bioinformatic simulations suggest how

the peptide interacts with the pockets of the recognition groove of the MHC molecule and give information that could be useful for rational vaccine design. As a case for studying, we predicted a highly immunogenic continuous epitope of HA of the influenza strain AH1N1 2009 [39–41]. Additionally, as an experimental counterpart, a plaque reduction neutralization test (PRNT) induced by virus-neutralizing antibodies was performed to evaluate the peptide functionality.

## Results

### 3D model selection of the HA of the human influenza H1N1

In early 2009, Di and coworkers reported a homology model of the HA H1N1 influenza strain and predicted some epitopes by SEPPA program [25]. Later, in 2010, Xu and coworkers reported the crystallographic coordinates of influenza HA trimer with a Protein Data Bank (PDB) code 3LZG [42]. Although both 3D models show high similarity, in this work, we used 3LZG and its corresponding protein sequence.

### Prediction of the epitope

Two epitope prediction methods were used, that is, sequence-based and structure-based predictors. Structural predictors, according to their strategy, localize more exposed sequences of amino acids and discard epitopes in hidden domains. Likewise, epitopes located in  $\alpha$ -helix and  $\beta$ -folded regions were discarded because, despite these regions having less mobility, they could be difficult to recognize by the MHC and usually are hidden inside the protein. In contrast, loops or tails are more recognizable and become accommodated in the corresponding pockets by the MHC molecule because of their flexibility. Furthermore, these

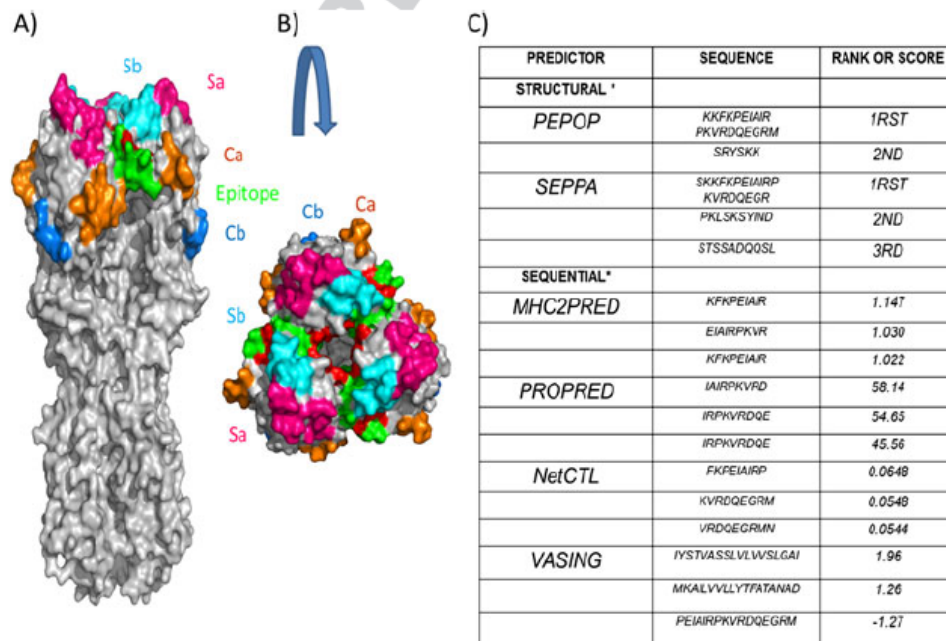


**Figure 1.** Antigenic sites of HA and scores obtained from computational epitope predictors. (A) Three-dimensional representation of the HA trimer by Xu and coworkers. The antigenic sites of the HA highlighted in colors Sa, Sb, Ca, and Cb. The localization of the epitope predicted by PEPOP and its core are highlighted in green and red, respectively. (B) Superior view of the globular head of the HA trimer. (C) Rankings or scores of the sequence predicted according to the scale in the context of each software predictor.



structures were considered for the structural modeling of the immunogenic peptide [43,44]. The first system of prediction used was that implemented in the PEPOP server, and its results were compared with the other predictors (Figure 1C). PEPOP played the role of the initial reference because of its several features (length, amino acids, beta-turns, and hydrophobicity) that filter and refine the epitope search for the best structural prediction. In this initial approach, three more conditions were required: high score for MHC II recognition, presence of the epitope in a conserved region, and at the same time belonging to a structurally exposed domain. Therefore, we submitted into the PEPOP server two main chains, those corresponding to the HA trimer retrieved from 3LZG. A 20-residue-length epitope was requested to obtain a domain that could be recognized or processed by the immune system, in particular, by the MHC II [45–47]. Several amino acid sequences were predicted; however, owing to the absence of scientific reports and to our knowledge about these sequences, the epitope sequence KKFKEIAIRPKVRDQEGRM (211–230 of chain A) was selected. The interest for this epitope is also due to it being located in the globular head of the HA. This surface portion is near a Ca2 antigenic site and includes the receptor binding region (Figure 1A and B) [48]. Also, it is known that residue 225 affects the receptor binding specificity of avian and human H1N1 viruses [49]. The epitope prediction presents a core of 10 amino acids (EIAIRPKVRD); according to the score of the PEPOP software, these represent the highest content of immunogenicity. When we compared the result of PEPOP with the other predictors, this sub-sequence (core) was also preferred by the epitope–MHC II and epitope–B cell predictors (Figure 1C).

A characterization of the predicted peptide was performed by the Peptide Property Calculator program ([www.genscript.com/ssl-bin/site2/peptide\\_calculation.cgi](http://www.genscript.com/ssl-bin/site2/peptide_calculation.cgi)), showing that its sequence has 40% hydrophobicity, 50% hydrophilicity, 15% acidic composition, and 35% basic composition. These proportions are essential for the peptide because they are related to immunogenicity [50,51]. The corresponding sequence of the epitope was submitted to a Protein–Protein Basic Local Alignment Search and Position-specific Iterated Basic Local Alignment Search (<http://blast.ncbi.nlm.nih.gov/>), resulting in it having a complete identity (100%) with a human protein related to a methyl-CpG-binding group (UNIPROT code: Q8WWY6) [52]. This protein is localized to the nucleus and restricted to the round spermatids in the postmeiotic stages of the male germ cell development. The score for identity was 100% only in the residues KVRDQEGR, and in the rest of the BLAST, alignments showed less than 90% of identity because of gaps. It is worthy to mention that the predicted epitope might not induce an autoimmune response because the methyl-CpG-binding trait is confined to the nucleus.

#### Docking and MD simulations of the peptide with the MHC class II

Three-dimensional models of the peptides and MHC II were used to describe the interactions between them by docking studies with AutoDock 4.0.1 (focused) and blind docking with CLUSPRO program [53,54]. The CLUSPRO program depicts free energy of the molecular interaction between the peptides and MHC II as the best free energy values (data not shown). The results demonstrate that the epitope predicted by PEPOP can be bonded by the MHC II recognition groove, with blind or restricted docking. A characteristic of docking is that the target, in this case MHC II, neglects the flexibility and the explicit solvent effects [55].

Therefore, from a complex obtained by AutoDock, MD simulations for 100 ns were performed to refine the epitope–MHC II complex with GROMACS [56–59]. To describe the epitope–MHC II interactions, we focused on the epitope recognition by the well-known MHC II pockets (P1, P4, P6, P7, and P9) located inside the recognition groove (Figure 2A). These regions participate in the formation of the epitope–MHC II complex necessary for the antigen presentation, and MD simulations provided evidence that the epitope reaches all MHC pockets [46,47]. The last structure reached by the MD simulations shows some changes in all the pockets, especially in P1 and P4. Also, during the simulations, Lys1 approaches the P1 (Gly86 in chain B) rapidly, although it interacts with residues nearby the P4 (Cys79 and Arg80 in chain B). Lys2, with less mobility, also interacts with P4; in particular, sharing with the Lys1 an interaction with the Cys79 (data not shown). Phe3 plays an interesting role because, during MD simulation, it interacts with residue of both chains Ile8 (chain A) and His13 (chain B, P4), suggesting that hydrophobic amino acids play a significant role in antigen processing. Also, the interaction formed by Tyr78 (chain B, P4) and Arg10 was evidenced as stabilizing. Regarding P6 and P7, the Val65 (chain A) and Leu67 (chain B) were nearby Glu6 and Arg19, respectively (Figure 2).

To examine the epitope–MHC II complex interactions during the MD simulations, we analyzed the root mean square deviation (RMSD) and root mean square fluctuation (RMSF) values (Figure 3). The RMSD analysis showed that the model reaches convergence approximately at 20 ns and remains stable during the rest of the MD simulation (100 ns) (Figure 3A) [60–62]. Also, the RMSF values were retrieved from the three chains of the complex (chain A spanning from 4 to 181, B from 2 to 190, both of the MHC II, and C corresponding to 20 of the peptides) (Figure 3B and C). The MHC II was analyzed in each chain; chain A shows many long movements in a region, spanning from residues 30 to 60, that involves the pocket 1 and the initial part of the pocket 6. The RMSF values studied from chain B have first pick; this phenomenon was due to the flexibility of the amino acids in the amino-terminal region (residues 2, 3, and 4). Other regions present a local maximum because of the lack of some amino acids in the chain; this gap spans from residues 105 to 113 of chain B. The chain B residues that were involved in long movements were from the region near pockets 1, 7, and 9 (Figure 2B). The RMSF values show that the Phe3 of the peptide is the only amino acid that has limited movements compared with the rest of the peptide. The limited changes are due to the P1 and especially P4 with the His13, which is one of the unique binding residues of the P4. All the rest of the residues have variable movements, but when the complex achieves convergence, the residues become more limited in their movements (Figure 3C).

#### Design of the peptides

The peptide was revised to explore the versatility of the epitope in order to improve it by editing its residue sequence according to the literature and the analysis *in silico* [63–65]. The epitope predicted was modified to reduce its possible autoimmune response due to its complete homology with a human protein related to spermatogenesis. These modifications included the removal of the last five residues that belong to the homology region of the protein related to a methyl-CpG-binding group (KKFKPEIAIRPKVRDQEGRM). The second modification obeys the MD simulations results where the amino-terminal region showed

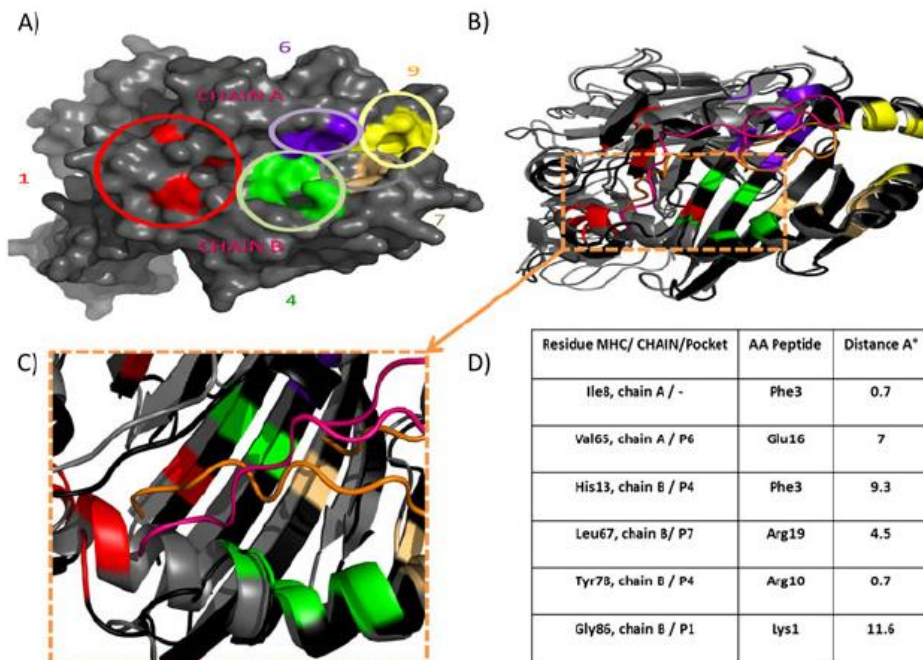


**Figure 2.** Pockets of the MHC and their interaction with the epitope. (A) Three-dimensional surface representation of the MHC molecule, circled and highlighted in color the pockets that involve the interaction with the epitope predicted by PEPOP (P1 = red, P4 = green, P6 = blue, P7 = light orange and P9 = yellow). (B) Superposition of the final docking map (gray) and the 100 ns simulation (black). (C) Zoom near the pockets 1 and 4 of the recognition groove. (D) Distances obtained by a contact map analysis, some of these interactions are with specific amino acids of the pockets 1, 4, 6, and 7.

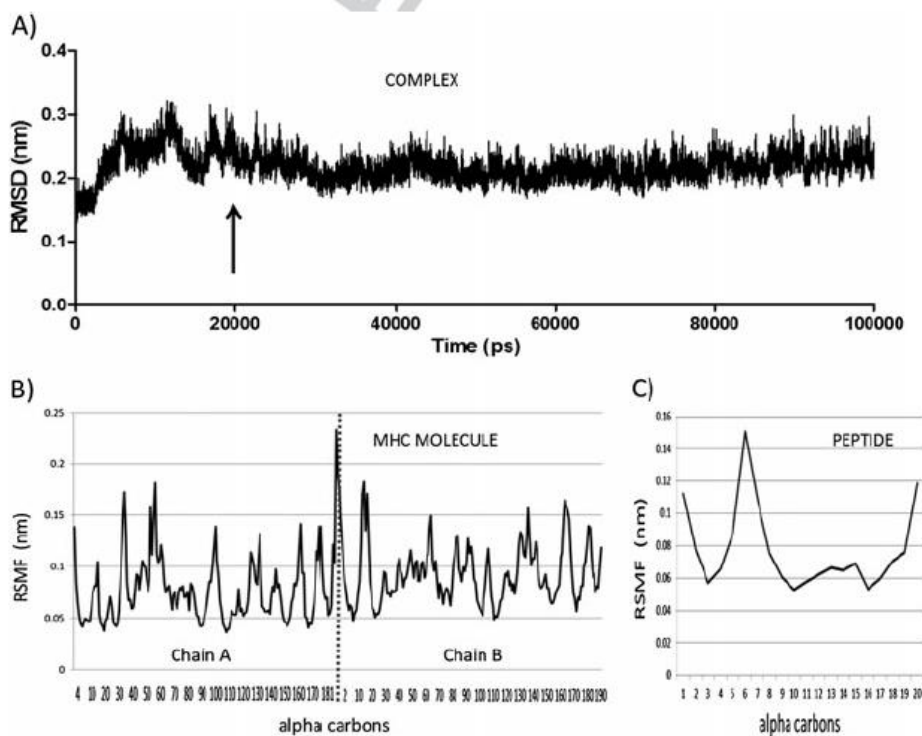


**Figure 3.** RMSD and RMSF parameters. (A) RMSD of the complex. (B) RMSF of the two chains of the MHC molecule. (C) Epitope of 20 amino acids.



a better interaction with the recognition groove. This result coincides with the report of Yano and coworkers, where it is mentioned that the KK linker sequence is preferred by cathepsin B to process antigens [66]. Thus, it is also consistent with the presence of the Lys1 and Lys2 in the amino-terminal region of the peptide; therefore, these residues remained unchanged. We named this peptide as p1 (KKFKPEIAIRPKVRD). The second peptide called peptide 2 (p2) conserves the sequence of p1 with an additional cysteine at the amino-terminal that functions as a linker for hemocyanin (KLH) [67]. This modification will provide evidence of the importance of the amino-terminal lysines (KLH-C-KKFKPEIAIRPKVRD). Another sequence of interest is RGD because it is preferred by the antigen process molecules and enhances the immune response [68]. Fortunately, the sequence of the peptide presented Arg and Asp residues in the carboxyl-terminal sequence, and taking advantage of this situation, we inserted a Gly between these residues, resulting in the peptide 3 (p3) (KKFKPEIAIRPKVRGD). In summary, we obtained four candidate peptides as potential immunogenic agents: the original is predicted by PEPOP (KKFKPEIAIRPKVRDQEGRM) and its derivatives p1 (KKFKPEIAIRPKVRD), p2 (KLH-C-KKFKPEIAIRPKVRD), and p3 (KKFKPEIAIRPKVRGD).

#### Human IgG antibodies to the peptides

To elucidate the immunogenic and antigenic potential of the p1 and p2, an enzyme-linked immunosorbent assay (ELISA) was performed with sera of two volunteer groups. These groups were integrated by sera obtained from individuals who were considered pre-pandemic (i.e., sera samples obtained before 2009); these were in storage before the 2009 outbreak. The second group of sera was found to be pandemic because these samples were collected during the outbreak. This ELISA was based on the binding of human Ab (IgG) to the p1 and p2 (Figure 4) [69,70]. The IgG antibodies identified the p1 in the sera of the two groups with no significant statistical difference (analysis of variance (ANOVA)). These results show that the general population had antibodies against the p1 prior to the immunization or infection with other viruses or exposure to influenza A virus (H1N1). In

other words, this epitope presumably is conserved among the pandemic and seasonal strains. Thus, the peptide is antigenic in humans. Results are presented as box-and-whisker plots. The boxes define the 25th and 75th percentiles, with error bars defining the 10th and 90th percentiles. Both peptides recognized human sera. Isotype response in serum from patients infected with influenza A p/H1N1/2009 IgG2 is the primary isotype of IgG antibodies against the p1. Although no differences were found in the levels of total IgG antibodies between pre-pandemic and pandemic sera, we analyzed the contribution of each subclass or isotype in response to p1 [71]. The antibody levels were significantly higher in the pandemic group compared with the pre-pandemic group (negative controls) for IgG2 ( $P=0.025$ , Mann-Whitney *U*-test) and IgG4 subclasses ( $P=0.007$ ). In the rank order, IgG2 (0.6 vs. 0.5, median) > IgG4 (0.08 vs. 0.07, median). Peptide 1 is immunogenic and induced antibodies to the native form of HA. The rabbits immunized with p1 peptide and human infected with p/H1N1 virus showed a definite immune response against wild-type viral antigens immobilized with concanavalin A (Con A, Sigma-Aldrich Corporation, St. Louis, MO, USA) (Figure 5). Rabbits immunized with p1 showed a stronger antibody response against the immobilized wild-type virus than human positive control. These results are significant and demonstrate that the p1 is highly immunogenic in rabbits and probably in humans, and it induces antibodies capable of interacting with the native form of HA [72].

#### Neutralizing antibodies induced by HA peptides in rabbits

Serum samples from rabbit immunized with p1 and from two vaccinated individuals and two patients infected with influenza A p/H1N1/2009 were titrated for neutralizing antibodies (PRNT50). p1 induces 1:533 neutralizing titers in rabbit, whereas the titers were 1:246 and 1:600 in vaccinated individuals and 1:400 and 1:250 in infected patients. On the other hand, p2, which is the p1 conjugated to hemocyanin (KLH-C-KKFKPEIAIRPKVRD), and p3, in which a glycine was added between the arginine and the aspartate of the p1 sequence, induced neutralizing

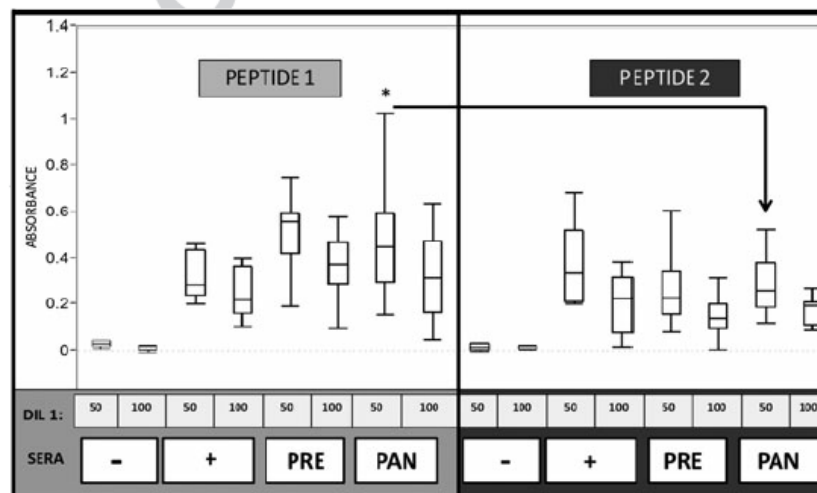


**Figure 4.** Detection of the p1 and p2 peptides by the human IgG Ab. Microplates were coated with p1 or p2 and sera from pre-pandemic and pandemic individuals were used. The IgG Ab to the HA peptide was detected with a secondary Ab specific for human IgG. \*Statistical analysis of the ELISA,  $p < 0.05$ , Pandemic—p1 versus Pandemic—p2, dilution 1:50, one-way ANOVA, Tukey–Kramer honestly significant difference.

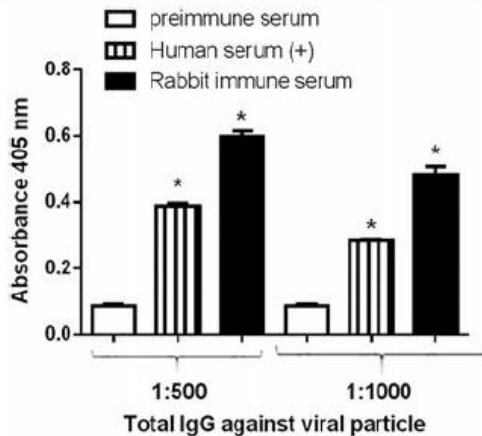


**Figure 5.** Levels of IgG against viral particle in serum of infected individuals or from rabbit immunized with peptide 1. IgG levels were determined by ELISA using viral antigens immobilized with Con A, and the IgG antibodies were detected with a secondary antibody specific for human or rabbit IgG. Data are expressed as the mean  $\pm$  SD. The levels were significantly higher in human serum and rabbit antiserum ( $p < 0.05$ , Kruskal–Wallis).

antibodies in minor quantity in the infected or vaccinated group F6 (titer 1: 103 and 1: 160, respectively) (Figure 6) [73,74].

## DISCUSSION

Predicting of possible epitopes and testing its immunogenicity involve a full effort and intervention of diverse scientific disciplines. There are different epitope prediction methods based

on biochemical properties, such as conserved sequences, special amino acids, length, hydrophobicity, secondary structure, and structure stability. Many studies focus on the sequence and its relation to B-cell immunity response; others take into account the recognition by MHC molecules or the 3D data of the proteins. Our workgroup has combined the epitope prediction and molecular modeling studies to obtain a peptide whose immunogenicity was assessed by experimental assays [70]. The area of opportunity for these studies is reflected by the fact that, until now, websites such as Immune Epitope Data Base (<http://www.tedb.org/>) that gather information on this topic are scarce [75,76]. In this work, we used the PEPPOP epitope predictor because of its features and previous results. Later, we analyzed the localization of the epitope and its relationship with antigenic sites using the 3D model of HA (PDB ID: 3LZG). Once the sequence in 3D model of HA is localized, we identified that the epitope was located among the amino acids that conform to the Ca antigenic site and near Sa and Sb antigenic sites (Figure 1A and B). Interestingly, this finding initiates a discussion about the definition of continuous or discontinuous epitopes: if the sequence is not reported as a discontinuous epitope, at least, it is part of a continuous epitope. Thus, the ELISA could suggest that this sequence is part of the same antigenic site; more experimental assays are necessary to prove this asseveration [78,79]. To confirm the immunological capabilities of the epitopes initially predicted, these were submitted to other epitope predictors to select those that were found at least in three of these predictors (Figure 1C) [80,81]. Also, the conservation of the sequence should be considered in designing an epitope [82,83]. HA has different epitopes reported elsewhere; an example is the sequence IAI that is part of a peptide that produces efficient immune response for paracoccidioidomycosis granulomatous disease caused by *Paracoccidioides brasiliensis*, a thermal dimorphic fungus [84]. In the peptide reported in this work, the sequence IAI is between

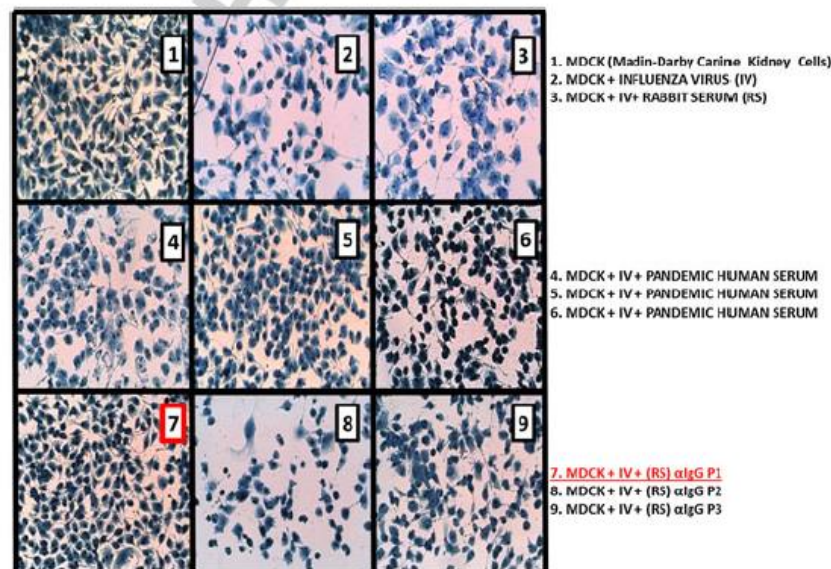


**Figure 6.** Plaque reduction neutralization test. Panel 1—MDCK cells, panel 2—MDCK cell with 30 plaque-forming units (PFU) influenza virus, panel 3—MDCK cells with influenza virus and rabbit serum (not immunized). Panels 4–6—MDCK cell with 30 PFU and human sera, the three panels were controls. Panels 7–9—infected MDCK cells with immunized rabbit sera with peptides 1, 2, and 3.



residues 216 and 225 of the subunit 1 of the HA (3LZG). Rothbard and coworkers reported an extensive analysis of the DR1 epitopes, proposing different sequences and combinations of residues that could be recognized [85]. More recently, Yano and coworkers suggested the use of RGD sequence in vaccine design [86]. Our results showed that p3, with the sequence RGD, produces neutralizing antibodies, but it does not have the same reaction when compared with p1 in the neutralization assays, possibly because of the introduction of the Gly. Some of the structural changes have been studied by Dayan and coworkers, explaining the reason of this phenomenon [87]. Other authors have analyzed how the loss of the recognition is due to the flexibility of the interaction of MHC with peptide [88]. In the docking assay, we prepared the simulation to produce a high flexibility in the peptide and a rigid structure for the MHC molecule. However, the MD simulations allowed us to increase the relaxing of the epitope-MHC II complex in order to refine the 3D model of interaction. The structural analysis showed that the carboxy-terminal sequence maintains a rigid behavior, preventing an unfolding of the extreme of the peptide or the stretching out of the recognition groove. This conformation produced a strong turn that was maintained during the simulation between the P4 and P6, and it coincided with possible interaction with the Met20. The groove recognized three initial residues of the amino-terminal sequence; however, the size of the residues spanning from Lys12 to Ile17 of the peptide hinders the anchoring with the groove completely. Also, the two Arg residues of the peptide, the Asp and the Gln, could be a hindrance to an adequate docking given their hydrophobicity. Several authors have reported that the binding to the pocket P1 stabilizes the epitope-MHC II complex [89–91]. Herein, the computational simulations show that Lys1, Lys2, and Phe3 bind the hydrophobic pocket P1 and P4 (Figure 2). On the contrary, possibly, the presence of KHL interferes (hindrance effects) with the recognition by the antibodies. Lys1 and Lys2 could facilitate the antigen processing and the pocket anchoring. Further analyses are needed to explain this phenomenon. P4 was the most important anchoring element after the 100 ns of MD simulations, as is shown by the interactions with at least four residues of the peptide (Lys1, Lys2, Phe3, and Arg10). Mainly, the P4 of chain B plays the most important role. Thus, the RMSF analysis shows fewer fluctuations in the P4, which contains the residues of anchorage. Furthermore, P4 has been reported to elicit a suitable spatial disposition of the residues nearby. In turn, certain residues in P6 modify the conformation of those in P9. For instance, the binding of positively charged amino acids at P6 can reduce the cavity of P9, limiting the ability to interact with residues with hydrophobic side chains. In contrast, the binding of negatively charged amino acids at P6 enlarges P9, rendering P9 capable of accepting residues with large side chains. The strength of linear peptides to bind to each other is regularly associated with hydrophobic complementarity. This occurs when peptides of different hydrophobicity bind to each other because hydrophilic amino acids in a peptide are located toward the aqueous solvent and release a space that could include a hydrophobic residue of the other peptide. The specificity of interactions between both peptides is improved by the ability of amino acids to create complementary protrusions and cavities and by the presence of residues of opposite charge [34]. According to MD simulations, the alpha helices of the recognition groove are unstable, particularly, in the alpha helices of both chains close to P1 and P4. Possibly, these changes are promoted by the interaction of the

peptide (by Lys1, Lys2, and Phe3) with the lateral chains of MHC II, searching an appropriate interaction.

Peptide 1 manifested its immunogenicity by inducing antibodies in rabbits as shown in the neutralization assays. This property could be based on the molecular size, rigidity, chemical complexity, interaction with B-cell receptors, or MHC and activation of helper T cells [92]. The p1 proved to be an antigen that is recognized by the IgG Ab from immunized rabbits and infected individuals, using the methodology reported for other peptides [93–95]. IgG antibodies in human serum, mainly the IgG2 isotype, demonstrate that clinical or subclinical infections with the influenza virus induced IgG to the peptide. Thus, the peptide is immunogenic and antigenic in humans. Although we did not directly demonstrate the interaction of p1 with MHC II molecules in infected subjects, we believe that this interaction took place because class switching to produce IgG requires activated helper T cells that recognize the antigen (p1) in association with the MHC II protein on the surface of an antigen-presenting cell, such as B cells or dendritic cells. Moreover, the interaction of p1 with MHC II molecules and T helper cells (CD4 T cells) was demonstrated by the class switch of the IgG isotype, which is mediated by cytokines produced by T helper cell activation after recognition of the peptide on MHC II molecules and the engagement of the CD40 receptor on B cells by CD40 L [96–98]. Peptides are protected against proteolytic degradation because B cells contain much lower levels of lysosomal proteases than macrophages. This condition favors the presentation of antigenic peptides on MHC II molecules by limiting the complete destruction of the peptide determinants [99,100]. In addition, the B-cell receptor may protect the peptide from proteolytic enzymes (selective processing) [101]. Through these two mechanisms, p1 could interact with MHC II molecules as well as activated T helper cells and the production of IgG antibodies in humans and rabbits. To serve as an antigen, a molecule typically must have a relative molecular mass of at least 4000 Da, and the peptide under study is approximately 1.9 kDa (1825.21 Da, 15 amino acid residues). Interestingly, this p1 is one of the few substances with low molecular weight (below 2000) having immunogenic and antigenic properties [70]. Immunogenicity of a peptide is related to its amino acid composition and its diversity. As we mentioned earlier, Lys1, Lys2, and Phe3 contained in p1 interact with the pockets 1 and 4. In the native HA, the epitope corresponding to p1 is exposed, providing accessibility to Ab binding. Also, the polar residues are situated on the surface much more frequently than nonpolar residues; thus, the regions of highest average polarity within a polypeptide sequence have the highest likelihood of being targets for Ab binding. Evidence shows that mimic epitopes are continuous epitopes, specifically the sera from all the individual of our trial recognized the peptide p1. Therefore, we confirmed that is a B-cell epitope, and it has been circulated previously in Mexican population, where clinical or subclinical infections with the influenza virus induced IgG Ab to the peptide p1. The antibodies against p1 were mainly isotype IgG2, which is the most abundant in human sera. IgG2 isotype is less efficient for complement activation and antibody dependent cell-mediated cytotoxicity than other isotypes, such as IgG1 [102,103]. We propose that the effect of IgG2 isotype against peptide 1 could be the neutralization of the free virus, producing antiviral activity through the binding of antibodies to the receptor binding site of the HA and preventing the infection by the influenza virus [42]. Moreover, the protection with IgG2 is

noteworthy because patients with a severe infection with influenza H1N1 have lower levels of this isotype and p1 peptide induces this isotype. Nevertheless, it is necessary to determine the neutralizing activity of the IgG2 isotype [104]. Finally, the results of the Con A and PRNT assays demonstrate that the peptides induce antibodies that can react with the protein of wild-type virus and neutralize it. The titers in vaccinated individuals were 1:246 and 1:600 and in infected patients were 1:400 and 1:250. These results suggest that the p1 induce a reaction similar to vaccine or in infected patients with titers of 1:533 and might be a candidate to be used as a peptide-based vaccine or in a diagnosis tool of the human influenza AH1N1.

## MATERIAL AND METHODS

### Ethics statement

The protocols for rabbits were reviewed and approved by the Committee of Bioethics and Research of the Escuela Nacional de Medicina y Homeopatía del IPN, Mexico City. The animals were handled in accordance with the Mexican Official Regulation (NOM-062-Z00-199—technical specifications for production, care, and use of laboratory animals). All serum samples for experiments were obtained from donors after they signed a written informed consent according to the Declaration of Helsinki.

### Epitope prediction

The crystal structure used for this study was the HA reported by Xu and coworkers (PDB code: 3LZG) [42]. All predictions were performed with the sequence and structure of 3LZG. Six programs of epitope predictions, four sequential predictors, and two structural predictors were used. To obtain MHC II epitope predictions, PROPED2 was utilized (<http://www.imtech.res.in/raghava/propred/>); its predictions are based on locating the promiscuous regions that can bind HLA-DR alleles [28], including the 47 HLA-DRB1s, which are the most representative. The MHC2PRED program (<http://www.imtech.res.in/raghava/mhc2pred/info.html>) was also used to obtain MHC II epitope predictions. Each peptide is represented by a 20-dimensional vector (SMV) using 12 alleles of its matrix (10 HLA-DRB1, 1 HLA-DRB5, and 1 HLA-DRB4) [26]. NetCTL 1.2 server predicts CTL epitopes in protein sequences that expand the MHC class I binding prediction to 12 MHC supertypes [105]. Finally, the last sequential predictor used was Vaxign [106] that is a vaccine target prediction and analysis system based on the principle of reverse vaccinology. Using 3D coordinates of the two chains of the model, we submit to both structural predictors, PEPOP (<http://pepop.sysdiag.cnrs.fr/PEPOP/>) [24] and SEPPA (<http://lifecenter.sgst.cn/seppa/>) [107]. We used the coordinates of the two chains of the model and submitted them to both predictors (Figure S1).

### Docking the epitope with the MHC II

Once the best epitope was obtained, a docking study was employed to describe the epitope and MHC II interactions. The crystal structure of MHC II for this analysis was HLA-DRB1\*0401 (PDB ID: 1D5M). HLA-DRB1 was previously reported to predict response profiles in donors when HLA haplotypes in the H1N1 virus were chosen at random [108]. Importantly, this HLA-DR allele is present in the majority of the human population [109]. We performed a non-restricted docking with the CLUSPRO automated docking program [54]. Docking calculations were also

performed with AutoDock 4.0.1 [110]. The search space was restricted to a rectangular box that included  $\beta$ -folded chains and  $\alpha$ -helix chains targeting the binding site of the epitope and the MHC II. A rectangular grid ( $70 \times 100 \times 90 \text{ \AA}$ ) with points separated by  $0.375 \text{ \AA}$  was generated. The docking parameters of 100 runs with 100 million energy evaluations for each test and a population size of 100 individuals were used. The docking results were analyzed with AutoDock Tools and PyMol software [53].

### Molecular dynamics simulation

The software GROMACS performed the MD simulations. First, the system was embedded in a solvated water box, and then the system was neutralized. The system had undergone an equilibration process before MD simulations were performed. The equilibration started with an initial minimization and was followed by whole minimization. Then an MD simulation of water molecules was carried out with all backbone atoms fixed. Finally, a 100-ns MD simulation was achieved under ensemble NVT. Tools of GROMACS were used to calculate the RMSD and RMSF [111].

### Contact map

To analyze the contacts and distances of the complex, a program of the Weizmann Institute of Science in Israel (<http://ligin.weizmann.ac.il/cma>) was performed to generate the contact map.

### Peptide synthesis

Three peptides were purchased for immunological assays as crude material from Mimotopes (Minneapolis, MN, USA and Clayton, Victoria, Australia): peptide 1 (p1: KKFKEAIRPKVRD), peptide 2 (p2: KLH-CKKFKEAIRPKVRD) conjugated with hemocyanin (KLH) linked to a cysteine with the sequence of the p1, and peptide 3 (p3: KKFKEAIRPKVRGD) with the addition of a glycine between the arginine and the aspartate.

### Enzyme-linked immunosorbent assay

Blood was obtained according to previously reported procedures [70] from healthy individuals who were living in Mexico City before the outbreak of the influenza H1N1 virus in 2009 and volunteers after the peak of the pandemic. Anti-HA peptide levels were evaluated in serum samples from infected and asymptomatic persons. The Ab levels in the serum samples were quantified by an indirect ELISA; 96-well plates were coated with either p1 or p2. One microgram per milliliter of peptide in carbonate bicarbonate buffer (15 mM  $\text{Na}_2\text{CO}_3$  and 35 mM  $\text{NaHCO}_3$  at pH9.6) was used. The plates were incubated for 2 h at  $37^\circ\text{C}$  and washed three times with 0.05% Tween-20 in phosphate-buffered saline (PBST). Blocking was performed by treating with PBST plus 6% fat-free milk and by further washing with PBST. Each sample was tested in duplicate. Serum samples from individuals were diluted 1:50 or 1:100. Afterward, the plates were incubated overnight at  $4^\circ\text{C}$  and washed with PBST. Dilutions of 1:1000, 1:2000, and 1:4000 goat anti-mouse IgG (Santa Cruz Biotechnology) or rabbit anti-human IgG (1:1000, Santa Cruz Biotechnology) were added to each well, and the plates were incubated for 2 h at room temperature. The plates were washed with PBST, and the enzymatic reactions were begun by adding substrate solution (0.5 mg/mL o-phenylenediamine plus 0.01%  $\text{H}_2\text{O}_2$  in 0.05 M citrate buffer 291 at pH5.2). After 15 min, the reactions were stopped with  $25 \mu\text{L}$  of 2.5 M  $\text{H}_2\text{SO}_4$ , and the



absorbance at 492 nm (A<sub>492</sub>) was measured using a Multiscan Ascent (Thermo Labsystems Inc., Philadelphia, PA, USA) microplate reader [112].

### Immunization of rabbits

Three rabbits were immunized with the three designed peptides (p1, p2, and p3). The immunization schedule was as follows. On day 1 (first immunization), 300 µg of peptide plus complete Freund's adjuvant (Sigma Chemical Co., St. Louis, MO, USA) was administered through the subcutaneous route. On day 8 (second immunization), 300 µg of peptide plus incomplete Freund's adjuvant was administered through the subcutaneous route. On day 15 (third immunization), 300 µg of peptide in 5 mL of saline solution was supplied via intramuscular injection. Seven days after the last immunization, the rabbits were anesthetized with pentobarbital, and serum samples were obtained from blood extracted by cardiac puncture and stored at -70 °C [70].

### Cells and influenza viruses

Madin-Darby canine kidney (MDCK) cells were grown in Dulbecco's Modified Eagle Medium Nutrient Mixture F-12 (DMEM/F-12) (Gibco, Grand Island, NY, USA), supplemented with 10% fetal bovine serum (Invitrogen) at 37 °C and 5% CO<sub>2</sub>. The strain influenza A Puerto Rico/916/34 (PubMed identifier: 24146939) was gently donated by Dr. Blanca Lilia Barrón, and the stock was prepared and stored as previously described [113].

### Concanavalin A enzyme-linked immunosorbent assay

Viral particles isolated and purified (FBS free) from infected MDCK cells were immobilized in wells coated with Con A, which binds the glycoproteins of enveloped viruses. Briefly, 96-well plates (Costar) were coated with 100 µL per well of Con A at 50 µg/mL in PBS, pH 7.4 for 1 h. The wells were washed and incubated with solubilized influenza A Puerto Rico/916/34 (serum-free virus stock) in PBS containing 0.1% Triton-X (PBS-Tx) for 1 h. After the wells had been washed with PBS-Tx, the unbound Con A binding sites were blocked with Roswell Park Memorial Institute medium 1640 containing 10% FBS for 1 h. Serial dilutions of the serum samples were incubated for 1 h at room temperature. Serum from influenza-positive patients was used as a positive control. Rabbit pre-immune serum samples were used as negative controls. After the wells had been washed again, they were incubated with 100 µL of peroxidase-conjugated secondary antibody anti-IgG (H + L) (Invitrogen) [72].

### Neutralization assay

Neutralizing antibodies were titrated as described previously by Morens and coworkers. Briefly, serial dilutions of the heat-inactivated test sera in triplicate started from 1:20 were mixed with 20 plaque-forming units of influenza A Puerto Rico/916/34 virus for 1 h at 37 °C and added to MDCK at a density of 1.2 × 10<sup>5</sup> cells per well in 24-well plates. At 1 h after infection, serum-free DMEM/F-12 medium with 2 µg of L-1-tosylamide-2-phenyl ethyl

chloromethyl ketone-treated trypsin was added to each well for 10 min at 37 °C. Then 500 µL of overlay medium was added to each well, and plates were incubated for 3 days under the same conditions. The supernatant was discarded, and the plaques were visualized with naphthol blue-black dye. The cytopathic effect was evaluated to determine the highest serum dilution that protected 50% of the cells from cytopathology in these wells. Positive and negative control sera and virus back titration were included in the assay to confirm the viral inoculum [73,74].

### Isotype response in serum from patients infected with pandemic influenza AH1N1 2009

IgG isotype antibodies against p1 peptide were measured by ELISA in 96-well polyvinyl plates (Nunc) coated with each peptide (2 µg/mL). We assayed 40 sera from patients infected with influenza AH1N1 2009 and 40 pre-pandemic sera at 1:100 dilutions for 1 h at 37 °C. Then the anti-human immunoglobulin peroxidase-conjugated secondary antibodies were added (anti-human IgG1, 2, 3, or 4, all Invitrogen) for 1 h at 37 °C. After H<sub>2</sub>O<sub>2</sub> and 2,2'-azino-bis(3-ethylbenzothiazoline-6-sulfonic acid) (Sigma-Aldrich Corporation, St. Louis, MO, USA) were added as substrates. The absorbance values were determined at 405 nm [71].

### Statistical analysis

Statistical analyses were performed using JMP Statistical Software (SAS Institute, Cary, NC, USA) (<http://www.jmp.com/>). Normally distributed data were analyzed by one-way ANOVA test to compare the groups. The differences among the groups were analyzed by a Tukey-Kramer honestly significant difference test; differences were considered significant at  $p < 0.05$ . Isotype differences were analyzed by ANOVA and Mann-Whitney U-test, t-test, nonparametric test, and Mann-Whitney post-test using GraphPad Prism 6 program (GraphPad Software, Inc., CA, USA) to determine the significance of the differences between groups, denoted by asterisks as follows: \* $p < 0.05$ , \*\* $p < 0.01$ .

## CONCLUSION

In addition to offering an atomistic description of the interaction of a peptide with the MHC, this study showed that *in silico* experiments (prediction of immunogenic epitopes, docking, and MD simulation) are useful tools for the rational design of epitope vaccines. An example is offered in this work using the HA protein of the influenza AH1N1 virus, whose resultant peptide can be used as a diagnostic tool or as an immunogenic agent. This strategy includes an experimental evaluation of immunogenic epitopes and could decrease the economic investment and the time needed to obtain epitope vaccines and diagnostic tools. Our research indicates that the selected peptide is immunogenic, antigenic, and efficient in inducing a strong immune response. Therefore, it should be a good candidate for the development of a peptide-based vaccine or diagnostic tool.

## REFERENCES

- Meltzer MI, Cox NJ, Fukuda K 1999. The economic impact of pandemic influenza in the United States: priorities for intervention. *Emerg Infect Dis* 5: 659-671. DOI: 10.3201/eid0505.990507.
- Eccles R 2005. Understanding the symptoms of the common cold and influenza. *Lancet Infect Dis* 5: 718-725. DOI: 10.1016/S1473-3099(05)70270-X.

3. Simonsen L, Matthew JC, Lawrence BS, Nancy HA, Nancy JC, Keiji F. 1998. Pandemic versus epidemic influenza mortality: a pattern of changing age distribution. *J Infect Dis* **178**: 53–60. DOI: 10.1086/515616.
4. Steinhauer DA, Skehel JJ. 2002. Genetics of influenza viruses. *Annu Rev Genet* **36**: 305–332. DOI: 10.1146/annurev.genet.36.052402.152757.
5. Wood JM. 2001. Developing vaccines against pandemic influenza. *Philos Trans R Soc Lond B Biol Sci* **29**: 1953–1960. DOI: 10.1098/rstb.2001.0981.
6. Kaiser J. 2006. A one-size-fits-all flu vaccine? *Science* **5772**: 380–382. DOI: 10.1126/science.312.5772.380.
7. Lu Y, Ding J, Liu W, Chen YH. 2002. A candidate vaccine against influenza virus intensively improved the immunogenicity of a neutralizing epitope. *Int Arch Allergy Immunol* **127**: 245–250. DOI: 10.1159/000053869.
8. Plotkin JB, Dushoff J. 2003. Codon bias and frequency-dependent selection on the hemagglutinin epitopes of influenza A virus. *Proc Natl Acad Sci U S A* **100**: 127152–127157. DOI: 10.1073/pnas.1132114100.
9. Ekiert DC, Bhabha G, Eisliger MA, Friesen RH, Jongeneelen M, Throsby M, Goudsmit J, Wilson IA. 2009. Antibody recognition of a highly conserved influenza virus epitope. *Science* **324**: 246–251. DOI: 10.1126/science.117149.
10. Novotný J, Handschumacher M, Haber E, Bruccoleri RE, Carlson WB, Fanning DW, Smith JA, Rose GD. 1986. Antigenic determinants in proteins coincide with surface regions accessible to large probes (antibody domains). *Proc Natl Acad Sci U S A* **83**: 226–230.
11. Liu W, Peng Z, Liu Z, Lu Y, Ding J, Chen YH. 2004. High epitope density in a single recombinant protein molecule of the extracellular domain of influenza A virus M2 protein significantly enhances protective immunity. *Vaccine* **23**: 366–371. DOI: 10.1016/j.vaccine.2004.05.028.
12. Zou P, Liu W, Chen YH. 2005. The epitope recognized by a monoclonal antibody in influenza A virus M2 protein is immunogenic and confers immune protection. *Int Immunopharmacol* **5**: 631–635. DOI: 10.1016/j.intimp.2004.12.005.
13. Garten RJ, Davis CT, Russell CA, Shu B, Lindstrom S, et al. 2009. Antigenic and genetic characteristics of swine-origin 2009 A(H1N1) influenza viruses circulating in humans. *Science* **325**: 197–201. DOI: 10.1126/science.1176225.
14. Goh GK, Dunker AK, Uversky VN. 2009. Protein intrinsic disorder and influenza viruses: the 1918 H1N1 and H5N1 viruses. *Viral J* **6**: 69. DOI: 10.1186/1743-422X-6-69.
15. Heiny AT, Miotto O, Srinivasan KN, Khan AM, Zhang GL, Brusic V, Tan TW, August JT. 2007. Evolutionarily conserved protein sequences of influenza viruses, avian and human, as vaccine targets. *PLoS One* **2**(11): e1190. DOI: 10.1371/journal.pone.0001190.
16. Shih AC, Hsiao TC, Ho MS, Li WH. 2007. Simultaneous amino acid substitutions at antigenic sites drive influenza A hemagglutinin evolution. *Proc Natl Acad Sci U S A* **104**: 6283–6288. DOI: 10.1073/pnas.0701396104.
17. Gogolák P, Simon A, Horváth A, Réthi B, Simon I, Berkics K, Rajnavölgyi E, Tóth GK. 2000. Mapping of a protective helper T cell epitope of human influenza A virus hemagglutinin. *Biochem Biophys Res Commun* **270**: 190–198. DOI: 10.1006/bbrc.2000.2384.
18. Caton AJ, Brownlee GG, Yewdell JW & Gerhard W. 1982. The antigenic structure of the influenza virus A/PR/8/34 hemagglutinin (H1 subtype). *Cell* **31**: 417–427. DOI: 10.1016/0092-8674(82)90135-0.
19. Wilson DB, Pinilla C, Wilson DH, Schroder K, Boggiano C, Judkowski V, Kaye J, Hemmer B, Martin R, Houghten RA. 1999. Immunogenicity. I. Use of peptide libraries to identify epitopes that activate clonotypic CD4+ T cells and induce T cell responses to native peptide ligands. *J Immunol* **163**: 6424–6434.
20. Seyed N, Zahedifard F, Safaiyan S, Gholami E, Doustdari F, Azadmanesh K, Mirzaei M, Saeedi Eslami N, Khadem Sadegh A, Eslami Far A, Sharifi I, Rafati S. 2011. In silico analysis of six known *Leishmania major* antigens and in vitro evaluation of specific epitopes eliciting HLA-A2 restricted CD8 T cell response. *PLoS Negl Trop Dis* **5**(9): e1295. DOI: 10.1371/journal.pntd.0001295.
21. Wang LF, Yu M. 2004. Epitope identification and discovery using phage display libraries: applications in vaccine development and diagnostics. *Curr Drug Targets* **5**: 1–15. DOI: 10.2174/1389450043490668.
22. Schwaiger J, Aberle JH, Stiasny K, Knapp B, Schreiner W, Fae I, Fischer G, Scheinost O, Chmelik V, Heinz FX. 2014. Specificities of human CD4+ T cell responses to an inactivated Flavivirus vaccine and infection: correlation with structure and epitope prediction. *J Virol* **88**: 7828–7842. DOI: 10.1128/JVI.00196-14.
23. Chen P, Rayner S, Hu KH. 2011. Advances of bioinformatics tools applied in virus epitopes prediction. *Viral Sin* **26**: 1–7. DOI: 10.1007/s12250-011-3159-4.
24. Moreau V, Fleury C, Piquier D, Nguyen C, Novali N, Villard S, Laune D, Granier C, Molina F. 2008. PEPPOP: computational design of immunogenic peptides. *BMC Bioinf* **9**: 71. DOI: 10.1186/1471-2105-9-71.
25. Di W, TianLei X, Jing S, JianXin D, GuoHui D et al., 2009. Structure modeling and spatial epitope analysis for HA protein of the novel H1N1 influenza virus. *Chin Sci Bull* **54**: 2171–2173. DOI: 10.1007/s11434-009-0429-3.
26. Wang L, Pan D, Hu X, Xiao J, Gao Y, Zhang H, Zhang Y, Liu J, Zhu S. 2009. BiodMHC: an online server for the prediction of MHC class II-peptide binding affinity. *J Genet Genomics* **36**: 289–296. DOI: 10.1016/S1673-8527(08)60117-4.
27. Lata S, Bhasin M, Raghava GP. 2007. Application of machine learning techniques in predicting MHC binders. *Methods Mol Biol* **409**: 201–215. DOI: 10.1007/978-1-60327-118-9\_14.
28. Singh H, Raghava GP. 2001. ProPred: prediction of HLA-DR binding sites. *Bioinformatics* **17**: 1236–1237. doi: 10.1093/bioinformatics/17.12.1236.
29. Malito E, Rappuoli R. 2013. Finding epitopes with computers. *Chem Biol* **20**: 1205–1206. DOI: 10.1016/j.chembiol.2013.10.002.
30. Zoete V, Irving M, Ferber M, Cuendet MA, Michielin O. 2013. Structure-based, rational design of T cell receptors. *Front Immunol* **4**: 268. DOI: 10.3389/fimmu.2013.00268.
31. Sela-Culang I, Benhnia MR, Matho MH, Kaever T, Maybeno M, Schlossman A, Nimrod G, Li S, Xiang Y, Zajonc D, Crotty S, Ofran Y, Peters B. 2014. Using a combined computational-experimental approach to predict antibody-specific B cell epitopes. *Structure* **22**: 646–657. DOI: 10.1016/j.str.2014.02.003.
32. Hoze E, Tsaban L, Maman Y, Louzoun Y. 2013. Predictor for the effect of amino acid composition on CD4+ T cell epitopes preprocessing. *J Immunol Methods* **391**: 163–173. DOI: 10.1016/j.jim.2013.02.006.
33. Van Regenmortel MH (2009) Synthetic peptide vaccines and the search for neutralization B cell epitopes *The Open Vaccine Journal* **2**: 33–44.
34. Van Regenmortel MH. 2014. Specificity, polyspecificity, and heterospecificity of antibody-antigen recognition *J Mol Recognit* **27**: 627–639. DOI: 10.1002/jmr.2394.
35. Flower DR, Macdonald IK, Ramakrishnan K, Davies MN, Doytchinova IA. 2010. Computer aided selection of candidate vaccine antigens. *Immunome Res* **6**: S1. DOI: 10.1186/1745-7580-6-S2-5.
36. Chen J, Wang Y, Guo D, Shen B. 2012. A systems biology perspective on rational design of peptide vaccine against virus infections. *Curr Top Med Chem* **12**: 1310–1319 DOI: 10.2174/156802612801319043.
37. Ponomarenko JV & Bourne PE. 2007. Antibody-protein interactions: benchmark datasets and prediction tools evaluation. *BMC Struct Biol* **7**: 64. DOI: 10.1186/1472-6807-7-64.
38. Krawczyk K, Liu X, Baker T, Shi J, Deane CM. 2014. Improving B-cell epitope prediction and its application to global antibody-antigen docking. *Bioinformatics* DOI: 10.1093/bioinformatics/btu190.
39. Knapp B, Omasits U, Schreiner W, Epstein MM. 2010. A comparative approach linking molecular dynamics of altered peptide ligands and MHC with in vivo immune responses. *PLoS One* **5**(7): e11653. DOI: 10.1371/journal.pone.0011653.
40. Stavrakoudis A. 2010. Conformational flexibility in designing peptides for immunology: the molecular dynamics approach. *Curr Comput Aided Drug Des* **6**: 207–222. DOI: 10.2174/157340910791760073.
41. Somvanshi P, Singh V, Seth PK. 2008. Prediction of epitopes in hemagglutinin and neuraminidase proteins of influenza A virus H5N1 strain: a clue for diagnostic and vaccine development. *OMICs* **12**: 61–69. DOI: 10.1089/omi.2007.0037.
42. Xu R, Ekiert DC, Krause JC, Hai R, Crowe JE Jr, Wilson IA. 2010. Structural basis of preexisting immunity to the 2009 H1N1



- pandemic influenza virus. *Science* **328**: 357–360. DOI: 10.1126/science.1186430.
43. Jørgensen KW, Buus S, Nielsen M. 2010. Structural properties of MHC class II ligands, implications for the prediction of MHC class II epitopes. *PLoS One* **5**(12): e15877. DOI: 10.1371/journal.pone.0015877.
  44. Sinigaglia F, Hammer J. 1994. Rules for peptide binding to MHC class II molecules. *APMIS* **102**: 241–248. DOI: 10.1111/j.1699-0463.1994.tb04871.x.
  45. Madden DR, Garboczi DN, Wiley DC. 1993. The antigenic identity of peptide–MHC complexes: a comparison of the conformations of five viral peptides presented by HLA-A2. *Cell* **75**: 693–708 DOI: 10.1016/0092-8674(93)90490-H.
  46. Trombetta ES, Mellman I. 2005. Cell biology of antigen processing in vitro and in vivo. *Annu Rev Immunol* **23**: 975–1028. DOI: 10.1146/annurev.immunol.22.012703.104538.
  47. Villadangos JA. 2001. Presentation of antigens by MHC class II molecules: getting the most out of them. *Mol Immunol* **38**: 329–346. DOI: 10.1016/S0161-5890(01)00069-4.
  48. Wiley DC, Skehel JJ. 1987. The structure and function of the hemagglutinin membrane glycoprotein of influenza virus. *Annu Rev Plant Physiol Plant Mol Biol* **56**: 365–394 DOI: 10.1146/annurev.pl.56.070187.002053.
  49. Meroz D, Yoon SW, Ducatez MF, Fabrizio TP, Webby RJ, Hertz T, Ben-Tal N. 2011. Putative amino acid determinants of the emergence of the 2009 influenza A (H1N1) virus in the human population. *Proc Natl Acad Sci U S A* **108**: 13522–13527. DOI: 10.1073/pnas.1014854108.
  50. Ménez R, Bossus M, Muller BH, Sibai G, Dalbon P, Ducancel F, Jolivet-Reynaud C, Stura EA. 2003. Crystal structure of a hydrophobic immunodominant antigenic site on hepatitis C virus core protein complexed to monoclonal antibody 19D9D6. *J Immunol* **170**: 1917–1924.
  51. Kropshofer H, Max H, Müller CA, Hesse F, Stevanovic S, Jung G, Kalbacher H. 1992. Self-peptide released from class II HLA-DR1 exhibits a hydrophobic two-residue contact motif. *J Exp Med* **175**: 1799–1803. DOI: 10.1084/jem.175.6.1799.
  52. Walavalkar NM, Gordon N, Williams DC Jr. 2013. Unique features of the antiparallel, heterodimeric coiled-coil interaction between methyl-cytosine binding domain 2 (MBD2) homologues and GATA zinc finger domain containing 2A (GATAD2A/p66a). *J Biol Chem* **288**: 3419–3427 DOI: 10.1074/jbc.M112.431346.
  53. Seeliger D, de Groot BL. 2010. Ligand docking and binding site analysis with PyMOL and AutoDock/Vina. *J Comput Aided Mol Des* **24**: 417–422 DOI: 10.1007/s10822-010-9352-6.
  54. Comeau SR, Gatchell DW, Vajda S, Camacho CJ. 2004. ClusPro: an automated docking and discrimination method for the prediction of protein complexes. *Bioinformatics* **20**: 45–50. DOI: 10.1093/bioinformatics/btg371.
  55. Amaro RE, Baron R, McCammon JA. 2008. An improved relaxed complex scheme for receptor flexibility in computer-aided drug design. *J Comput Aided Mol Des* **22**: 693–705. DOI: 10.1007/s10822-007-9159-2.
  56. Terentiev AA, Moldogazieva NT, Levtsova OV, Maximenko DM, Borozdenko DA, Shaitan KV. 2012. Modeling of three dimensional structure of human alpha-fetoprotein complexed with diethylstilbestrol: docking and molecular dynamics simulation study *J Bioinform Comput Biol* **10**: 1241012. DOI: 10.1142/S0219720012410120.
  57. Carlsson J, Boukharta L, Aqvist J (2008) Combining docking, molecular dynamics and the linear interaction energy method to predict binding modes and affinities for nonnucleoside inhibitors to HIV-1 reverse transcriptase. *J Med Chem* **51**: 2648–2656. DOI: 10.1021/jm7012198.
  58. Shahlaei M, Madadkar-Sobhani A, Mahnam K, Fassihi A, Saghale L & Mansourian M. 2011. Homology modeling of human CCR5 and analysis of its binding properties through molecular docking and molecular dynamics simulation. *Biochim Biophys Acta* **1808**: 802–817. DOI: 10.1016/j.bbame.2010.12.004.
  59. Król M, Chaleil RA, Tournier AL, Bates PA. 2007. Implicit flexibility in protein docking: cross-docking and local refinement. *Proteins* **69**: 750–757. DOI: 10.1002/prot.2169.
  60. Senda Y, Fujio M, Shimamura S, Blomqvist J, Nieminen RM. 2012. Fast convergence to equilibrium for long-chain polymer melts using a MD/continuum hybrid method. *J Chem Phys* **137**: 154115. DOI: 10.1063/1.4759036.
  61. Grossfield A, Feller SE, Pitman MC. 2007. Convergence of molecular dynamics simulations of membrane proteins. *Proteins* **67**: 31–40. DOI: 10.1002/prot.21308.
  62. Smith LJ, Daura X, Van Gunsteren WF. 2002. Assessing equilibration and convergence in biomolecular simulations. *Proteins* **48**: 487–496. DOI: 10.1002/prot.10144.
  63. Sundaram R, Lynch MP, Rawale SV, Sun Y, Kazanji M, Kaumaya PT. 2004. De novo design of peptide immunogens that mimic the coiled coil region of human T-cell leukemia virus type-1 glycoprotein 21 transmembrane subunit for induction of native protein reactive neutralizing antibodies. *Biol Chem* **279**: 24141–24151 DOI: 10.1074/jbc.M313210200.
  64. Kaumaya PT, VanBuskirk AM, Goldberg E, Pierce SK. 1992. Design and immunological properties of topographic immunogen determinants of a protein antigen (LDH-C4) as vaccines. *J Biol Chem* **267**: 6338–6346.
  65. Wang CY, Chang TY, Walfield AM, Ye J, Shen M, Ye J, Chen SP, Li MC, Lin YL, Jong MH, Yang PC, Chyr N, Kramer E, Brown F. 2002. Effective synthetic peptide vaccine for foot-and-mouth disease in swine. *Vaccine* **20**: 2603–2610. DOI: 10.1016/S0264-410X(02)00148-2.
  66. Yano A, Onozuka A, Asahi-Ozaki Y, Imai S, Hanada N, Miwa Y, Nisizawa T (2005) An ingenious design for peptide vaccines. *Vaccine* **23**: 2322–2326. DOI: 10.1016/j.vaccine.2005.01.031.
  67. Helling F, Shang A, Calves M, Zhang S, Ren S, Yu RK, Oettgen HF, Livingston PO. 1994. GD3 vaccines for melanoma: superior immunogenicity of keyhole limpet hemocyanin conjugate vaccines. *Cancer Res* **54**: 197–203.
  68. Yano A, Onozuka A, Matin K, Imai S, Hanada N, Nisizawa T. 2003. RGD motif enhances immunogenicity and adjuvanticity of peptide antigens following intranasal immunization. *Vaccine* **22**: 237–243. DOI: 10.1016/S0264-410X(03)00561-9.
  69. Mavrouli MD, Routsias JG, Maltezou HC, Spanakis N, Tsakris A. 2011. Estimation of seroprevalence of the pandemic H1N1 2009 influenza virus using a novel virus-free ELISA assay for the detection of specific antibodies. *Viral Immunol* **24**: 221–226. DOI: 10.1089/vim.2010.0137.
  70. Loyola PK, Campos-Rodríguez R, Bello M, Rojas-Hernández S, Zimic M, Quiliano M, Briz V, Muñoz-Fernández MA, Tolentino-López L, Correa-Basurto J. 2013. Theoretical analysis of the neuraminidase epitope of the Mexican A H1N1 influenza strain, and experimental studies on its interaction with rabbit and human hosts. *J Immunol Res* **56**: 44–60. DOI: 10.1007/s12026-013-8385-z.
  71. Burlington DB, Clements ML, Meiklejohn G, Phelan M, Murphy BR. 1983. Hemagglutinin-specific antibody responses in immunoglobulin G, A, and M isotypes as measured by enzyme-linked immunosorbent assay after primary or secondary infection of humans with influenza A virus. *Infect Immun* **41**: 540–545.
  72. Robinson JE, Holton D, Liu J, McMurdo H, Murciano A, Gohd R. 1990. A novel enzyme-linked immunosorbent assay (ELISA) for the detection of antibodies to HIV-1 envelope glycoproteins based on immobilization of viral glycoproteins in microtiter wells coated with concanavalin A. *J Immunol Methods* **132**: 63–71. DOI: 10.1016/0022-1759(90)90399-G.
  73. Chan KH, To KK, Hung IF, Zhang AJ, Chan JF, Cheng VC, Tse H, Che XY, Chen H, Yuen KY. 2011. Differences in antibody responses of individuals with natural infection and those vaccinated against pandemic H1N1 2009 influenza. *Clin Vaccine Immunol* **18**: 867–873. DOI: 10.1128/CVI.00555-10.
  74. Morens DM, Halstead SB, Repik PM, Putvatana R, Raybourne N. 1985. Simplified plaque reduction neutralization assay for dengue viruses by semimicro methods in BHK-21 cells: comparison of the BHK suspension test with standard plaque reduction neutralization. *J Clin Microbiol* **22**: 250–254.
  75. Geysen HM, Barteling SJ, Meloen RH. 1985. Small peptides induce antibodies with a sequence and structural requirement for binding antigen comparable to antibodies raised against the native protein. *Proc Natl Acad Sci U S A* **82**: 178–182. doi:10.1073/pnas.82.1.178.
  76. Peters B, Sidney J, Bourne P, Bui HH, Buus S, Doh G, Fleri W, Kronenberg M, Kubo R, Lund O, Nemazee D, Ponomarenko JV, Sathiamurthy M, Schoenberger S, Stewart S, Surko P, Way S, Wilson S, Sette A. 2005. The immune epitope database and analysis resource: from vision to blueprint. *PLoS Biol* **3**(3): e91. DOI: 10.1371/journal.pbio.0030091.

99. Wiegiers KJ, Wetz K, Dernick R. 1990. Molecular basis for linkage of a continuous and discontinuous neutralization epitope on the structural polypeptide VP2 of poliovirus type 1. *J Virol* **64**: 1283–1289.
78. Moreau V, Granier C, Villard S, Laune D, Molina F. 2006. Discontinuous epitope prediction based on mimotope analysis. *Bioinformatics* **22**: 1088–1095. DOI: 10.1093/bioinformatics/btl012.
79. Flower DR. 2003. Towards in silico prediction of immunogenic epitopes. *Trends Immunol* **24**(12): 667–674. DOI: 10.1016/j.it.2003.10.006.
80. Yu K, Petrovsky N, Schönbach C, Koh JY, Brusci V. 2002. Methods for prediction of peptide binding to MHC molecules: a comparative study. *Mol Med* **8**: 137–148.
81. Igarashi M, Ito K, Yoshida R, Tomabechi D, Kida H, et al., 2010. Predicting the antigenic structure of the pandemic (H1N1) 2009 influenza virus hemagglutinin. *PLoS One* **5**(1): e8553. DOI: 10.1371/journal.pone.0008553.
82. Du L, Zhou Y, Jiang S. 2010. Research and development of universal influenza vaccines. *Microbes Infect* **12**: 280–286. DOI: 10.1016/j.micinf.2010.01.001.
83. Taborda CP, Juliano MA, Puccia R, Franco M, Travassos LR. 1998. Mapping of the T-cell epitope in the major 43-kilodalton glycoprotein of *Paracoccidioides brasiliensis* which induces a Th-1 response protective against fungal infection in BALB/c mice. *Infect Immun* **66**: 786–793.
84. Rothbard JB, Taylor WR. 1988. A sequence pattern common to T cell epitopes. *EMBO J* **7**: 93–100.
85. Yano A, Miwa Y, Kanazawa Y, Ito K, Makino M, Imai S, Hanada N, Nisizawa T. 2013. A novel method for enhancement of peptide vaccination utilizing T-cell epitopes from conventional vaccines. *Vaccine* **31**: 1510–1515. DOI: 10.1016/j.vaccine.2012.12.083.
86. Dayan FE, Daga PR, Duke SO, Lee RM, Tranel PJ, Doerksen RJ. 2010. Biochemical and structural consequences of a glycine deletion in the alpha-8 helix of protoporphyrinogen oxidase. *Biochim Biophys Acta* **1804**: 1548–1556. DOI: 10.1016/j.bbapap.2010.04.004.
87. Insaïdo FK, Borbulevych OY, Hossain M, Santhanagopalan SM, Baxter TK, Baker BM. 2011. Loss of T cell antigen recognition arising from changes in peptide and major histocompatibility complex protein flexibility: implications for vaccine design. *J Biol Chem* **286**: 40163–40173. DOI: 10.1074/jbc.M111.283564.
88. James EA, Moustakas AK, Bui J, Nouv R, Papadopoulos GK, Kwok WW. 2009. The binding of antigenic peptides to HLA-DR is influenced by interactions between pocket 6 and pocket 9. *J Immunol* **183**: 3249–3258. DOI: 10.4049/jimmunol.0802228.
89. Cárdenas C, Ortiz M, Balbín A, Villaveces JL, Patarroyo ME. 2005. Allele effects in MHC-peptide interactions: a theoretical analysis of HLA-DRbeta1\*0101-HA and HLADRBeta1\*0401-HA complexes. *Biochem Biophys Res Commun* **330**: 1162–1167. DOI: 10.1016/j.bbrc.2005.03.102.
90. Painter CA, Cruz A, López GE, Stern LJ, Zavala-Ruiz Z. 2008. Model for the peptide-free conformation of class II MHC proteins. *PLoS One* **3**(6): e2403. DOI: 10.1371/journal.pone.0002403.
91. Benjamin DC, Berzofsky JA, East IJ, Gurd FRN, Hannum C, Leach SJ, et al., 1984. The antigenic structure of proteins: a reappraisal. *Annu Rev Immunol* **2**: 67–101. DOI: 10.1146/annurev.iy.02.040184.000435.
100. Madhumathi J, Prince PR, Anugraha G, Kiran P, Rao DN, et al., 2010. Identification and characterization of nematode specific protective epitopes of *Brugia malayi* TRX towards development of synthetic vaccine construct for lymphatic filariasis. *Vaccine* **28**: 5038–5048. DOI: 10.1016/j.vaccine.2010.05.012.
111. Benkirane N, Friede M, Guichard G, Briand JP, Van Regenmortel MH, Muller S. 1993. Antigenicity and immunogenicity of modified synthetic peptides containing D-amino acid residues. *J Biol Chem* **268**: 26279–26285.
94. Pandiaraja P, Arunkumar C, Hoti SL, Rao DN, Kaliraj P (2010) Evaluation of synthetic peptides of WbSXP-1 for the diagnosis of human lymphatic filariasis. *Diagn Microbiol Infect Dis* **68**: 410–415. DOI: 10.1016/j.diagmicrobio.2010.07.015.
95. Rudolph MG, Stanfield RL, Wilson IA. 2006. How TCRs bind MHCs, peptides, and coreceptors. *Annu Rev Immunol* **24**: 419–466 DOI: 10.1146/annurev.immunol.23.021704.115658.
96. Stavnezer J, Guikema JE, Schrader CE. 2008. Mechanism and regulation of class switch recombination. *Annu Rev Immunol* **26**: 261–292. DOI: 10.1146/annurev.immunol.26.021607.090248.
97. Smith-Garvin JE, Koretzky GA, Jordan MS. 2009. T cell activation. *Annu Rev Immunol* **27**: 591–619. DOI: 10.1146/annurev.immunol.021908.132706.
98. Lennon-Duménil AM, Bakker AH, Maehr R, Fiebiger E, Overkleef HS, Roseblatt M, Ploegh HL, Lagaudrière-Gesbert C. 2002. Analysis of protease activity in live antigen-presenting cells shows regulation of the phagosomal proteolytic contents during dendritic cell activation. *J Exp Med* **196**: 529–540. DOI: 10.1084/jem.20020327.
99. Delamarre, L, Pack M, Chang H, Mellman I, Trombetta ES. 2005. Differential lysosomal proteolysis in antigen-presenting cells determines antigen fate. *Science* **307**: 1630–1634. DOI: 10.1126/science.1108003.
100. Jemmerson, R, Paterson Y. 1986 Mapping epitopes on a protein antigen by the proteolysis of antigen-antibody complexes. *Science* **232**: 1001–1004. DOI: 10.1126/science.2422757.
101. Frazer J, Capra J. 1999. Immunoglobulins: structure and function. Fundamental immunology. Paul W. E (eds). Philadelphia-New York: Lippincott-Raven: 37–74.
102. Srivastava V, Yang Z, Hung IF, Xu J, Zheng B, Zhang MY. 2013. Identification of dominant antibody-dependent cell-mediated cytotoxicity epitopes on the hemagglutinin antigen of pandemic H1N1 influenza virus. *J Virol* **87**: 5831–5840. DOI: 10.1128/JVI.00273-13.
103. Gordon CL, Holmes NE, Grayson ML, Torresi J, Johnson PD, Cheng AC, Charles PG. 2012. Comparison of immunoglobulin G subclass concentrations in severe community-acquired pneumonia and severe pandemic 2009 influenza A (H1N1) infection. *Clin Vaccine Immunol* **19**: 446–448. DOI: 10.1128/CVI.05518-1164.
104. Larsen MV, Lundegaard C, Lamberth K, Buus S, Lund O, Nielsen M. 2007. Large-scale validation of methods for cytotoxic T-lymphocyte epitope prediction. *BMC Bioinf* **8**: 424. DOI: 10.1186/1471-2105-8-424.
105. He Y, Xiang Z, Mobley HL. 2010. Vaxign: the first web-based vaccine design program for reverse vaccinology and applications for vaccine development. *J Biomed Biotechnol* **2010**: 297505 DOI: 10.1155/2010/297505.
106. Sun J, Wu D, Xu T, Wang X, Xu X, Tao L, Li YX, Cao ZW. 2009. SEPPA: a computational server for spatial epitope prediction of protein antigens. *Nucleic Acids Res* **37**: W612–W616. DOI: 10.1093/nar/gkp417.
107. Schanen BC, De Groot AS, Moise L, Ardito M, McClaine E Martin W, Wittman V, Warren WL, Drake DR 3rd. 2011. Coupling sensitive in vitro and in silico techniques to assess cross-reactive CD4(+) T cells against the swine-origin H1N1 influenza virus. *Vaccine* **29**: 3299–3309. DOI: 10.1016/j.vaccine.2011.02.019.
108. Southwood S, Sidney J, Kondo A, del Guercio MF, Appella E, Hoffman S, Kubo RT, Chesnut RW, Grey HM, Sette A. 1998. Several common HLA-DR types share largely overlapping peptide binding repertoires. *J Immunol* **160**: 3363–3373.
109. Morris GM, Huey R, Olson AJ. 2008. Using AutoDock for ligand-receptor docking. *Curr Protoc Bioinformatics* Chapter 8: Unit 8.14. DOI: 10.1002/0471250953.bi0814s24.
110. Hess B, Kutzner C, Van der Spoel K, Lindahl E. 2008. GROMACS 4: algorithms for highly efficient, load-balanced, and scalable molecular simulation. *J Chem Theory Comput* **4**: 435–447 DOI: 10.1021/ct700301q.
111. Ciacci-Zanella JR, Vincent AL, Prickett JR, Zimmerman SM, Zimmerman JJ. 2010. Detection of anti-influenza A nucleoprotein antibodies in pigs using a commercial influenza epitope-blocking enzyme-linked immunosorbent assay developed for avian species. *J Vet Diagn Invest* **22**: 3–9. DOI: 10.1177/104063871002200102.
112. Rimmelzwaan GF, Baars M, Claas EC, Osterhaus AD. 1998. Comparison of RNA hybridization, hemagglutination assay, titration of infectious virus and immunofluorescence as methods for monitoring influenza virus replication in vitro. *J Virol Methods* **74**: 57–66. DOI: 10.1016/S0166-0934(98)00071-8.
113. Haste-Andersen P, Nielsen M, Lund O. 2006. Prediction of residues in discontinuous B-cell epitopes using protein 3D structures. *Protein Sci* **15**: 2558–2567 DOI: 10.1110/ps.062405906.

## SUPPORTING INFORMATION

Additional supporting information may be found in the online version of this article at the publisher's web site.